Inaugural dissertation

for

obtaining the doctoral degree

of the

Combined Faculty of Mathematics, Engineering and Natural Sciences

of the

Ruprecht - Karls - University

Heidelberg

Presented by

M. Sc. Sevgican Demir

born in: Istanbul/Turkey

Oral examination: 07.12.2022

Novel molecular mechanisms

of TSC22D4 action

in development of diabetes mellitus

Referees: Prof. Dr. Marc Freichel

Prof. Dr. Peter Angel

Table of Contents

Acknowledgments

I would like to express my gratitude to all those who supported me during my Ph.D. studies. First of all, I would like to thank Dr. Bilgen Ekim-Üstünel for giving me the opportunity to perform my doctoral thesis in her group. Her passion for science has always motivated me to plan more experiments to produce more and more data. Working with her side-by-side and spending quite some time trying to detect a fainted western blot band was priceless! After all the hard work and exhausting days, I completed my Ph.D. project with great support of her. Thank you, hocam!

I am so grateful being part of the IDC group. I would like to thank Prof. Stephan Herzig for his endless support and guidance throughout my Ph.D. project. His valuable inputs on my project led us always to think deeper and go further. I would also like to thank all the IDC members in Heidelberg for creating a friendly environment. I specifically thank Dr. Gretchen Wolff and Dr. Mina Sakurai for helping me with daily struggles and for guiding me when I needed! Lunch and coffee breaks in case of "emergency" helped me to get through the day. I really appreciate your suggestions and detailed discussions of my results. Gretchen, thank you for helping me with the primary hepatocyte experiments which comprised a big part of my research. I would also like to thank Dr. Maik Brune for his help in producing Adenoviruses.

I would like to thank Annika Wieder and Oksana Hautzinger for their technical assistance during my Ph.D. I could not have performed all the qPCRs and Western blots without your support! Annika, thank you very much for your assistance with all the last-minute experiments. I appreciate how you were always willing to create a spot for me on your calendar!

I would like to thank Prof. Marc Freichel and Prof. Peter Angel for being my thesis committee members. Their advice and guidance during my Ph.D. were invaluable. I would like to also thank Prof. Dr. Karin Müller-Decker and Prof. Ursula Klingmüller for evaluating my thesis and accepting being part of my committee.

I would like to thank two of my close friends, Özge and Cagatay, for the nights that we came together to discuss our problems related to our projects. I loved how we always ended up dancing and shaking our daily struggles away! I would also like to thank Steffi for her warm friendship during our Ph.D. years!

Last but not least, I would like to thank my family for supporting my decisions and having faith in me. I cannot thank enough my husband, Aykut, for always being there and cheering me up at my lowest. In the Ph.D. journey that we have been through together, you were my biggest motivation! Thanks for being my other half! Finally, I would like to thank my mom, Gönül, for her unconditional love and endless support. Annem, tüm emeğin ve desteğin için teşekkürler! Bu tez senin için!

1. Abstract

The pathogenesis of Type 2 Diabetes (T2D) manifests itself with elevated blood glucose and insulin levels. At the molecular level, dysregulations in the insulin signaling pathway cause disruptive cellular processes modulated by distinct regulators. Akt plays a key role in the insulin signaling cascade regulating glucose and lipid metabolism, cell survival and proliferation. In my Ph.D. project, I identified Transforming Growth Factor β1 (TGFβ1) Stimulated Clone 22 D4 (TSC22D4) as a novel Akt-interacting protein. TSC22D4 interacts specifically with Akt1 via its D2 domain, which is located in the intrinsically disordered region of TSC22D4. Starvation or energy deprivation promotes TSC22D4-Akt1 interaction, while refeeding mice or stimulating cells with glucose and insulin impairs the interaction. Having identified the interaction site of TSC22D4 with Akt1, we produced the D2+TSC allele which constitutively interacts with Akt1, independent of nutrient availability. The strong interaction of TSC22D4 and Akt1 (via D2+TSC allele) improves glucose handling, insulin sensitivity and lipid accumulation in AAV-transduced TSC22D4$^{hep-/-}$ mice. Altogether, TSC22D4 plays a role in regulating insulin signaling via interacting Akt and contributes to its function on glucose and lipid metabolism.

2. Zusammenfassung

Die Pathogenese des Typ-2-Diabetes (T2D) äußert sich in erhöhten Blutzucker- und Insulinspiegeln. Auf molekularer Ebene führen Dysregulationen im Insulin-Signalweg zu störenden zellulären Prozessen, die von verschiedenen Regulatoren moduliert werden. Akt spielt eine Schlüsselrolle in der Insulin-Signalkaskade, die den Glukose- und Fettstoffwechsel, das Überleben und die Proliferation von Zellen reguliert. In meinem Promotionsprojekt habe ich den durch den Transforming Growth Factor β1 (TGFβ1) stimulierten Klon 22 D4 (TSC22D4) als neuartiges Akt-interagierendes Protein identifiziert. TSC22D4 interagiert über seine D2-Domäne, welche sich in der intrinsisch ungeordneten Region von TSC22D4 befindet, spezifisch mit Akt1. Hungern oder Energieentzug fördern die Interaktion zwischen TSC22D4 und Akt1, während die erneute Fütterung von Mäusen oder die Stimulierung von Zellen mit Glukose und Insulin die Interaktion beeinträchtigt. Nachdem wir die Interaktionsstelle von TSC22D4 mit Akt1 identifiziert hatten, erzeugten wir das D2+TSC-Allel, das unabhängig von der Verfügbarkeit von Nährstoffen konstitutiv mit Akt1 interagiert. Die starke Interaktion von TSC22D4 und Akt1 (über das D2+TSC-Allel) verbessert die Glukoseverarbeitung, die Insulinsensitivität und die Lipidakkumulation in AAV-transduzierten TSC22D4$^{hep-/-}$ Mäusen. Zusammen genommen spielt TSC22D4 eine Rolle bei der Regulierung der Insulinsignalübertragung über die Interaktion mit Akt und trägt zu dessen Funktion im Glukose- und Fettstoffwechsel bei.

3. Introduction

3.1. Diabetes Mellitus as a life-threatening disease

Diabetes is a metabolic disease characterized by increased blood glucose levels (hyperglycemia), which results in serious damage to the organs, including the heart, kidneys, liver and nerves. According to the World Health Organization (WHO), around 422 million people had diabetes worldwide in 2014, and the majority of those people belong to low- and middle-income countries. In 2019, diabetes was one of the fatal diseases and around 2 million people lost their lives due to diabetes and its complications [1].

There are two main types of diabetes: Type 1 Diabetes (T1D) and Type 2 Diabetes (T2D). T1D is an autoimmune disorder where the immune system fails to recognize the insulin-producing β-cells of the pancreas and destroys them [2]. T2D, on the other hand, is a metabolic disorder resulting in hyperglycemia due to insulin resistance in metabolic organs such as the liver and adipose tissue [3].

In a healthy state, carbohydrates are broken down to glucose in the postprandial state, leading blood glucose levels to rise and stimulating the pancreatic β-cells to release insulin into the bloodstream. Glucose-induced insulin secretion helps glucose uptake into metabolic organs such as skeletal muscle and adipose tissue as the energy source. After a meal, the liver stores excess glucose as glycogen or fat for a later time to metabolize it. The liver produces and/or stores glucose depending on the glucose needs of the body. Insulin-mediated glucose uptake by metabolic organs is balanced by pancreatic hormones insulin and glucagon in the liver. Non-insulin mediated glucose uptake is regulated by another pancreatic hormone somatostatin which inhibits insulin and glucagon secretion [4], [5].

As circulating glucose is taken up by metabolic organs, blood glucose levels decrease, and the pancreas stops releasing insulin. In case of insulin resistance, a primary feature in T2D, the metabolic organs cannot respond normally to the insulin hormone. The insulin-secreting pancreatic β-cells temporarily increase their number and secrete more insulin (hyperinsulinemia) to compensate for the elevated glucose levels in the circulation. Due to increased insulin levels, constitutive activation of insulin signaling pathways at target tissues initiates several negative feedback loops towards insulin signaling, contributing to insulin resistance. In insulin resistance, cells of the metabolic tissues fail to respond to circulating insulin levels and activate the PI3K/Akt signaling pathway. A constant hyperglycemic state causes an extra burden on β-cells which results in β-cell malfunctioning and failure; a.k.a β-cell exhaustion. In T2D, β-cell mass in the pancreatic islets is decreased by around 60% and glucose-stimulated insulin secretion (GSIS) capacity is impaired [6].

T2D is a complex and heterogenic disease with several risk factors causing insulin resistance. Genetic factors, being overweight and having a sedentary lifestyle are some of the primary causes of T2D. T2D can be subclassed into different groups: mild obesity-induced diabetes, severe insulin-resistant diabetes, severe

insulin-deficient diabetes, mild age-related diabetes, and severe autoimmune diabetes [6, 7]. Since T2D results from dysregulations in different metabolic organs and tissue-specific signaling pathways, patients with diabetes can also experience various complications affecting organs such as the retina, liver, kidney, and vital body systems such as the cardiovascular and nervous systems.

Insulin resistance is one of the dominant features of metabolic syndrome. The metabolic syndrome manifests itself with hyperglycemia, high blood pressure and abnormal lipid levels such as decreased high-density lipoprotein (HDL) cholesterol, elevated triglyceride levels, and low-density lipoprotein (LDL) cholesterol. Elevated triglyceride levels can cause increased liver fat content, leading to non-alcoholic fatty liver disease (NAFLD). Due to lipotoxicity induced-inflammation in the liver, NAFLD may develop further into non-alcoholic steatohepatitis (NASH), liver cirrhosis and liver cancer (hepatocellular carcinoma).

Although T1D cannot be currently prevented, onsets of T2D can be delayed or even avoided by applying some practices. Performing regular exercise and healthy eating habits help maintain good health and to control blood glucose and lipid levels. It is important to diagnose diabetes in its early stages via periodic assessments of blood glucose and insulin levels. Since the longer a person lives with diabetes without a diagnosis, the worse their complications and health outcomes might become. Regular screening of kidneys, feet, cardiovascular system and eyes reduces the risk of serious complications caused by diabetes.

Even though early detection of the symptoms would help avoid the worse outcomes, there is still no cure for diabetes. Drugs and dose-dependent insulin injections are used only in the later stages of the disease. There are still unknown molecular mechanisms that help maintain blood glucose and lipid levels to prevent T2D beforehand. In my Ph.D. project, I aim to identify the underlying molecular mechanisms and contribute to the field for the development of novel therapies.

3.2. Role of β-cells in insulin secretion

β-cells, located in the Langerhans islet of the pancreas, are connected to each other and surrounded by other hormone-secreting cells: α (alpha) cells and δ (delta) cells (Fig. 1a). With the islets' vascularized structure, the pancreas regulates the trafficking of growth factors. Having an appropriate number of functional insulin-secreting β-cells (known as β-cell mass) is one of the requirements of insulin secretion. Insulin is secreted via granules and insulin secretion is tightly mediated by regulatory signals such as free fatty acids, amino acids, hormones and, most importantly, circulating glucose concentration [6].

Glucose transporter-2 (Glut2) is a transmembrane protein that is abundantly located on the β-cells surface and senses the circulating blood glucose levels. In the cells, Glut2-dependent glucose uptake results in the closure of ATP-sensitive potassium channels on the membrane (K_{ATP} channels), leading to voltage-gated

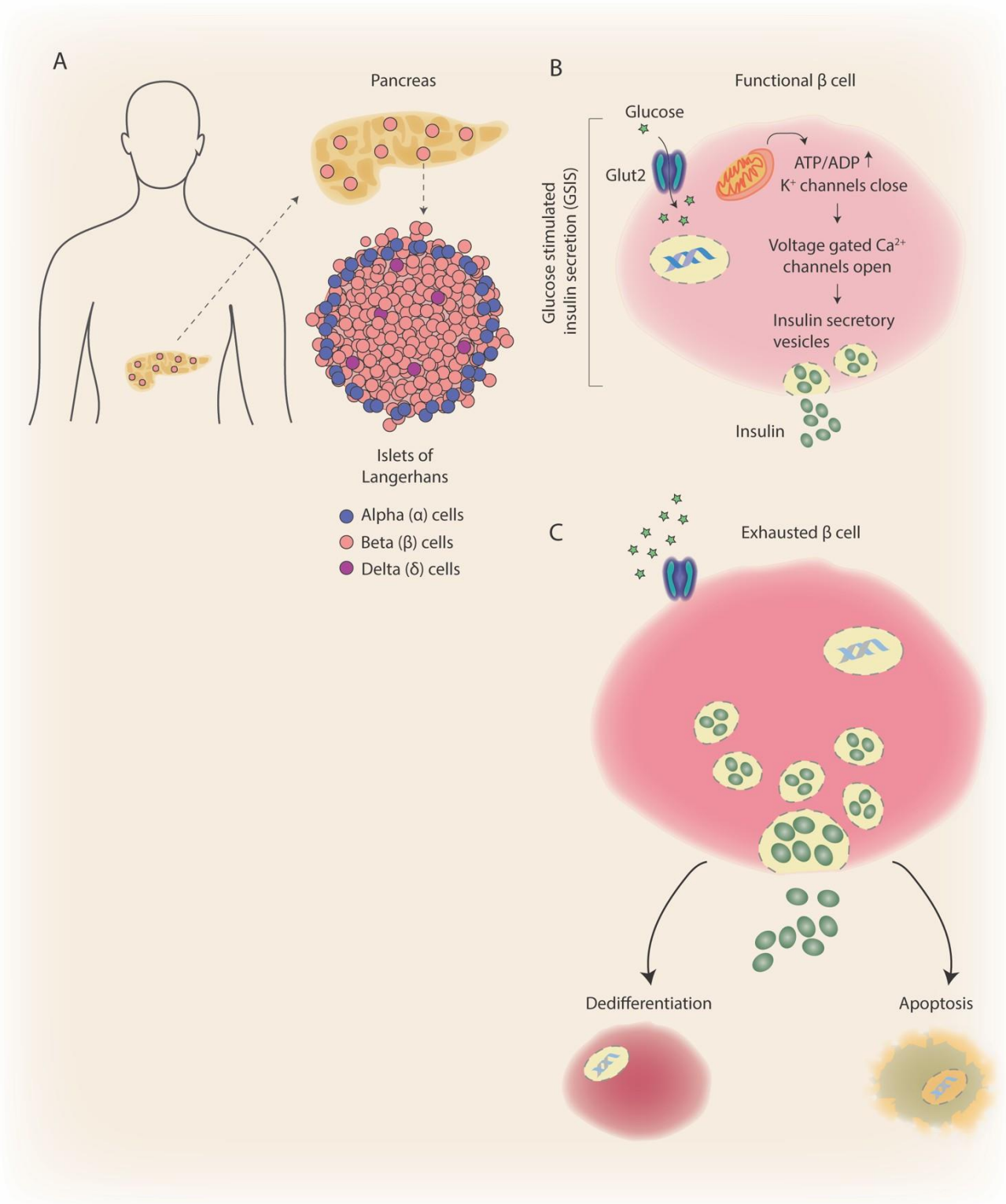

Figure 1: Role of beta (β) cells in insulin secretion.

A. Illustration of pancreatic cell types (α, β, δ cells) located in the islets of Langerhans. **B**. Functional β cells maintain islet function by regulating insulin release upon glucose stimulation. **C**. Exhausted β cells in type 2 diabetes increase their size and secrete more insulin. The fate of the exhausted β cells can be either dedifferentiation or apoptosis. (*Figure adapted from Demir et al, [6]*).

calcium channels to open. Eventually, β-cells secrete insulin into the bloodstream to target metabolic organs (Fig. 1b).

In T2D, exhausted β-cells, which produced extreme amounts of insulin to compensate for high glucose, can either dedifferentiate or undergo apoptosis (Fig. 1c) [6], [8]. Interestingly, under stress conditions, healthy and functional β-cells can also lose their differentiated form and dedifferentiate to a precursor state. Unfortunately, this event also results in a decrease in the β-cell mass and malfunctioning β-cells give rise to cytotoxic events aggravating symptoms of T2D.

3.3. Role of liver in metabolic syndrome

The liver acts as a critical hub for metabolic homeostasis and it is one of the key organs that contribute to the regulation of glucose metabolism. The liver regulates the synthesis and storage of glucose in the fasting and fed states, respectively (Fig. 2) [9], [10].

There are four main cell types in the liver: hepatocytes, hepatic stellate cells (HSCs), Kupffer cells and liver sinusoidal endothelial cells. Hepatocytes constitute ~80% of the total liver population. Glucose enters hepatocytes via Glut2 which is a dominant glucose sensor found also in hepatocytes. With glycolysis, glucose is metabolized into pyruvate in the cytoplasm to eventually generate ATP with the tricarboxylic acid (TCA) cycle and oxidative phosphorylation in the mitochondria [6].

The liver not only metabolizes glucose with glycolysis but also converts glucose into fatty acids when carbohydrates are abundant. In the postprandial state, products of glycolysis are used for fatty acid synthesis through lipogenesis. Additionally, fatty acids released from adipose tissue can also be taken by the liver from the bloodstream. Produced and/or received fatty acid chains are further used as building blocks of triacylglycerol and cholesterol in hepatocytes and stored in lipid droplets or secreted into the bloodstream as very-low-density protein (VLDL). On the other hand, in the fasting state, glycogen breaks down to glucose through glycogenolysis, and the liver secretes glucose into the bloodstream. Overall, hepatic glucose production is the primary source of energy for cells to maintain their functions.

The relationship between blood glucose levels and the liver is governed by a hepatic homeostatic mechanism that responds to the level of glycemia in the fasting or postprandial state. Metabolic activity in the liver is regulated via various factors, particularly hormonal stimulations of the pancreas. While insulin induces glycolysis, glycogen production and lipogenesis, it suppresses gluconeogenesis, allowing liver cells to metabolize and/or store glucose and lower glycemia. On the other hand, as opposed to insulin, glucagon induces gluconeogenesis. In T2D, malfunctioning insulin action results in constantly active (sustained) gluconeogenesis and overly promoted lipogenesis. This phenomenon is also known as selective insulin resistance.

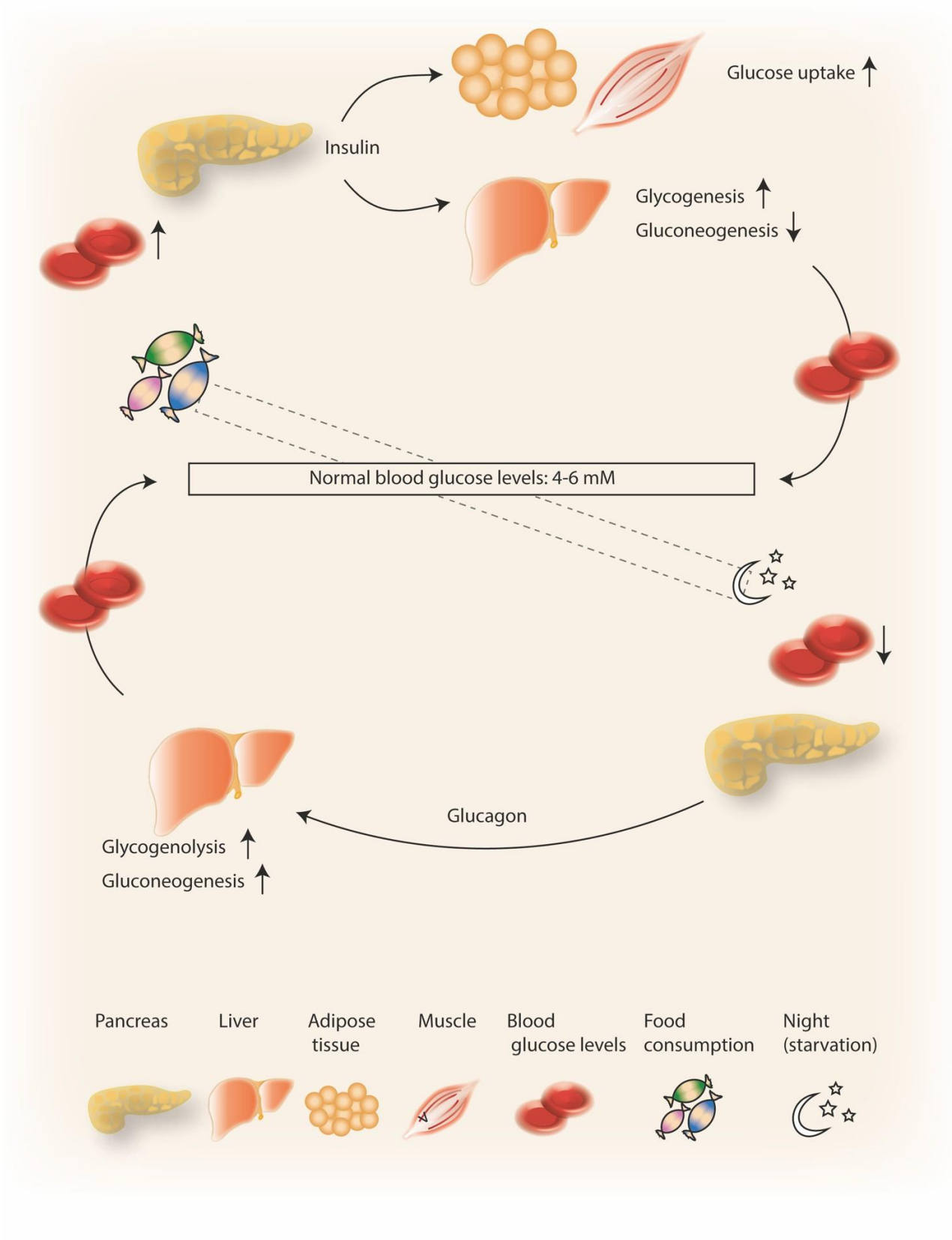

Figure 2: Role of liver in glucose metabolism.

Liver plays a key role maintaining blood glucose levels together with pancreas. In the postprandial state, blood glucose levels increase and the pancreas secretes insulin. While glycogenesis rate increases in the liver, gluconeogenesis rate decreases to reach normal blood glucose levels. Upon starvation, blood glucose levels decrease and the pancreas secretes glucagon to induce glycogenolysis and gluconeogenesis in the liver.

At the molecular level, various transcription factors regulate liver energy metabolism by controlling rate-limiting steps of metabolic pathways in the liver. In the healthy state, upon insulin binding, Akt, as a key serine/threonine kinase in the insulin signaling pathway, suppresses gluconeogenesis by inhibiting Forkhead box O1 (FoxO1) transcription factor. On the other hand, upon starvation, glucagon signaling induces the expression of FoxO1 and Peroxisome proliferator-activated receptor gamma coactivator 1-alpha (PGC1α) to regulate gluconeogenesis and lipogenesis.

3.4. Canonical insulin signaling pathway

The insulin signaling pathway plays a central role in regulating metabolic actions of growth factors by controlling a wide range of cellular processes.

The insulin binding to the insulin receptor (IR), a tyrosine kinase receptor, initiates a cascade of phosphorylation events (Fig. 3). Insulin-bound IR homodimerizes and phosphorylates insulin receptor substrates 1 and 2 (IRS1/2), which phosphorylates the lipid kinase phosphoinositide 3-kinase (PI3K). Activated PI3K then phosphorylates phosphatidylinositol (3,4)-bisphosphate (PIP2) and converts it to phosphatidylinositol (3,4,5)-trisphosphate (PIP3). The phosphorylation cascade leads PIP3 to recruit 3-phosphoinositide-dependent protein kinase 1 (PDK1) and protein kinase B (PKB)/Akt to the cell membrane. Akt is phosphorylated on distinct residues on Akt1 (S473, T308), Akt2 (S474, T309) and Akt3 (S472, T305) by mammalian target of rapamycin complex 2 (mTORC2) and PDK1, respectively. Although in the absence of phosphorylation at S473, T308-phosphorylated Akt can still phosphorylate some of its effectors [11], phosphorylation of both S473 and T308 residues is required for Akt to be fully and catalytically active. Once activated, Akt isoforms translocate to different subcellular compartments such as mitochondria, endoplasmic reticulum, Golgi and nucleus to contribute to its function. Akt modulates numerous cellular events through distinct effectors, regulating glucose metabolism, glycogen and lipid synthesis, cell cycle, proliferation and survival [12], which will be detailed in sections 3.6 and 3.7.

3.5. Akt isoforms: Akt1, Akt2 and Akt3

Protein kinases are generally expressed in different isoforms with a high degree of similarities. Although they share sequence similarities and protein structures, each of those isoforms might serve a distinct function in a tissue-specific manner. The sequence differences might lead to conformational changes in the protein, resulting in alteration of binding partners, effectors or targets for each of the isoforms.

Akt belongs to AGC kinase family, and it consists of three highly conserved isoforms: Akt1, Akt2 and Akt3. The Akt isoforms share a high degree of sequence homology in their catalytic domain. With the divergence in the N-terminal Pleckstrin (PH) domain and C-terminal regulatory domain, the interacting partners of Akt

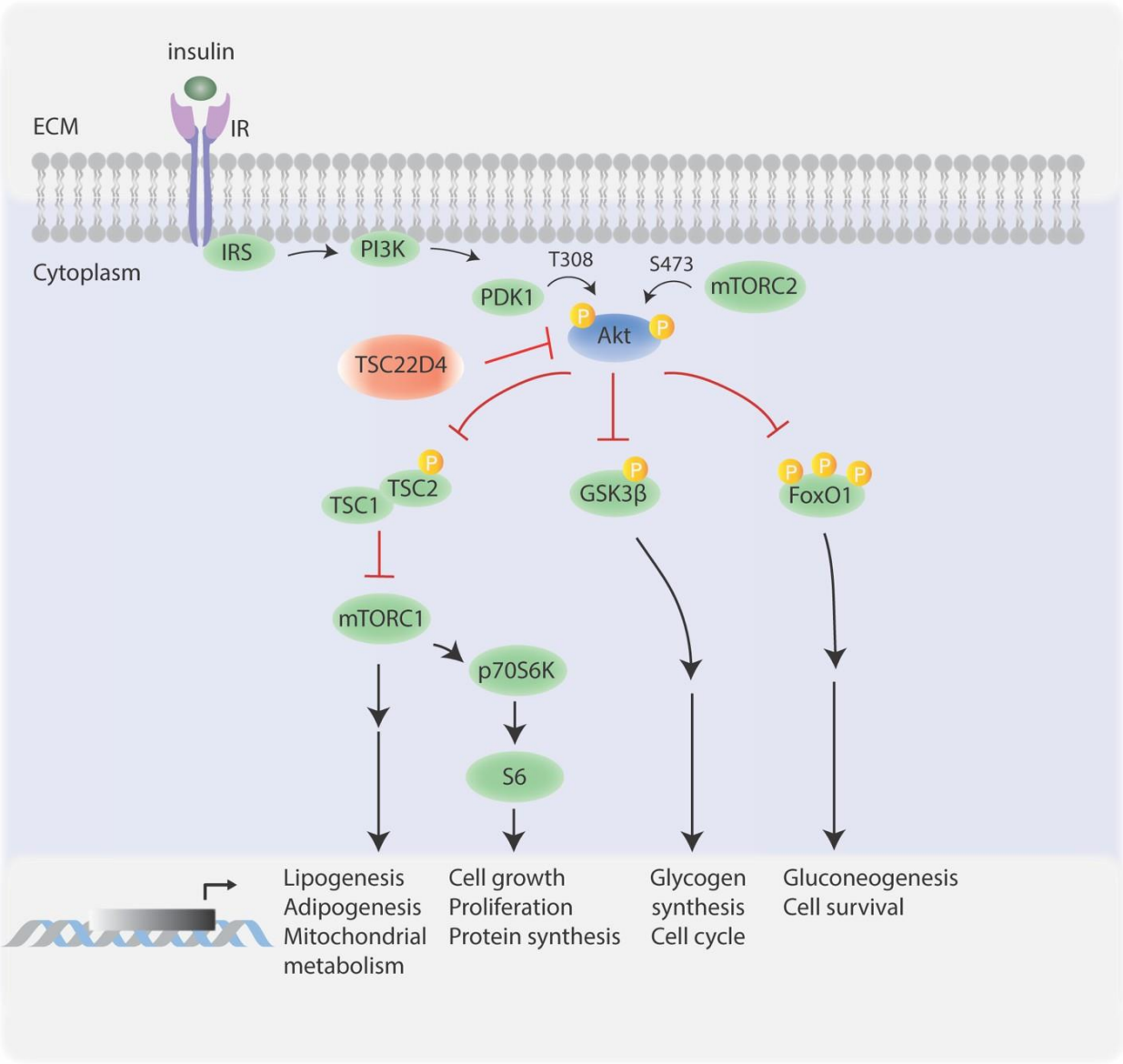

Figure 3: Canonical insulin signaling pathway.

Upon insulin binding to the insulin receptor (IR), a phosphorylation cascade becomes activated. Activated IRS phosphorylates PI3K, which recruits PDK1 to the cell membrane. Akt is phosphorylated by PDK1 and mTORC2 at T308 and S273 residues, respectively. Activated Akt regulates main metabolic events via its downstream targets such as TSC1/TSC2, GSK3β and FoxO1. (*Figure adapted from Demir et al, [6]*).

isoforms may differ. As a protein kinase located at the intersection of numerous effectors, all three isoforms of Akt are activated in response to growth factors and hormones via PI3K signaling.

In the liver, different cell types including hepatocytes, HSCs and Kupffer cells, contribute to the progression of alcoholic liver disease, liver fibrosis, and ultimately cirrhosis. For the fatty liver diseases, the activities of Akt isoforms are unique in regulating downstream effectors in a tissue-dependent manner. For example, Akt1 and Akt2 are both involved in HSC proliferation, while only Akt2 plays a role in migration in ethanol and LPS-induced liver fibrosis. On the other hand, while only Akt1 or Akt2 absence does not affect liver regeneration, hepatic-specific Akt1 and Akt2 deficient mice impaired liver regeneration and increased mortality [13]. Furthermore, in colon cancer cell lines, knocking out of either Akt1, Akt2, or both Akt1/2 reduced lactate and alanine levels, eventually resulting in malfunctioning carbohydrate metabolism. Genes playing a role in glucose metabolism diminished and fatty acid metabolism was impaired in Akt1 KO and Akt2 KO cells [14].

Whole-body knockout mouse studies have shown that Akt1 plays more role in cell survival and proliferation, Akt2 is essential in regulating glucose metabolism, and Akt3 has more role in brain development [14], [15]. On the other hand, double Akt isoform knockout mice showed both specific and overlapping roles of the Akt family isoforms. To understand the extensive functions of each Akt isoform, *in vivo* conditional and tissue-specific knockout studies and *in vitro* studies in different cell types are required [16].

3.6. Role of Akt in glucose metabolism

In the liver, Akt activation upon insulin stimulation is essential for suppressing hepatic glucose production and inducing lipid synthesis. Akt suppresses glucose production via its phosphorylation-mediated inhibition of its downstream target FoxO1 transcription factor (Fig. 3), which induces key gluconeogenic enzymes Phosphoenolpyruvate carboxykinase (PEPCK) and Glucose 6-phosphate (G6P) during fasting. Insulin-Akt signaling also regulates *de novo* lipid synthesis through the Sterol regulatory element-binding protein 1 (SREBP1) transcription factor [17]. Other Akt effectors playing role in glucose metabolism include glycogen synthase kinase 3β (GSK3β), AS160 and PFKFB2. GSK3β inhibits insulin-dependent glycogen synthesis, and increased GSK3β expression is positively correlated in diabetic and obese animals [18]. Further, Akt modulates protein synthesis by inhibiting Tuberous sclerosis complex 2 (TSC2) and indirectly promoting mTORC1/p70 S6K/S6 axis [17], [19].

PI3K becomes active within seconds to minutes of growth factor stimulation and reaches the maximum function mostly in an hour. Then, it is downregulated with timing dependent on cell type and stimulus. This transient signaling event is balanced with Phosphatase and tensin homolog deleted chromosome 10 (PTEN) action in combination with the temporary inactivation of PI3K [17]. PTEN is a negative regulator of the PI3K-Akt signaling, and it inhibits PIP_3 activation by dephosphorylating PIP_3 at the D3 position [20]. Protein phosphatase

2A (PP2A) and the PH domain leucine-rich repeat protein phosphatases (PHLPP1 and PHLPP2) also inactivate Akt function by dephosphorylating Akt on T308 and S473, respectively [17].

3.7. Akt binding partners

Protein-protein interaction can cause conformational changes in the binding proteins by stabilizing or destabilizing them. Alternatively, some proteins can act as anchors, creating large molecule complexes to modulate signaling events [21].

Akt is a key effector signaling molecule in the insulin signaling pathway. It regulates a wide range of downstream proteins essential for metabolism, energy homeostasis, cell growth, and survival. Akt directly phosphorylates numerous targets that are transcription factors, protein and lipid kinases, cell cycle regulators and enzymes. Those targets, which Akt phosphorylates on S and T residues, share a consensus motif:R-X-R-X-X-S/T [17].

Akt consists of three domains as PH domain, kinase domain and regulatory C-tail. Each interaction partner prefers a different binding domain of Akt depending on the conformation and affinity to the interaction site. It has been reported that the PH domain is critical for Akt to interact with phosphoinositides and other protein partners. PIP_3, for example, interacts with the PH domain of Akt to stimulate its translocation to the plasma membrane, whereas PDK1 interacts with Akt via the C-tail of Akt.

Another protein that interacts specifically with the PH domain of Akt is JNK interacting protein 1 (JIP1). JIP1 involves in a complex regulating JNK signaling and Akt-JIP1 interaction modulates apoptosis. Growth factor receptor-binding protein 10 (Grb10) also interacts with the PH domain of Akt. Interestingly, via its SH2 domain, Grb10 can bind to tyrosine kinase receptors, including insulin receptor (IR) which enhances Akt activation [22]. Additionally, Akt has a conserved proline-rich sequence (PXXP) at the C-terminus, enabling Akt to bind to SH3 domain-containing proteins such as tyrosine kinase Src and Arg-binding protein 2 (ArgBP2γ). ArgBP2γ binds to the PXXP region of Akt and p21-activated protein kinase (PAK21) to generate the Akt-ArgBPg-PAK1 complex to regulate cell survival [23].

Upon insulin stimulation and other growth factors, Tribbles homolog 3 (Trb3) interacts with the kinase domain of Akt to inhibit its activation by interfering with phosphorylation sites at T308 and S473 [24]. Trb3 expression is enhanced in the normal liver upon fasting, and Trb3 expression levels are significantly higher in the liver of db/db mice [24]，[21]. Endosomal adaptor protein containing PH domain, PTB domain and leucine zipper motif (APPL1) interacts with the kinase domain of Akt to block Akt-Trb3 interaction through direct competition. Therefore, APPL1 promotes Akt translocation to the plasma membrane to enhance its activation. Interestingly, hepatic APPL1 overexpression in db/db mice promotes hyperglycemia and insulin resistance [25], and the APPL1-Akt complex dissociates upon insulin stimulation [26].

3.8. Intrinsically disordered proteins (IDPs)

Intrinsically disordered proteins (IDPs) consist of highly flexible and dynamic polypeptide chains which do not have stable and defined tertiary structures (Fig. 4a). The unstructured polypeptide regions in IDPs tend to have secondary structures such as alpha helices or beta sheets that enable them to change their conformational state for binding with other proteins, nucleic acids and a wide range of small molecules. The function of the known IDPs typically involves modulating signal transduction events and transcriptional regulation [27], [28]. IDPs are prone to have numerous posttranslational modifications (PTMs) such as acetylation, glycosylation, and ubiquitination, yet phosphorylation appears to be particularly important. The phosphorylation sites located in the disordered regions can have a stabilizing effect on transient tertiary structures. Based on the studies on IDPs, a short stabilization motif was identified: S/T-P-(3)-R/K in which S/T represents a phosphorylation site [29]. Proteins that were identified containing the stabilization motif have diverse functions and structures. However, most of them emerged to be kinases or kinase-interacting proteins such as mitogen-activated protein kinase kinases (MAPKK), the calcium/calmodulin dependent kinases (CaMKs) or the protein kinase C (PKC) binding proteins. TSC22 family proteins also contain intrinsically disordered regions and, notably, TSC22D4, contains the stabilization motif in its disordered region (Fig. 4b) [29]. The transition from a disordered to an ordered state is regulated through phosphorylation for IDPs to bind to the interacting proteins. Once a helical structure is stabilized via phosphorylation, it accelerates other proteins' binding efficacy to contribute to the IDPs function [29], [30]. Therefore, phosphorylation in the intrinsically disordered regions acts as a signal to stimulate molecular interactions.

Moreover, some of the IDPs lack stable secondary structures which allow them to act more dynamic and reversible compared to IDPs having defined secondary structures. Having more flexibility in the protein makes them extremely sensitive environmental sensors. In addition to ligands and binding partners, they can also sense chemical signals, mechanical stress, and light or pH changes [31]. In IDPs, structural heterogeneity is determined by amino acid proportion, and the majority of IDPs are enriched in polar and charged amino acids such as Pro, Gly, Gln, Ser, Glu, Lys, and Ala rather than bulky hydrophobic amino acids. Notably, the amino acid composition of TSC22D4 mostly consists of Pro, Gly and Ser residues (Fig. 4c).

3.9. TSC22 family proteins and their functions

Transforming growth factor-beta 1 (TGFβ1)-Stimulated Clone (TSC) 22 family consists of 4 proteins (TSC22D1, TSC22D2, TSC22D3 and TSC22D4) each with alternatively spliced isoforms. All TS22 family members share a highly conserved TSC Box, but also belong to the IDP category with unstructured peptide sequences flanking the TSC box. Therefore, these proteins might contribute to various signaling events with distinct protein-protein interactions due to their conformational flexibility.

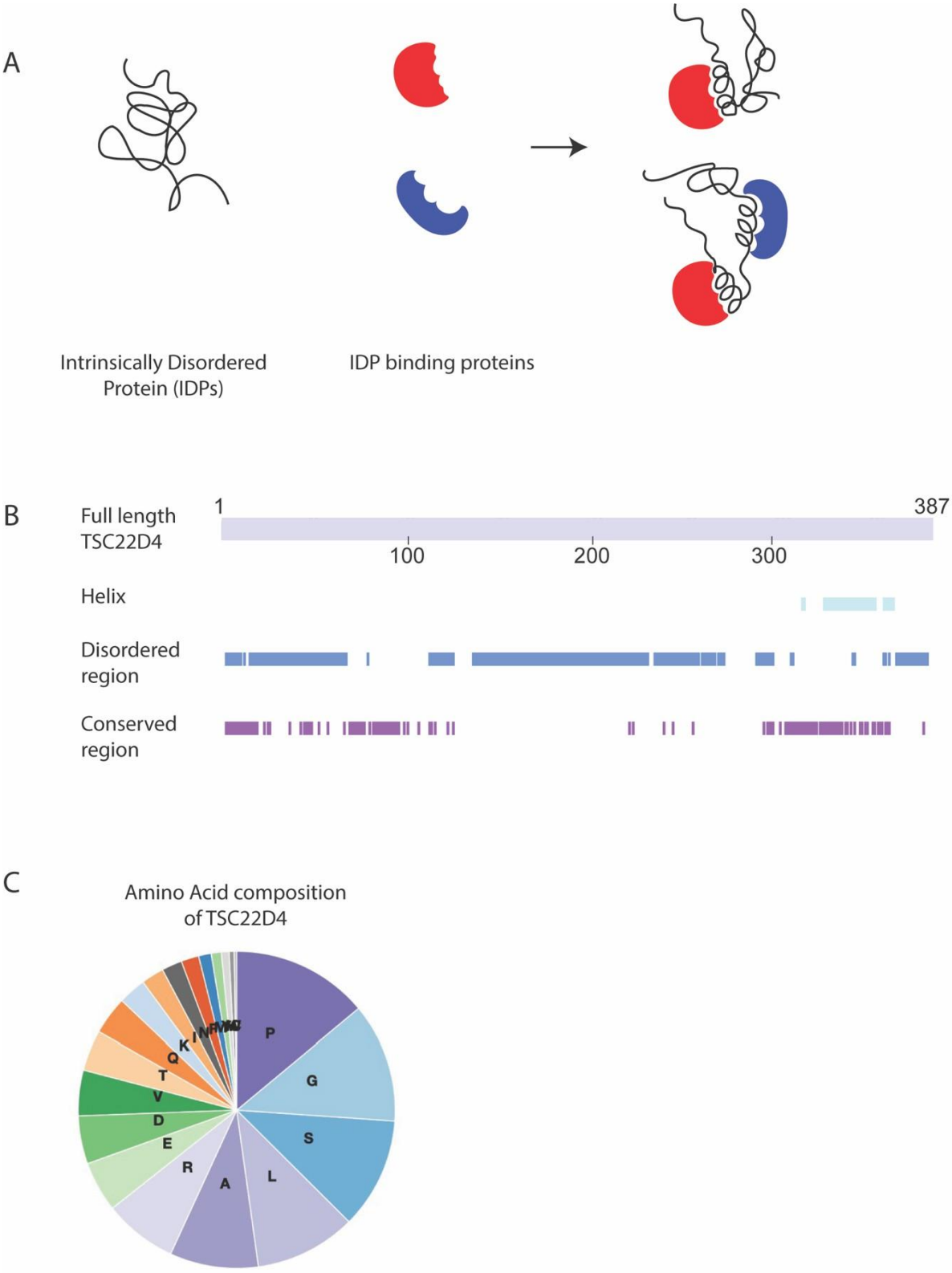

Figure 4: TSC22D4 as an intrinsically disordered protein (IDP).

A. Illustration of an IDP, its binding partners and possible interactions due to the flexible conformational changes of the IDP. **B**. Structural analysis of TSC22D4 (*Figure adapted from [32]*) **C**. Amino acid composition of TSC22D4 (*Figure adapted from [32]*).

TSC22 (which was later re-named as TSC22D1) was first isolated as a TGFβ1 inducible gene in mouse osteoblastic cells by a differential screening, a common method to identify differentially expressed genes in distinct physiological conditions [33]. TSC22 is expressed ubiquitously in mice and humans, and its expression varies in different cell lines upon stimulants such as TGFβ1, serum or dexamethasone [34], [35], [36]. All TSC22 family members have a leucine zipper (ZIP) motif in the conserved TSC Box. Interestingly, the ZIP domain in TSC22 proteins does not have the consensus sequence, N-(2)-A-A-(2)-(C/S)-R, and it lacks the basic region found in most basic region/leucine zipper (bZIP) proteins. In the bZIP-containing transcription factors, the upstream basic region acts as a DNA binding domain, while the leucine zipper motif enables protein dimerization. Due to the lack of a basic region in their ZIP domain, the potential DNA binding capacity of TSC22 family proteins remain elusive [37]. Nevertheless, like in bZIP proteins, ZIP also facilitates forming of homodimers and heterodimers to contribute to transcriptional regulation. Indeed, TSC22 family proteins appeared as transcriptional regulators which play role in both gene activation and repression [33], [38], [36]. Furthermore, TSC22 family proteins can homodimerize and heterodimerize with other TSC22 family proteins via the ZIP motif located in TSC Box. TSC22D4 heterodimers with TSC22D3 to enhance binding of NRBP1 complex assembly [39]. In addition, TSC22D1 isoforms dimerize with TDC22D4 to regulate antagonist events for cell fate. While TSC22D1.1 dimerizes with TSC22D4 to promote cell proliferation/survival, TSC22D1.2-TSC22D4 complex promotes senescence which is a state of irreversible growth arrest against DNA damage and oxidative stress [40]. A study on TSC22D4 was shown that TSC22D4 KO esophageal tumor cells delayed cellular senescence with decreased cyclin-dependent kinase (CDK) inhibitor P21 levels [41]. Further, in human medulloblastoma cells (DAOY cells), silencing TSC22D4 expression reduced cell-cycle progression from G1 to S phase, indicating increased cell-cycle arrest [36].

As in TSC22D1, posttranslational modifications give TSC22D4 isoforms heterogeneity and functional complexity. To illustrate, TSC22D4 isoforms were found in distinct subcellular localizations in mouse cerebellar granule neurons (CGNs) upon cell differentiation and postnatal cerebellum development [40]. In developing mouse brains, TSC22D4 plays role in proliferation, migration and differentiation by being expressed in specific brain areas responsible for mature and immature brain cells. In early embryonic brain development, TSC22D4 was found upregulated in areas specified for granule cell precursors. Thus, it plays role in differentiation of immature brain cells. In the adult stages, TSC22D4 was found activated in different brain areas for controlling cell proliferation and growth [36], [42]. Further, TSC22D4 was shown to play role in mitochondrial redox metabolism by dimerizing apoptosis-inducing factor (AIF) [40].

Overall, TSC22 family proteins act as tumor suppressors and regulate cell proliferation, differentiation and apoptosis [40], [43], [36], [44], [35]. In different studies, many binding partners of TSC22 family proteins have been identified. Namely, TSC22D1 interacts with Smad and Tgfβ receptor to regulate Tgfβ induced cell death [36].

TSC22D2 interacts with pyruvate kinase isoform M2 (PKM2) [45] and WD repeat protein WDR77 [46] to modulate cell proliferation. TSC22D3 interacts with NFKB, Raf, Ras and p53 which in turn inhibits the action of the downstream targets [47], [48], [49], [50],[51].

3.10. Role of TSC22D4 in glucose and lipid metabolism in the liver

TSC22D4 was identified due to its consensus sequence similarity with the other TSC22 family members, TSC22D1 and TSC22D3. Indeed, as with the other members of the family, studies performed on TSC22D4 showed that TSC22D4 suppresses transcriptional activity when fused to DNA binding domains [33]. The biological and tissue-specific function of TSC22D4 has been widely studied by the research group in that I conducted my Ph.D. project.

In a previous publication published by my supervisor, TSC22D4 was identified as a novel regulator of the insulin signaling pathway [52]. It promotes insulin resistance, glucose intolerance and diabetic hyperglycemia in obese and type 2 diabetic murine models. Also, patients with type 2 diabetes have elevated levels of TSC22D4 in their livers, leading to insulin resistance.

Hepatic TSC22D4 expression was elevated in mice with fatty liver disease and fibrosis both in mice and human livers [52], [53]. In a recent publication in our lab, hepatocyte-specific deletion of TSC22D4 (TSC22D4$^{hep-/-}$), resulted in reduced lipid accumulation, decreased apoptosis and amelioration in inflammation in mice liver with Methionine/Choline deficient (MCD) diet [54]. MCD diet is commonly used to model the buildup of fat and progressed fatty liver disease, non-alcoholic steatohepatitis (NASH). Briefly, the deficiency of Methionine/Choline leads to abnormal mitochondrial β-oxidation and very low-density lipoprotein (VLDL) synthesis [55]. In this study, analysis in single-cell RNA sequencing of TSC22D4$^{hep-/-}$ mice demonstrated an enriched gene network plays role in mitochondrial processes such as TCA cycle and triglyceride metabolism, supporting the improvements in liver damage in mice with the tissue-specific loss of TSC22D4.

Different liver cell types, including hepatic stellate cells (HSCs), hepatocytes and hepatic macrophages, present intra-hepatic crosstalk in progressive liver diseases (i.e. NASH and fibrosis) [56]. Upon chronic liver damage and inflammation, TGFβ1-induced HSCs become active and secrete collagen, a marker of the cirrhotic liver, into the extracellular matrix [57], [58]. In one of our latest studies, TSC22D4 was shown as a downstream effector of TGFβ1 to contribute to HSCs function with elevated HSC activation markers, α-smooth muscle actin (αSMA), Smad3, and collagen type I α1 (Col1a1) [58]. In a human hepatic cell line (LX2 cells), TSC22D4 induced cell proliferation and migration, which are the main characteristics of activated HSCs. Additionally, RNA-sequencing performed in TSC22D4 knockdown LX2 cells revealed regulators of HSCs (i.e. CCL7 and IL1β) as downstream targets of TSC22D4.

Altogether, TSC22D4 emerges as a key regulator of glucose and lipid metabolism contributing to fatty liver diseases via hepatocytes. In addition, it promotes cell proliferation and migration in HSCs, contributing to cell survival.

4. Project-related previous results

Our lab has identified TSC22D4 as a novel regulator of hepatic lipid metabolism in mice with cancer cachexia, a wasting disorder causing an extreme loss in body and muscle weight [53]. In the livers of the cachectic mice, TSC22D4 levels were elevated and hepatocyte-specific acute TSC22D4 knockdown resulted in the induction of lipogenic genes. Since TSC22D4 levels were positively correlated with the body wasting degree of the cachectic mice, TSC22D4 appeared as one of the candidates that might also regulate systemic energy homeostasis. To determine the target gene network of TSC22D4, Dr. Bilgen Ekim Üstünel performed a high throughput analysis using primary hepatocytes of mice expressing adenovirus either with non-specific control or TSC22D4-specific shRNA. As a result of the KEGG pathway analysis, TSC22D4 emerged as a potent regulator of the insulin/Akt signaling pathway [52]. The subsequent functional assays showed that TSSC22D4 regulates hyperglycemia and insulin resistance in diabetic mouse models by impairing Akt phosphorylation and downstream signaling [52]. Liver-specific TSC22D4 knockdown upregulated phospho-Akt (pAkt) levels as well as phosphorylation of Akt downstream targets such as FoxO1 and GSK3β compared to control mice [52]. However, the phosphorylation of upstream regulators of Akt (e.g. mTOR and IR) remained unchanged.

To follow up the PI3K/Akt axis in the context of TSC22D4 regulatory metabolism in liver tissues, Dr. Ekim-Üstünel transiently transfected Hepa1-6 cells (murine hepatoma cell line) with Flag-TSC22D4 and HA-Akt1 tagged plasmids and performed co-immunoprecipitation (co-IP) with α-Flag antibody, to test if TSC22D4 exerts its inhibitory effects on Akt function via physical interaction. As a result, HA-Akt1 successfullyco-IPed with Flag-TSC22D4, indicating TSC22D4-Akt1 interaction (Demir et al [59]; Manuscript accepted; in press @Science Advances). Further, glucose and insulin stimulation impaired the interaction and increased pAkt levels. Dr. Ekim Üstünel performed also Flag-TSC22D4 IP from the liver lysates of WT mice overexpressing vector control or Flag-TSC22D4, and observed an enriched interaction of endogenous Akt1 in the Flag IPs. In agreement with her previous findings in starved and glucose/insulin stimulated cells, refeeding mice after overnight starvation impaired the hepatic TSC22D4-Akt1 interaction [59]. Moreover, to test if TSC22D4-Akt1 interaction is regulated by intracellular energy levels, she treated Flag-TSC22D4 and HA-Akt1 overexpressing Hepa1-6 cells with mitochondrial inhibitors rotenone and antimycin and performed co-IP. Consequently, rotenone and antimycin treatment promoted TSC22D4-Akt1 interaction and reduced pAkt levels [59].

Thus, the goal of my study is to elucidate the role of TSC22D4-Akt1 interaction in controlling Akt function and glucose metabolism.

5. Aim of the study

1) Verifying TSC22D4-Akt1 interaction *in vivo*

2) Comparing the levels of endogenous TSC22D4-Akt1 interaction in different diabetic mouse models with different diets

3) Identifying the required and sufficient TSC22D4 domains for establishing the Akt1 interaction

4) Identifying TSC22D4 peptides with therapeutic potential to modulate Akt function

5) Identifying the role of TSC22D4-Akt1 interaction in cultured Hepa1-6 cells and primary hepatocytes

6) Identifying the role of hepatic TSC22D4-Akt1 interaction in glucose and lipid metabolism *in vivo*

6. Results

6.1. TSC22D4 interacts with Akt1 *in vivo*

Based on the preliminary data on TSC22D4-Akt1 interaction in Hepa1-6 cells, we aimed to determine if TSC22D4 interacts with Akt1 in mouse livers *in vivo* and if so; whether the interaction levels are being affected upon fasting/feeding regimen.

First, I examined endogenous TSC22D4-Akt1 interaction levels in WT mice fed with control diet (CD) or high-fat diet (HFD) to mimic insulin resistance via hyperglycemia and hyperinsulinemia. Therefore, to test TSC22D4-Akt1 interaction *in vivo* and to compare the interaction levels in CD and HFD conditions, I prepared liver lysates and performed endogenous TSC22D4 IP by incubating the liver lysates with homemade α-TSC22D4 antibody overnight. Then, I conjugated antibody-antigen complex with protein A/G coupled beads via further incubation (Fig. 5a). To confirm TSC22D4 presence in the IPs and to test Akt1 interaction, I performed Western Blotting for α-TSC22D4 and α-Akt1 antibodies, respectively. As a result, TSC22D4 IPs were successful and TSC22D4 interacted with Akt1 in the livers of WT mice with a control diet and HFD (Fig. 5b). The interaction levels were similar in the CD and HFD. Furthermore, TSC22D4 interacted specifically with Akt1, since Akt2 levels in the TSC22D4 IPs did not show further enrichment compared to IgG controls.

Alternatively, a high fat/high sucrose diet (HF/HSD) is a widely used approach to induce rapid onset of metabolic syndrome including differential changes in genes responsible for insulin signaling, lipogenesis and inflammation [60]. After analyzing TSC22D4-Akt1 interaction in HFD mice, we examined if TSC22D4-Akt1 interaction was affected in mice fed with HF/HSD. To this end, from the liver lysates of WT mice in the CD and HF/HSD, I performed endogenous TSC22D4 IP and analyzed the Akt1 interaction levels by Western Blotting. Interestingly, TSC22D4-Akt1 interaction decreased in HF/HSD mice compared to CD fed mice (Fig. 5c). The results indicated that TSC22D4-Akt1 interaction was impaired in WT mice in the presence of hyperglycemia and hyperinsulinemia.

To further analyze TSC22D4-Akt1 interaction *in vivo*, we used db/db mice as a model for type 2 diabetes. Db/db mice lack leptin receptors and the absence of the receptors results in high body weight, reduced glucose tolerance, chronic hyperglycemia, hyperinsulinemia, and elevated levels of serum lipids. In order to test if there are any changes in TSC22D4-Akt1 interaction between WT mice fed with a chow diet and db/db mice fed with a control diet in starved conditions, I analyzed the Akt1 protein levels for endogenous TSC22D4 IP in the liver lysates. As a result, TSC22D4-Akt1 interaction levels were similar between the WT and db/db mice in the respective diet conditions (Fig. 5d).

Lastly, I examined livers from db/db mice in starved and 1-hour refed conditions to test if TSC22D4-Akt1 interaction levels change in the absence or presence of nutrients. Endogenous TSC22D4 IP and Akt1 Western

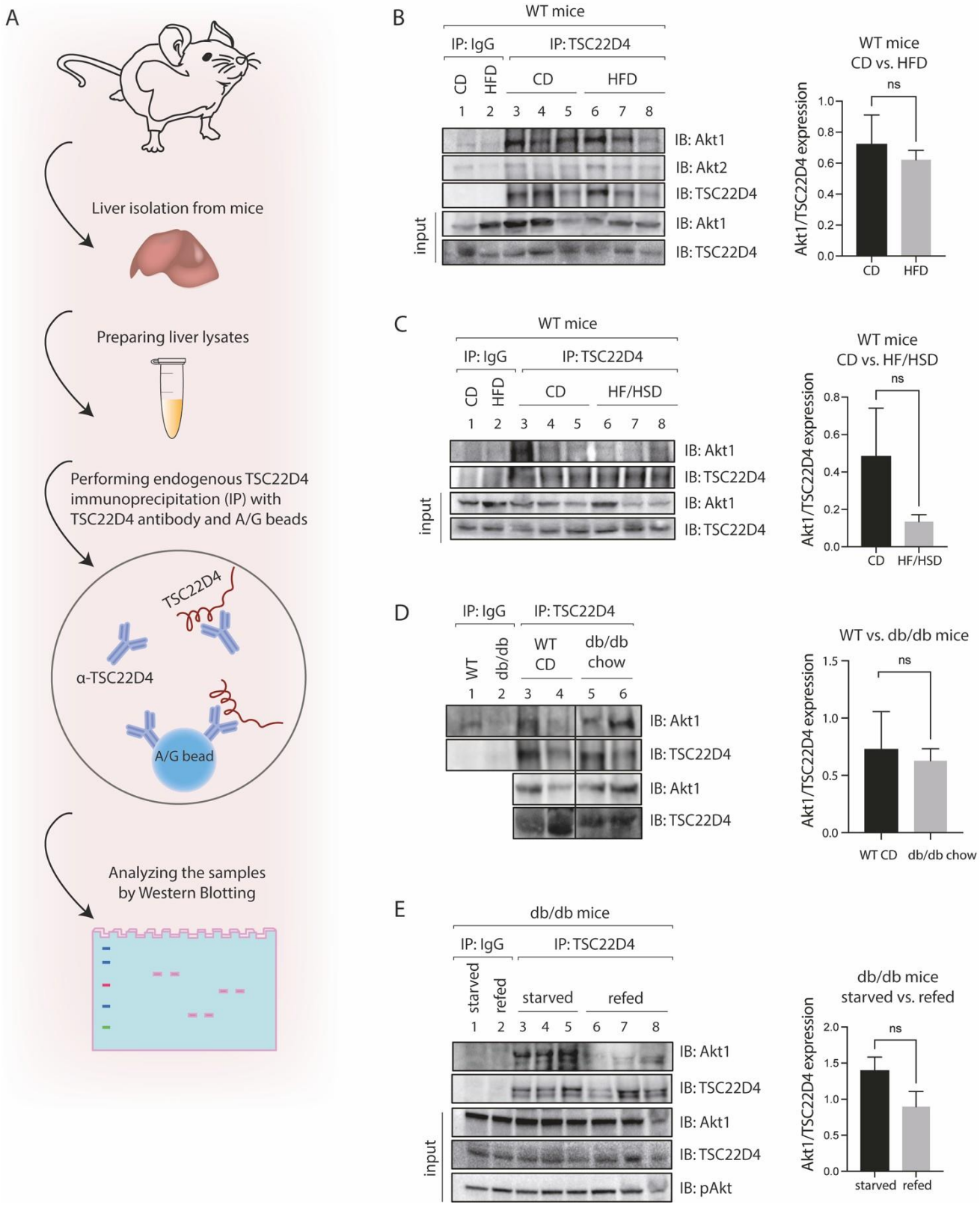

***Figure 5: TSC22D4 interacts with Akt1*.**

A. Isolated liver tissues from WT or db/db mice were lysed in CHAPS buffer by using a Dounce homogenizer. The lysates were incubated with homemade TSC22D4 antibody on a rotating rack at 4°C degrees overnight. Then, the antibody/antigen complex was pulled out using A/G-coupled agarose beads by incubating the mixture on a rotating rack

at 4°C degrees for 2 hours. After incubation, the immunoprecipitates were washed 3 times with CHAPS buffer with centrifugation steps. The immunoprecipitates were added 4x sample loading buffer and boiled at 95°C degrees to be analyzed by Western Blotting. **B.** TSC22D4 was IPed from the WT mice liver lysates fed with a control diet (CD) or high fat diet (HFD). **C.** TSC22D4 was immunoprecipitated (IP: TSC22D4) from WT mice liver lysates fed with a CD or high fat/high sucrose diet (HF/HSD). **D.** TSC22D4 was immunoprecipitated (IP: TSC22D4) from WT and db/db mice liver lysates fed with a CD or chow diet, respectively. **E.** TSC22D4 was immunoprecipitated (IP: TSC22D4) from db/db mice liver lysates fed with a chow diet in starved or refed conditions. **B-E**. The immunoprecipitates and the input liver lysates were immunoblotted (IB) with indicated antibodies. Right panels: Quantification of Akt1 enrichment in TSC22D4 co-IPs normalized to Akt1 levels in the input.

blots showed decreased TSC22D4-Akt1 interaction levels when the mice were refed in db/db mice (Fig. 5e). Therefore, the absence of nutrients promoted the interaction between TSC22D4 and Akt1, while the nutrient availability impaired the interaction, confirming our current publication [59].

Overall, these results indicated that TSC22D4 and Akt1 interact *in vivo*. Furthermore, in different diabetic mouse models which show hyperglycemia and hyperinsulinemia (e.g. WT mice fed with HF/HSD), TSC22D4-Akt1 interaction status changes. In WT mice, the interaction is stronger in the mice fed with CD compared to HF/HSD. For the db/db mice, the interaction is also stronger when the mice were starved. Therefore, TSC22D4 and Akt1 seem to interact more in case of energy depletion in WT and db/db mice [59].

6.2. D2 domain and TSC box are required for Akt1 interaction

TSC22D4 (387 aa, Fig.6a) contains evolutionarily conserved domains in the N-terminus and a TSC box in the C-terminus that contains a leucine zipper motif, which enables TSC22D4 to homodimerize or heterodimerize with the other members of the TSC family [33]. In addition, TSC22D4 has an intrinsically disordered region (IDR) that contains several post-translational modification (PTM) sites, including phosphorylation [61]. IDRs are functional and unique protein regions that play fundamental roles in protein-protein interactions due to their distinct conformational flexibility [62].

To identify the interaction site of TSC22D4-Akt1, we mapped TSC22D4 by creating different deletion mutants to analyze them in co-IP experiments. Several deletion mutants were already created and tested by my supervisor prior to my PhD program. Interestingly, deletion of the conserved regions at the N terminus (ΔRegion-1 (ΔR1, Δ1-20 aa), ΔRegion-2 (ΔR2, Δ70-100 aa) or ΔN-terminus (ΔN, Δ1-100 aa) did not show any less interaction with Akt1 compared to full-length TSC22D4. Therefore, the conserved regions at the N terminus of TSC22D4 might not have a significant role in TSC22D4-Akt1 interaction. Additionally, in the preliminary experiments, the N-terminus deletion of the IDR (ΔDomain 1, ΔD1, Δ105-205 aa) showed similar levels of Akt1 interaction in the co-IP experiments.

To further analyze the interaction site of TSC22D4 to Akt1, I created new mutants by deleting different parts of TSC22D4 (Fig. 6b) via PCR-based site-directed mutagenesis. To test its role in Akt1 interaction, we deleted the C-terminus of the IDR and created ΔDomain 2 (**ΔD2**, Δ206-318 aa) mutant. Additionally, to test if the TSC box, which contains the leucine zipper motif, plays a role in Akt interaction, we created **ΔTSC** (Δ319-378 aa) mutant (Fig. 6b). I co-transfected Hepa1-6 cells with HA-Akt1 with either Flag-WT-TSC22D4, ΔD2 mutant or ΔTSC mutant. I pulled down HA-Akt1 with anti-HA conjugated agarose beads and analyzed Flag levels in the IPs with Flag antibody by Western Blotting (Fig. 6c). For further validation, I performed a parallel set of experiments and did a reciprocal co-IP assay where I pulled down Flag antibody and analyzed the HA-Akt1 levels in the IPs for ΔD2 mutant (Fig. 6d). As a result, ΔD2 and ΔTSC mutants significantly blunted Akt1 interaction compared to WT-TSC22D4 overexpressing cells. Therefore, we identified the D2 domain and

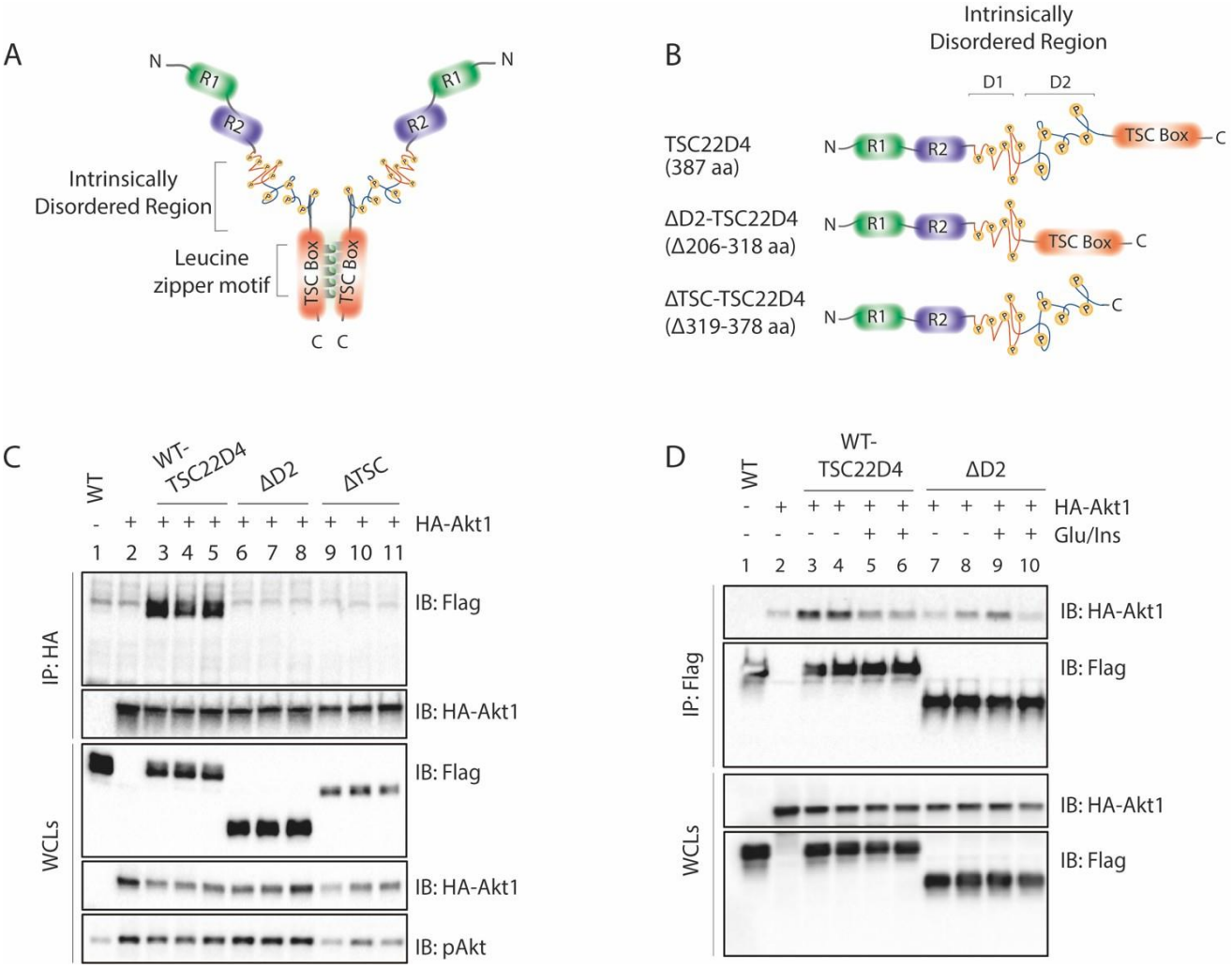

Figure 6: D2 and TSC domains are required for Akt1 interaction.

A. Illustration of TSC22D4 protein with evolutionarily conserved domains. **B..** Illustration of full-length TSC22D4, ΔD2 and ΔTSC mutants. **C.** Hepa1-6 cells were transiently co-transfected with Flag-TSC22D4-WT (2,5 µg), -ΔD2 (2,5 µg) or -ΔTSC (2,5 µg) deletion mutants and HA-Akt1 (2,5 µg). 48 hours post-transfection, HA-Akt1 was immunoprecipitated with anti-HA antibody (IP: HA) and the IPs and WCLs were immunoblotted (IB) with indicated antibodies. **D.** Hepa1-6 cells were transiently co-transfected with Flag-TSC22D4-WT (2,5 µg) or -ΔD2 (2,5 µg) and HA-Akt1 (2,5 µg) in the absence or presence of glucose [20 µM] and insulin [100 nM] upon overnight starvation. The immunoprecipitates (IP: Flag) and WCLs were immunoblotted (IB) with indicated antibodies**.**

TSC Box as the domains required for Akt1 interaction.

6.3. TSC22D1 and TSC22D3 interact with Akt1

All TSC22 family proteins (TSC22D1, TSC22D2, TSC22D3 and TSC22D4) share a conserved TSC box containing a leucine zipper motif [33], [37] (Fig. 7a). Since deletion of TSC Box in TSC22D4 caused impaired Akt1 interaction, we tested if other TSC22 family members could also interact with Akt1. I transiently co-transfected Hepa1-6 cells with HA-Akt1 with either Flag-TSC22D4, Flag-TSC22D1 or Flag-TSC22D3 (Fig. 7b). Flag IP results indicated that not only TSC22D4 (lanes 4-6) but also TSC22D1 (lanes 7-9) and TSC22D3 (lanes 10-12) interact with Akt1, even stronger than TSC22D4. In parallel, pAkt levels significantly decreased in TSC22D1 and TSC22D3 expressing cells compared to TSC22D4 in the cell lysates (Fig. 7b, lower right panel).

6.4. TSC22D4 homodimerizes with TSC22D1 and TSC22D3

Furthermore, we explored if TSC22D4 heterodimerizes with other TSC22 family members TSC22D1 and TSC22D3 in Hepa1-6 cells, since the dimerization of TSC22D4 might modulate Akt interaction and function. I co-transfected Hepa1-6 cells with Myc-TSC22D4 with either Flag-TSC22D1, Flag-TSC22D3 or Flag-TSC22D4 to compare homodimerization or heterodimerization levels of TSC22D4 with other TSC22 family members (Fig. 7c). Myc levels in the IPs showed that TSC22D4 homodimerizes with itself (lanes 6-8) and heterodimerizes with TSC22D1 (lanes 9-11) and TSC22D3 (lanes 12-14). Notably, heterodimerization of TSC22D4 with TSC22D1 was significantly stronger than with TSC22D3 as well as its homodimerization with itself (Fig. 7c, lower panel).

6.5. TSC Box but not the D2 domain is required for TSC22D4 homodimerization

Since the TSC box is required for both homodimerization and heterodimerization for TSC22 family proteins in previous studies, we tested if the D2 domain, which is required for Akt1 interaction, is also necessary for TSC22D4 homodimerization. I transiently co-transfected Hepa1-6 cells with Myc-tagged WT-TSC22D4 together with either Flag-WT-TSC22D4, Flag-ΔD2 or Flag-ΔTSC mutants to compare homodimerization levels of the mutants. I performed Flag IP and analyzed WT-TSC22D4 levels using the Myc antibody (Fig. 7d). While WT-TSC22D4 homodimerizes with Myc-WT-TSC22D4 (lanes 6-8), ΔD2 mutant (lanes 9-11) showed less homodimerization levels compared to WT-TSC22D4. On the other hand, ΔTSC mutant failed to homodimerize with WT-TSC22D4 completely (lanes 12-14). Therefore, we concluded that TSC Box is required for homodimerization of TSC22D4, whereas the D2 domain is not.

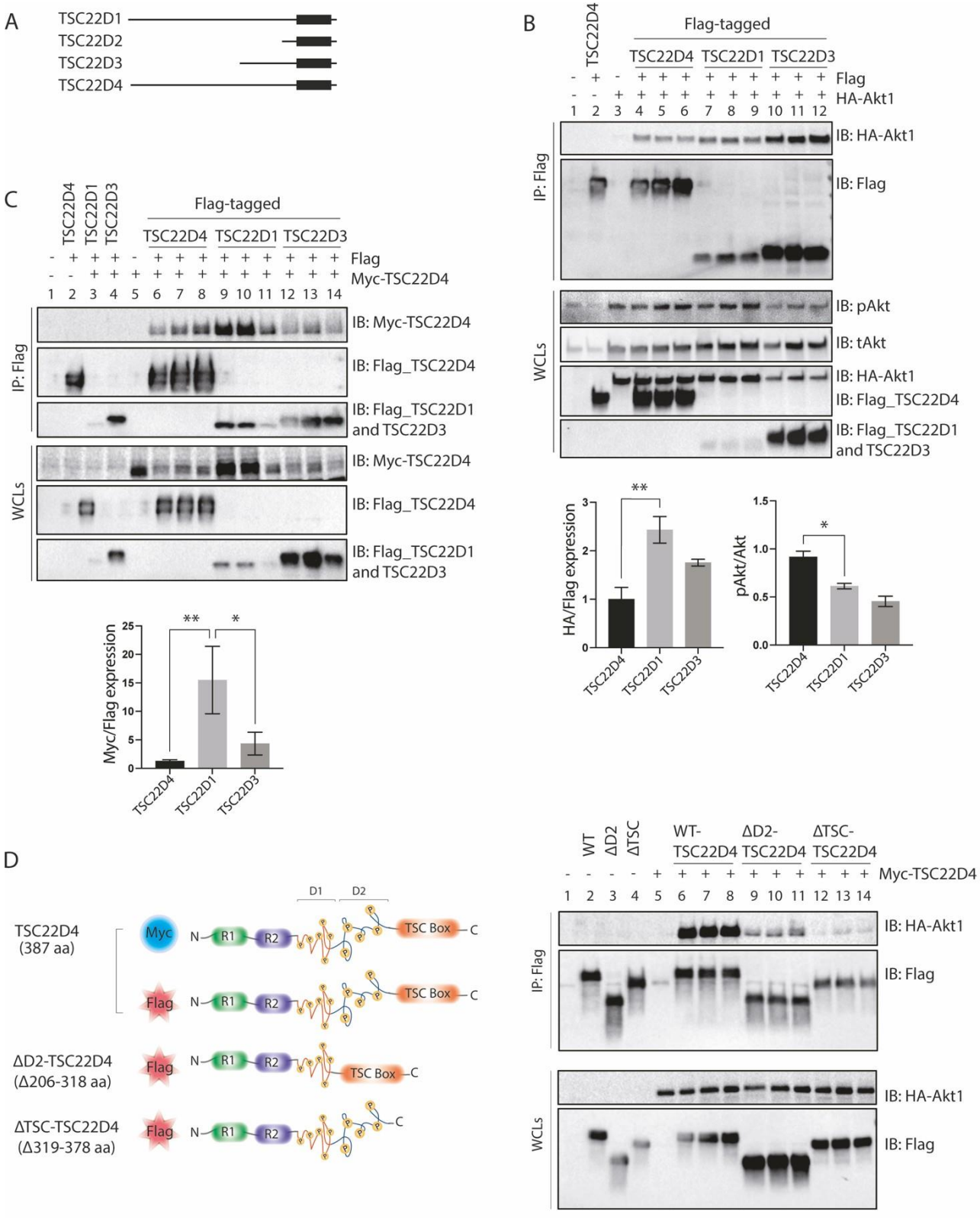

Figure 7: Analyses of TSC22 family members.

A. Illustration of TSC22 family members. **B.** Hepa1-6 cells were transiently co-transfected with Flag-TSC22D4 (2,5 µg), -TSC22D1 (4 µg) or -TSC22D3 (4 µg) and HA-Akt1 (2,5 µg). Lower panel: Quantification of HA-Akt1 enrichment in immunoprecipitates (IP: Flag) and quantification of pAkt levels in whole cell lysates (WCLs) normalized to the tAkt levels. **C.** Hepa1-6 cells were transiently co-transfected with Flag-TSC22D4 (2,5 µg), -TSC22D1 (4 µg) or -TSC22D3 (4 µg) and Myc-

WT-TSC22D4 (2,5 µg). Lower panel: Quantification of Myc-WT-TSC22D4 enrichment in Flag co-IPs normalized to the Flag levels. **D.** Hepa1-6 cells were transiently co-transfected with Flag-TSC22D4 (2,5 µg), ΔD2 (2,5 µg) or -ΔTSC (2,5 µg) deletion mutants and Myc-WT-TSC22D4 (2,5 µg). **B-D**. 48 hours post-transfection, Flag was immunoprecipitated (IP: Flag) with anti-Flag affinity gel and the IPs and whole cell lysates (WCLs) were immunoblotted (IB) with indicated antibodies.

6.6. D2+TSC interacts with Akt1 as strong as WT-TSC22D4

To understand whether the D2 domain and TSC box are sufficient to interact with Akt1, I designed primers to generate the cDNA that contains D2 domain together with the TSC box (**D2+TSC**, 206-378 aa) (Fig. 8a). I performed a co-transfection assay on Hepa1-6 cells using HA-Akt1 with either Flag-WT-TSC22D4,Flag-ΔD2-TSC22D4 or Flag-D2+TSC. After performing Flag IP with the cell lysates, I analyzed HA-Akt1 levels byWestern Blotting (Fig. 8b-c). Interestingly, the D2+TSC construct showed strong interaction with HA-Akt1 indicating D2 domain, together with the TSC box, is sufficient for Akt1 interaction. Additionally, I analyzed D2+TSC construct in starved (Fig. 8b, lanes 11-14, Fig. 8c, lanes 7-8) and glucose/insulin stimulated conditions (Fig. 8c, lanes 9-10). As observed before, WT-TSC22D4-Akt1 interaction was impaired in nutrient availability compared to starved conditions (Fig. 8c, lanes 5-6). On the other hand, D2+TSC-Akt1 interaction remained the same in basal and glucose/insulin stimulated conditions (Fig. 8c, lanes 7-10). Therefore, D2+TSC seems to interact with Akt1 constitutively and independent of metabolic stimulations. ΔD2 mutant, on the other hand,again failed to interact with Akt1 (Fig. 8b, lanes 7-10).

6.7. D2 domain is sufficient for Akt interaction, whereas TSC Box is not

Having shown that ΔD2 mutant and ΔTSC mutant fail to interact with Akt1, TSC Box is required for protein dimerization, and D2+TSC constitutively interacts with Akt1, we tested if D2 domain alone or TSC box alone would be sufficient for Akt interaction. Thus, we decided to shorten D2+TSC by designing primers to create the **D2 domain alone** (201-318 aa) and **TSC box alone** (318-380 aa) to determine which part of D2+TSC is sufficient for Akt interaction (Fig. 9a). I co-transfected Hepa1-6 cells with Flag-D2 or Flag-TSC Box together with HA-Akt1 (Fig. 9b). In the Flag IPs, the presence of only D2 domain was sufficient to interact with Akt1 (lanes 6-9), whereas only TSC Box failed to interact with Akt1 (lanes 10-13). Therefore, I was able to map our protein TSC22D4 successfully and narrowed down the peptide fragments to understand their roles in detail. While the D2 domain is required and sufficient for Akt1 interaction, TSC Box is not sufficient for Akt1 interaction. Instead, TSC Box is needed for protein dimerization. Furthermore, I analyzed pAkt levels and phosphorylation status of downstream targets of Akt in FBS starved and insulin-stimulated conditions in cells that were expressing Flag-D2 or Flag-TSC. (Fig. 9b, right panel). Notably, basal pAkt levels decreased in both D2 and TSC expressing cells compared to vector control. In addition, pAkt levels significantly increased in the D2 domain and TSC box expressing cells upon insulin stimulation compared to basal conditions. As one of the downstream targets, pS6K1 levels were significantly increased in insulin-stimulated TSC Box expressing cells compared to vector control and only D2 domain. pGSK3β, pFoxo1 and pS6 levels remained the same.

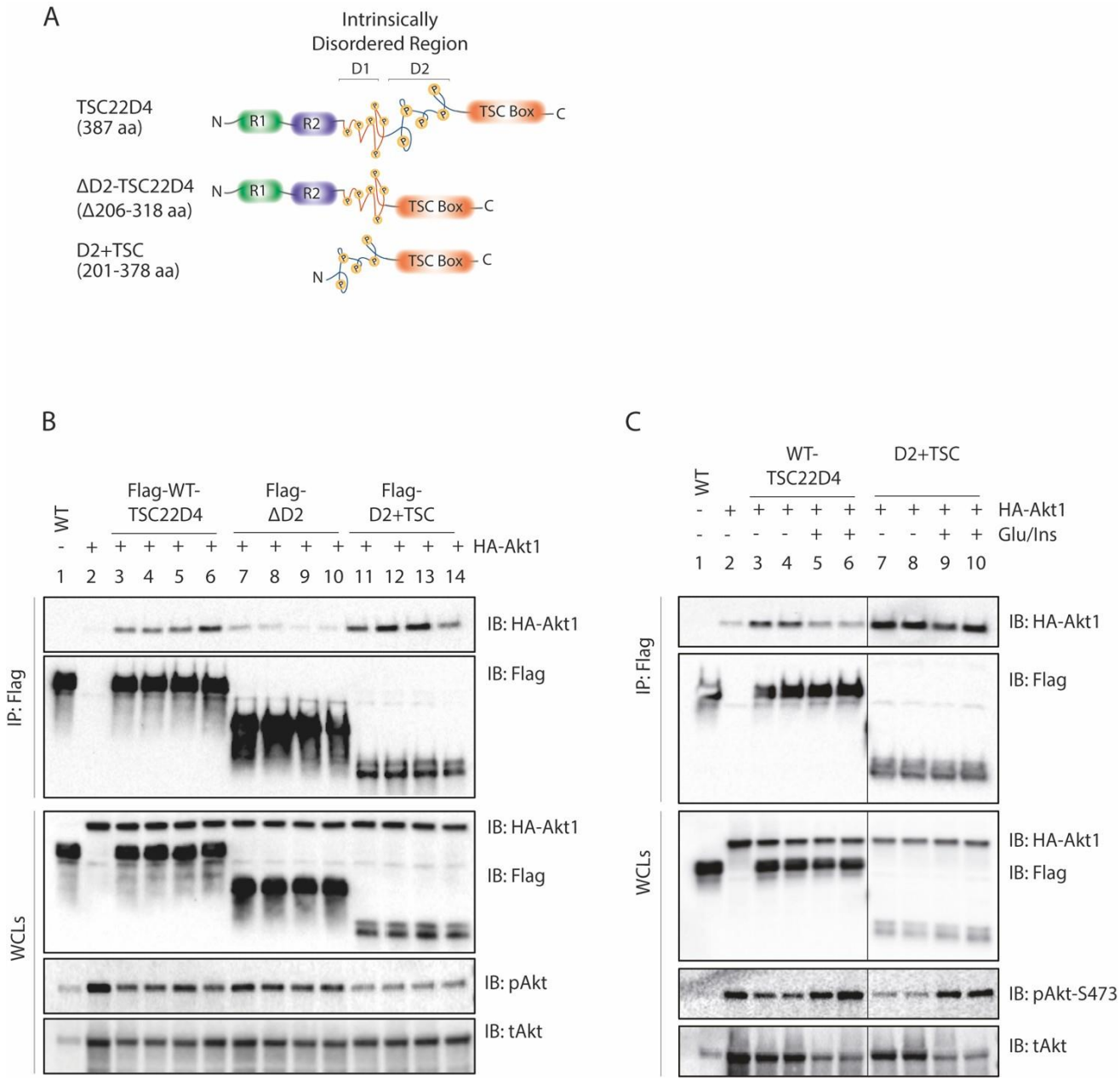

Figure 8: D2+TSC is sufficient for Akt1 interaction.

A. Illustration of full-length TSC22D4, ΔD2 and D2+TSC mutants. **B**. Hepa1-6 cells were transiently co-transfected with Flag-TSC22D4-WT (2,5 µg), -ΔD2 (2,5 µg) or D2+TSC (2,5 µg) and HA-Akt1(2,5 µg). **C.** Hepa1-6 cells were transiently co-transfected with Flag-TSC22D4-WT (2,5 µg) or D2+TSC (2,5 µg) and HA-Akt1 (2,5 µg) in the absence or presence of glucose [20 µM] and insulin [100 nM] upon overnight starvation. **B-C**. Flag was immunoprecipitated with anti-Flag affinity gel (IP: Flag) and the IPs and whole cell lysates (WCLs) were immunoblotted (IB) with indicated antibodies.

6.8. D2-ΔC is sufficient to interact with Akt1

Next, we aimed to shorten the interaction site, D2, as much as possible to test the small peptide *in vivo* for future translational studies [63]. TSC22D4 has 15 novel phosphorylation sites, identified by tandem mass spectrometry [61], of which 6 of them are found in the D2 domain of TSC22D4. Since the presence of these phosphorylation sites causes flexibility to the IDPs for establishing unique conformational structures, we hypothesized that the D2 domain might serve translational potential as a small peptide drug interfering with the TSC22D4-Akt1 interaction and inhibiting insulin resistance.

Although the D2 domain is a part of the intrinsically disordered region of TSC22D4 and does not have a defined 3D structure, we identified 6 aa length (TPPLSR, 223-228 aa) stabilizing motif followed by a 12 aa length alpha helix (RDGAVRLRMELV, 230 241 aa) at the N terminus of D2 peptide [29]. Additionally, via in silico analysis, we identified another peptide sequence prone to forming alpha-helix structure (GAAAAQSLSLARSMLAIS) at the C terminus of the D2 peptide (Fig. 9c). To begin with, we decided to divide D2 sequence into two parts and designed custom primers to create Flag-tagged **D2-ΔN** (266-318 aa) and **D2-ΔC** (201-265 aa) peptides (Fig. 9d). Therefore, we tested if the stabilizing motif or alpha helix structures regulate Akt function by performing co-IP assays. D2-ΔN peptide, which does not contain the stabilization motif but contains the alpha-helix structure, was not expressed in Hepa1-6 cells, and excluded from the candidate. On the other hand, when I analyzed D2-ΔC peptide expressing cells for pAkt levels in the whole cell lysates (WCLs), I observed that basal pAkt levels decreased compared to vector control (Fig. 9e). Also, pAkt levels increased in D2-ΔC expressing cells in insulin-stimulated conditions (lanes 13-14). Furthermore, D2-ΔC peptide showed the same interaction levels of Akt1 with the D2 peptide itself in the IPs (Fig. 9e, right panel). Since the D2-ΔC peptide contains a stabilization motif followed by a small alpha-helix structure, those secondary structures might be the specific regions required for Akt interaction.

To evaluate further and specify the required TSC22D4-Akt1 interaction site, I created smaller D2-ΔC peptides: **D2-ΔC-ΔN1** (223-265 aa), **D2-ΔC-ΔN2** (229-265 aa) and **D2-ΔC-ΔC** (201-241 aa) (Fig. 9d). We aimed to shorten the D2-ΔC peptide more from the N terminus (D2-ΔC-ΔN1 and -ΔN2) and C terminus (D2-ΔC-ΔC) to identify the smallest region sufficient for Akt1 interaction. D2-ΔC-ΔN1 contains the stabilization motif (TPPLSR, 223-228 aa) followed by a helix, whereas D2-ΔC-ΔN2 lacks the stabilization motif and contains only the helical structure. Therefore, by creating 2 different -ΔN mutants, we investigated if the stabilization motif plays a role in Akt1 interaction. Also, by using the D2-ΔC-ΔC peptide in the co-IP assays, we aimed to validate the required peptide region in the D2 domain. I performed co-IP assays by co-transfecting Flag-tagged small peptides and HA-Akt1 in Hepa1-6 cells. Flag-tagged mutants had expression problems at the protein level, possibly due to a lack of stabilization caused by their size. Thus, I could not assess their interaction levels with Akt1.

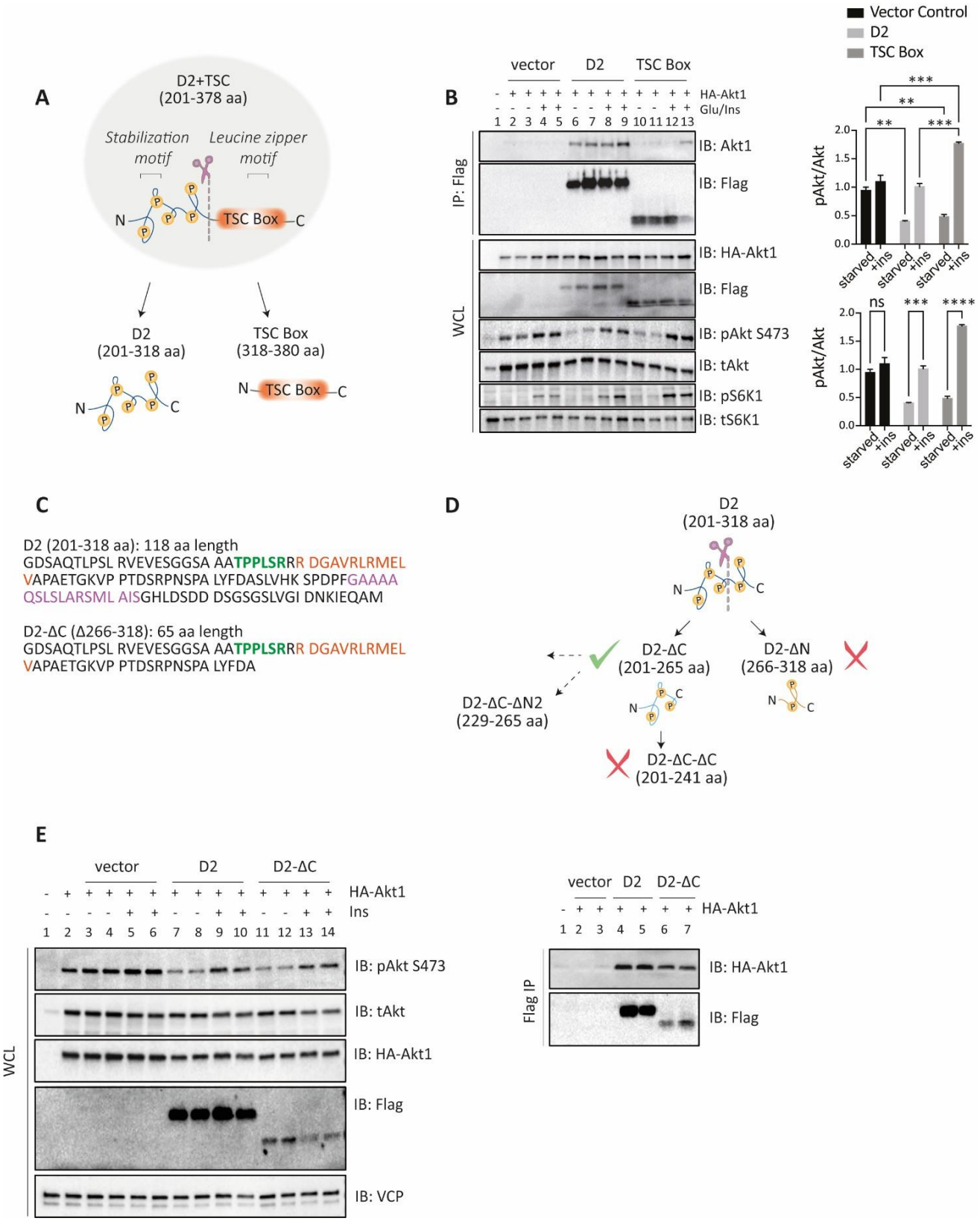

Figure 9: TSC22D4-D2 domain is sufficient for Akt1 interaction.

A. Illustration of D2+TSC, only D2 and only TSC Box deletion mutants. **B**. Hepa1-6 cells were transiently co-transfected with Flag-D2 (2,5 µg), -TSC (2,5 µg) and HA-Akt1(2,5 µg) in the absence or presence of glucose [20 µM] and insulin [100 nM] upon overnight starvation. **C.** Peptide sequence of D2 and D2-ΔC mutants. Green: stabilization motif, red and purple:

alpha helices. **D.** Illustration of D2 and D2 truncated deletion mutants. **E.** Hepa1-6 cells were transiently co-transfected with Flag-D2 (2,5 µg), -D2-ΔC (2,5 µg) and HA-Akt1(2,5 µg) in the absence or presence of glucose [20 µM] and insulin [100 nM] upon overnight starvation. **B, E**. Flag was immunoprecipitated with anti-Flag affinity gel (IP: Flag) and the IPs and whole cell lysates (WCLs) were immunoblotted (IB) with indicated antibodies.

6.9. TSC22D4 localizes in the cytoplasm in Hepa1-6 cells

Since TSC22D4 localizes both in the nucleus and cytoplasm in different cell types [43, 44], we explored the subcellular localization of TSC22D4 in Hepa1-6 cells and mouse liver sections by immunofluorescence (IF). In order to optimize commercial and our homemade α-TSC22D4 antibodies, I first started the analysis with Hepa1-6 cells.

Initially, I performed a co-staining of Hepa1-6 cells with a commercial TSC22D4 antibody and GAPDH as a housekeeping protein (Fig. 10a). While TSC22D4 localization was both in the cytoplasm and nucleus, GAPDH staining was only localized in the cytoplasm.

To test the specificity of our homemade TSC22D4 antibody, I transiently knocked down TSC22D4 in Hepa1-6 cells by using siRNA targeting TSC22D4. I stained the cells with our homemade α-TSC22D4 antibody (Fig. 10b). In the control cells transfected with scrambled control siRNA (siNC), I detected TSC22D4 signals in the nucleus and cytoplasm. In the TSC22D4 knockdown cells, the cytoplasmic signal was mostly lost and the nuclear signal remained the same. Also, the nucleus in the TSC22D4 knockdown cells seemed to be bigger compared to siNC cells. I quantified TSC22D4 signal intensity by choosing the area of each cell for both siNC and siTSC22D4 (Fig. 10c). As a result, the TSC22D4 signal was decreased by around 50% in siTSC22D4 compared to siNC cells. Additionally, I conducted quantitative PCR (qPCR) analysis of the parallel set of cells from the same experiment to analyze the relative mRNA expression. As shown in Fig. 10d, siTSC22D4 cells expressed ~50% less TSC22D4 than siNC. In summary, qPCR data supported the IF quantification results and our homemade TSC22D4 antibody is specific to cytoplasmic TSC22D4. Interestingly, the staining in the nucleus did not disappear after siRNA transfection. This might be due to relatively low knockdown efficiency or nonspecific binding of the antibody to a nuclear protein.

To test if we could observe the TSC22D4-Akt1 co-localization by IF, I overexpressed Flag-TSC22D4 and HA-Akt1 in Hepa1-6 cells and stained them with commercial α-Flag and α-HA immunofluorescent antibodies (Fig. 11a). While some cells were efficiently transfected both with Flag-TSC22D4 and HA-Akt1, others were transfected either with Flag-TSC22D4 or HA-Akt1. Consequently, TSC22D4 expression was visible in the cytoplasm, whereas we could detect Akt1 expression both in the nucleus and cytoplasm.

Overexpression of WT-TSC22D4 or D2+TSC does not change Akt1 localization

As shown in Fig. 8c, while WT-TSC22D4 strongly interacts with Akt1 upon starvation as opposed to the glucose/insulin stimulation, D2+TSC constitutively interacts with Akt1 independent of nutrient availability. Therefore, we tested if Akt1 localization differs when we overexpress WT-TSC22D4 vs. D2+TSC allele. To this end, I overexpressed Flag-WT-TSC22D4 or Flag-D2+TSC in Hepa1-6 cells and stained the cells with α-Flag and α-Akt1 immunofluorescent antibodies. We specifically focused on staining endogenous Akt1 to avoid

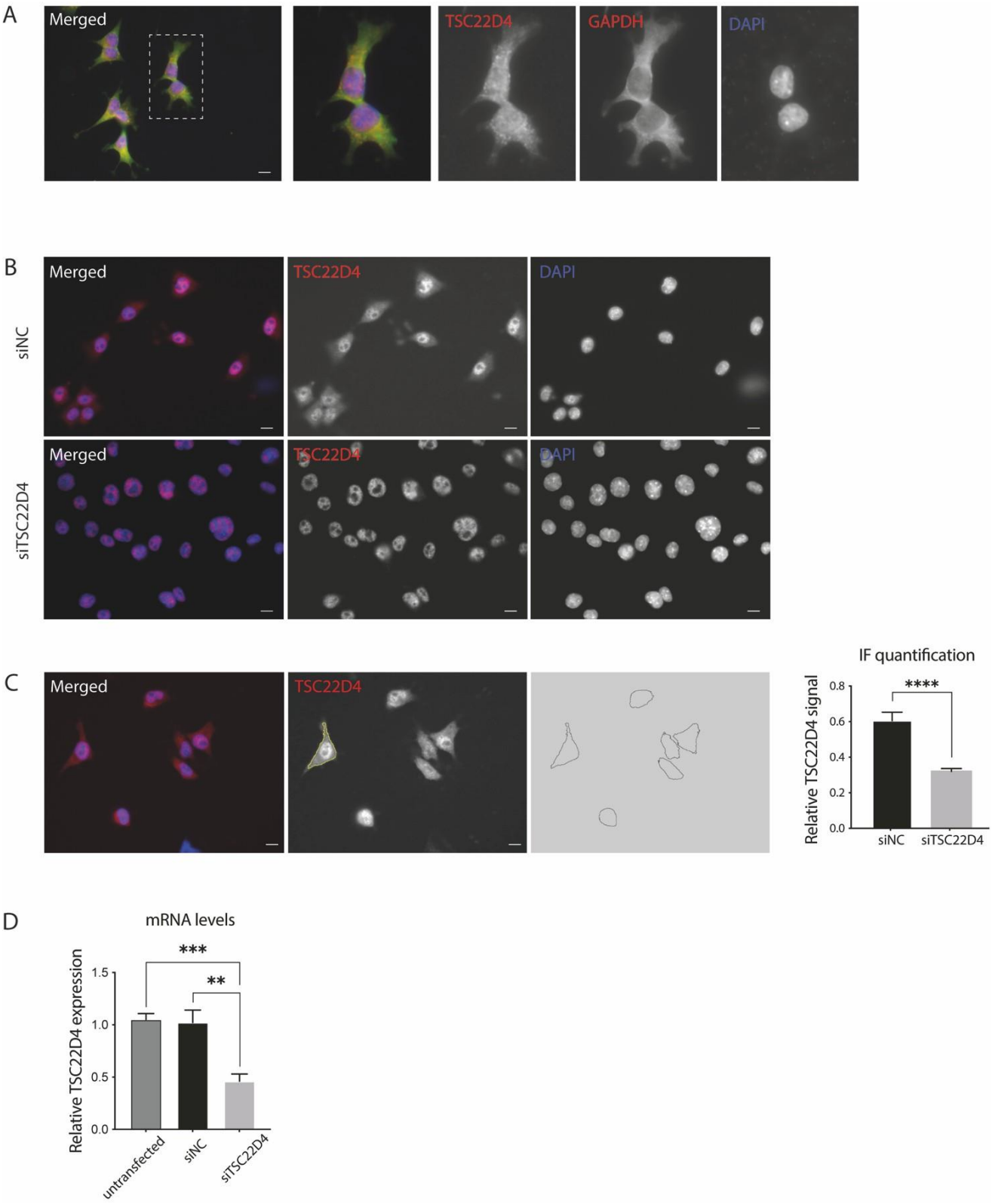

Figure 10: TSC22D4 localizes in the cytoplasm.

A. Untransfected Hepa1-6 cells were grown on chamber slides. The cells were fixed, permeabilized, blocked and stained with anti-TSC22D4 and anti-GAPDH antibodies. Alexa Fluor 488 (anti-GAPDH, green) or Alexa Fluor 568 (anti-TSC22D4, red) were used as secondary antibodies. A mounting medium with DAPI was used to detect the nucleus (blue). Zeiss fluorescence microscope with ZEN software was used to capture the images (40x, scale bar: 20 µM). Fiji, Image J was used for analyzing the images. **B**. Hepa1-6 cells, grown on chamber slides, were transfected with either scrambled siRNA

(siNC) or siTSC22D4 by using a Lipofectamine reagent. 48 hours post-transfection, the cells were stained with homemade α-TSC22D4 antibody and Alexa Fluor 568 antibody. **C**. TSC22D4 signal intensity was calculated in siNC or siTSC22D4 transfected Hepa1-6 cells by using Fiji, Image J. Cytoplasmic area was chosen in each cell and average signal intensities were compared. **D**. TSC22D4 mRNA levels of siNC or siTSC22D4 transfected cells were measured by quantitative real-time PCR (qRT-PCR) analysis.

inconsistent transfection efficiency of HA-Akt1 overexpression in the cells. As a result, endogenous Akt1 expression was detected both in the cytoplasm and nucleus when the cells were overexpressed either with WT-TSC22D4 or D2+TSC allele (Fig. 11b), indicating the subcellular localization of Akt1 does not change upon WT-TSC22D4 or D2+TSC overexpression.

TSC22D4 or Akt1 localization does not change upon anabolic stimuli

TSC22D4-Akt1 interaction is impaired in the presence of nutrients (Fig. 6e, Fig. 8c) and it strengthens upon mitochondrial inhibition with rotenone and antimycin treatment [59]. Since particular anabolic stimuli modulate TSC22D4-Akt1 interaction, we examined if the subcellular localization of TSC22D4 or Akt1 changes upon glucose [20 µM]/insulin [100 nM] or rotenone [1 µM]/antimycin [1 µM] treatments. To this end, I overexpressed Flag-TSC22D4 in Hepa 1-6 cells and stained them in starved or in glucose/insulin or rotenone/antimycin treated conditions (Fig. 11c, left panel). To test the subcellular localization of Akt1 in different conditions, I used untransfected Hepa 1-6 cells and stained the cells for endogenous Akt1 (Fig. 11c, right panel). Consequently, Flag-TSC22D4 expression remained the same as in the cytoplasm when the cells were starved or stimulated. Endogenous Akt1 expression, on the other hand, was mostly around the nucleus in starved, glucose/insulin or rotenone/antimycin stimulations (Fig. 8c).

Interestingly, when we overexpress the cells either with Flag-tagged TSC22D4 alleles or empty vector control, we observed endogenous Akt1 expression both in the nucleus and cytoplasm (Fig. 11b). On the other hand, we detected Akt1 expression only around the nucleus when the cells were not transfected (Fig. 11c). Therefore, the subcellular localization of endogenous Akt1 might change upon the presence of ectopic expression vectors in the Hepa1-6 cells.

PLA shows TSC22D4-Akt1 interaction in Hepa1-6 cells

After optimizing the working conditions of homemade and commercial TSC22D4 antibodies on Hepa1-6 cells, I performed a proximity ligation assay (PLA). PLA is an effective method that allows *in situ* detection of protein-protein interactions with high sensitivity. I observed discrete spots on Hepa1-6 cells, indicating TSC22D4-Akt1 interaction (Fig. 11d). Next, I used liver sections of hepatocyte-specific TSC22D4 KO mice and WT mice for analyzing the TSC22D4-Akt1 interaction by PLA. The staining protocol on liver sections did not work as successfully as in Hepa1-6 cells due to non-specific signals.

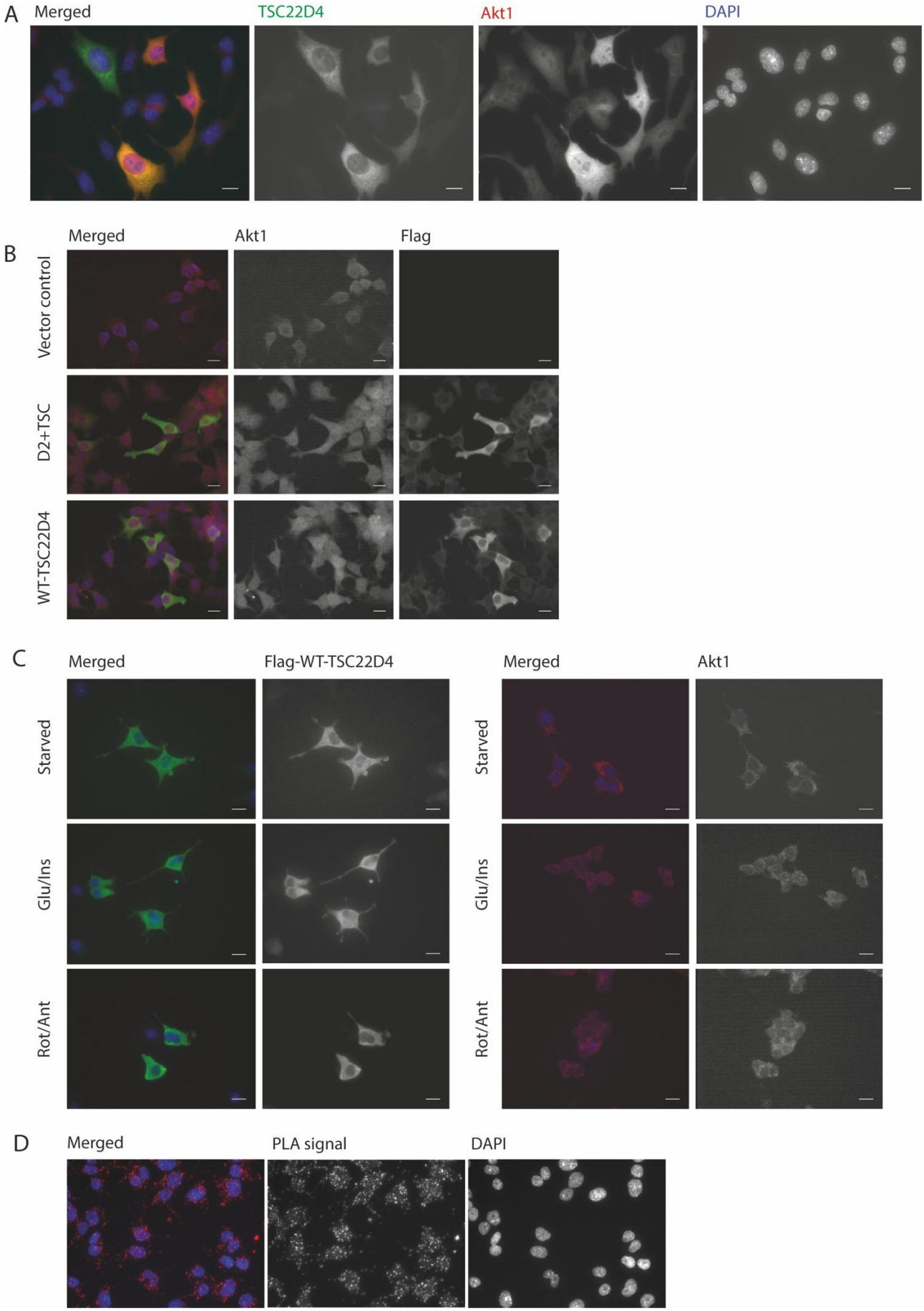
A
Merged
TSC22D4
Akt1
DAPI
B
Merged
Akt1
Flag
Vector control
D2+TSC
WT-TSC22D4
C
Merged
Flag-WT-TSC22D4
Merged
Akt1
Starved
Glu/Ins
Rot/Ant
Starved
Glu/Ins
Rot/Ant
D
Merged
PLA signal
DAPI

Figure 11: Subcellular localization of TSC22D4 and Akt1.

A. Hepa1-6 cells, grown on chamber slides, were co-transfected with Flag-TSC22D4 and HA-Akt1. 36 hours post-transfection, the cells were starved overnight. The cells were fixed, permeabilized, blocked and stained with anti-Flag and anti-HA antibodies. Alexa Fluor 488 (anti-Flag, green) or Alexa Fluor 568 (anti-HA, red) were used as secondary antibodies. A mounting medium with DAPI was used to detect the nucleus (blue). Zeiss fluorescence microscope with ZEN software was used to capture the images (40x, scale bar: 20 µM). Fiji, Image J was used for analyzing the images. **B**. Hepa1-6 cells were transiently transfected with vector control, Flag-WT-TSC22D4 or Flag-D2+TSC. 36 hours post-transfection, the cells were starved overnight and stained with anti-Akt1 antibody. **C**. Hepa1-6 cells, untransfected or transfected with Flag-WT-TSC22D4, were stained with anti-Flag (left) or anti-Akt1 (right) and analyzed in starved, glucose [20 µM]/insulin [100 nM] or rotenone [1 µM]/antimycin [1 µM] treated conditions. **D.** Proximity ligation assay performed for TSC22D4-Akt1 proximity in overnight starved Hepa1-6 cells.

6.10. Animal experiments

After identifying TSC22D4 as an Akt1 binding protein, we aimed to understand the function of TSC22D4-Akt1 interaction. To this end, we generated Adenoviruses (AV) and Adeno-associated viruses (AAV) expressing **WT-TSC22D4**, **ΔD2-TSC22D4**, **D2+TSC** and empty vector as a negative control to employ in functional assays in primary hepatocytes and in mice, respectively, as described below:

→ *in vitro:* Overexpression of AVs expressing TSC22D4 alleles in primary mouse hepatocytes isolated from hepatocyte-specific TCS22D4 KO (TSC22D4$^{hep-/-}$) mice

→ *in vivo*: Overexpression of hepatocyte targeted AAVs of TSC22D4 alleles into TSC22D4$^{hep-/-}$ mice

11.1.1. In vitro analyses: Primary hepatocytes experiments

TSC22D4 regulates Akt function

TSC22D4 deficiency enhances Akt function in primary hepatocytes. Additionally, acute hepatic knockdown of TSC22D4 in WT mice with AAVs expressing miRNA-TSC22D4 improved Akt function [52]. Based on these results, our lab established hepatocyte-specific TSC22D4 KO (TSC22D4$^{hep-/-}$) mice by crossing Albumin-cre mice to the *Tsc22d4* floxed/floxed mice [54] as a working model to understand the hepatocyte- specific role of TSC22D4 in mice.

We investigated if TSC22D4-Akt interaction regulates insulin-induced Akt phosphorylation in primary hepatocytes isolated from WT mice vs. TSC22D4$^{hep-/-}$ mice in starved and glucose/insulin-stimulated conditions. I examined the phosphorylation status of Akt and its downstream targets by Western blotting (Fig. 12a). As a result, pAkt, pFoxo1, pGSK3β and pS6K1 levels increased in TSC22D4 KO cells compared to WT cells, especially in glucose/insulin-stimulated conditions in agreement with our previous study [52]. Therefore,we confirmed that TSC22D4 downregulates insulin signaling cascade via interfering with Akt function in hepatocytes.

TSC22D4-Akt1 interaction regulates Akt function

To understand the function of TSC22D4-Akt1 interaction, I overexpressed TSC22D4 mutants in primary hepatocytes isolated from TSC22D4$^{hep-/-}$ mice and transduced the cells with AVs expressing empty vector control, WT-TSC22D4, ΔD2-TSC22D4 and D2+TSC. I analyzed the phosphorylation status of Akt and its effectors in starved or glucose [20 μM] and insulin [100 nM] stimulated conditions. As a result, basal pAkt levels were lower in cells expressing ΔD2 and D2+TSC mutants under starvation (Fig. 12b). Additionally, basal phosphorylation of FoxO1, GSK3β and S6 levels were lower in D2+TSC expressing starved cells. The phosphorylation levels of Akt and its effectors were similar for the primary hepatocytes stimulated with glucose/insulin in each group.

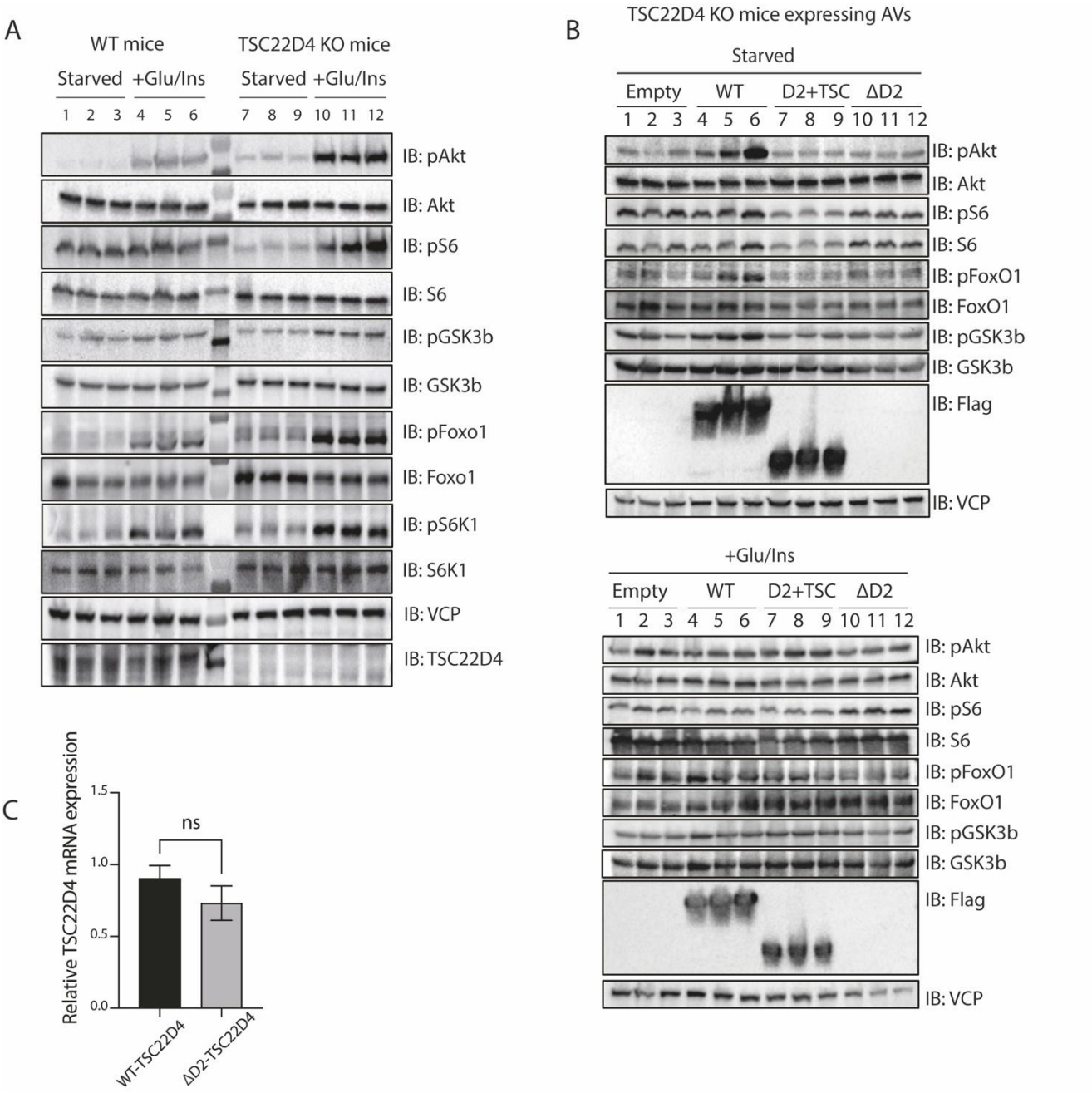

***Figure 12: TSC22D4-Akt1 interaction controls Akt signaling*.**

A. Primary hepatocytes from WT and hepatocyte-specific TSC22D4 KO mice (TSC22D4$^{hep-/-}$) were isolated. **B.** Primary hepatocytes from TSC22D4$^{hep-/-}$ mice were isolated and transduced with AVs expressing vector control or TSC22D4 alleles. **A-B**. After 36 hours, the cells were starved overnight, and the next day, stimulated without or with glucose [20 µM] and insulin [100 nM]. Cell lysates were immunoblotted (IB) with the indicated antibodies. **C**. Quantitative RT-PCR (qRT-PCR) analysis of TSC22D4 expression in primary hepatocytes transduced with AV-TSC22D4-WT or -ΔD2.

Interestingly, the ΔD2 mutant was detected at a lower size (~20 kDa) than its expected size (~35 kDa) by Western blotting in primary hepatocytes. Of note, we had previously tested the expression of all our constructs before recombination into adenoviral plasmids and its detections were successful in Hepa1-6 cells. To test if ΔD2 was truncated or not, we designed custom primers for ΔD2-TSC22D4 and confirmed that the ΔD2 mutant is fully expressed at the mRNA level (Fig. 12c). However, since the interaction deficient ΔD2 mutant failed to express at the protein level at the correct molecular weight, we preferred to exclude it in the following primary hepatocyte experiments.

D2+TSC and Akt1 interaction promotes PGC1α expression

Since Akt plays a significant role in suppressing the expression of gluconeogenic genes [64], we tested the effect of TSC22D4-Akt1 interaction in gluconeogenesis using primary hepatocytes from WT control vs. TSC22D4$^{hep-/-}$ mice. I transduced primary hepatocytes isolated from TSC22D4$^{hep-/-}$ mice with AVs expressing TSC22D4 alleles and starved in the absence or presence of forskolin [10 μM] which promotes cyclic adenosine monophosphate (cAMP) production [64]. I analyzed the mRNA expression of the main gluconeogenic genes: peroxisome proliferator-activated receptor gamma coactivator 1-alpha (PGC1α), phosphoenolpyruvate carboxykinase (PCK1) and glucose 6-phosphate (G6P) (Fig. 13a). PGC1α showed higher expression levels in D2+TSC overexpressing TSC22D4$^{hep-/-}$ cells, compared to WT-TSC22D4 and vector control expressing cells. Furthermore, in the presence of an Akt inhibitor (Akti 1/2, [5 μM]), D2+TSC transduced cells expressed significantly more PGC1α than WT-TSC22D4 and vector control, indicating D2+TSC expressing cells regulate PGC1α expression in an Akt dependent manner. PCK1 and G6P expressions also tended to increase upon Akti1/2 treatment compared to only forskolin treated group in D2+TSC expressing cells (Fig. 13a).

Notably, PGC1α, PCK1 and G6P levels were lower in TSC22D4$^{hep-/-}$ cells compared to the WT control cells. Chronic deletion of TSC22D4 in the TSC22D4$^{hep-/-}$ mice might have produced a compensatory mechanism for suppressing gluconeogenesis independent of Akt function.

In addition to the primary cell experiments, I showed that forskolin treatment promoted the TSC22D4-Akt1 interaction in Hepa1-6 cells (Fig. 13b). Further, D2+TSC overexpressing Hepa1-6 cells showed stronger interaction with Akt1 compared to WT-TSC22D4 overexpressing cells upon forskolin induction (Fig. 13c). Thus, the strong interaction of D2+TSC and Akt1 was promoted even more in the presence of forskolin.

D2+TSC might regulate not only glucose metabolism but also other metabolic events

In addition to gluconeogenesis, PGC1α also regulates cellular energy metabolism in the liver [64], [65], [66] during the fasting state by promoting β-oxidation of fatty acids and enhancing mitochondrial biogenesis. Therefore, we investigated if other fatty acid oxidation targets, such as peroxisome proliferator-activated

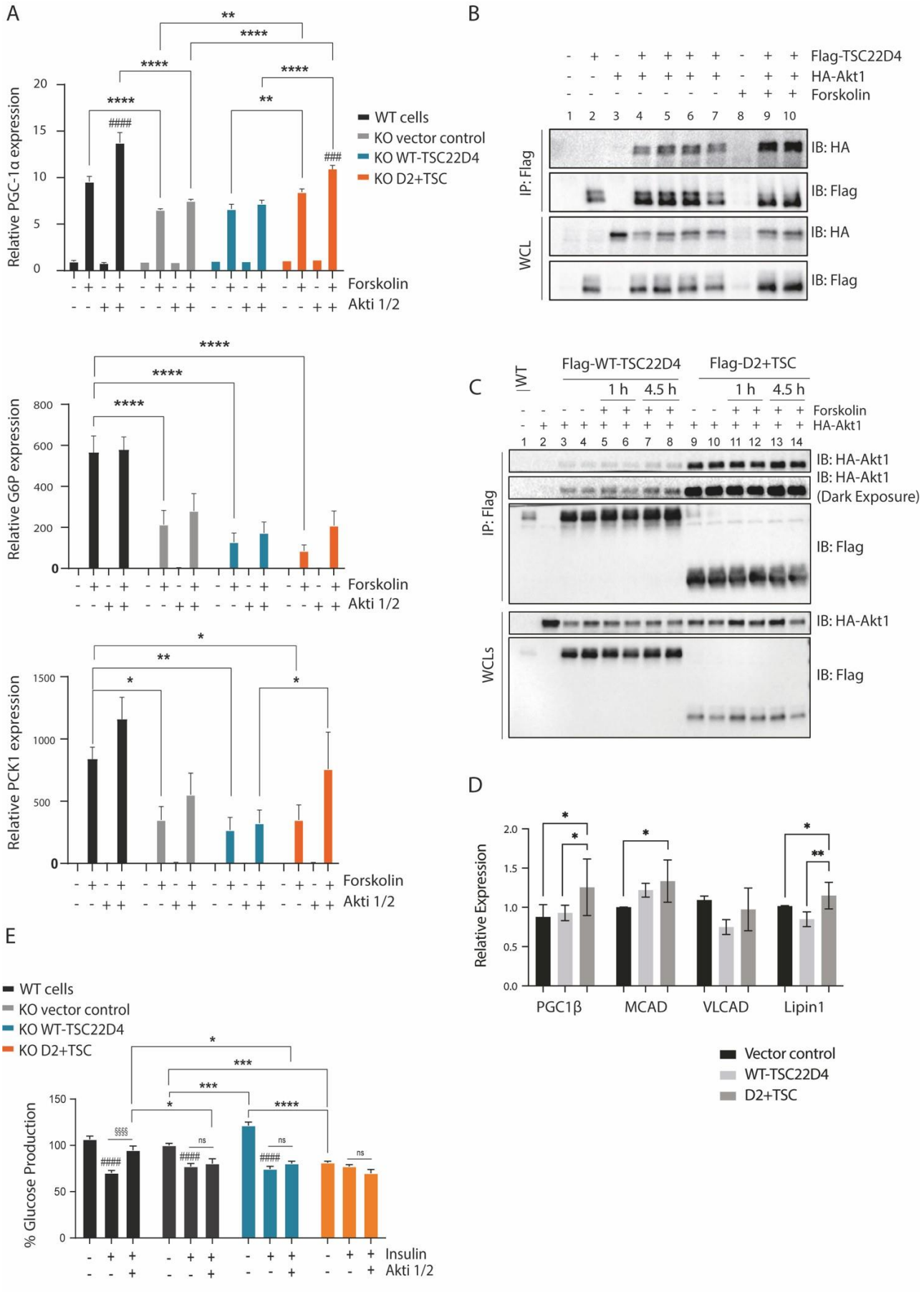
A
Relative PGC-1α expression
WT cells
KO vector control
KO WT-TSC22D4
KO D2+TSC
Forskolin
Akti 1/2
Relative G6P expression
Relative PCK1 expression
B
Flag-TSC22D4
HA-Akt1
Forskolin
IP: Flag
WCL
IB: HA
IB: Flag
C
WT
Flag-WT-TSC22D4
Flag-D2+TSC
1 h
4.5 h
IB: HA-Akt1
(Dark Exposure)
D
Relative Expression
PGC1β
MCAD
VLCAD
Lipin1
Vector control
WT-TSC22D4
D2+TSC
E
% Glucose Production
Insulin

Figure 13: TSC22D4-Akt1 interaction regulates Akt function in primary hepatocytes.

A. Primary hepatocytes from WT or TSC22D4$^{hep-/-}$ mice were isolated. Cells from TSC22D4$^{hep-/-}$ mice were transduced with AVs expressing vector control or TSC22D4 alleles. After 36 hours, the cells were starved overnight followed by forskolin [100 µM] treatment in the presence or absence of Akti 1/2 [5 µM] for 4.5 hours. Cells were collected in Trizol for RNA isolation and gluconeogenic gene expressions were measured by qRT-PCR. **B**. Hepa1-6 cells were co-transfected with Flag-WT-TSC22D4 and HA-Akt1. 36 hours post-transfection, the cells were starved overnight followed by forskolin [100 µM] treatment for 4.5 hours. Flag immunoprecipitates (IP:Flag) and whole cell lysates (WCLs) were immunoblotted (IB) with the indicated antibodies. (Data generated together with Dr. Ekim-Üstünel). **C.** Hepa1-6 cells were co-transfected with Flag-WT-TSC22D4 or Flag-D2+TSC and HA-Akt1. 36 hours post-transfection, the cells were starved overnightfollowed by forskolin [100 µM] treatment for 1 hours or 4.5 hours. Flag immunoprecipitates (IP:Flag) and whole cell lysates (WCLs) were immunoblotted (IB) with the indicated antibodies. (Data generated together with Dr. Ekim-Üstünel).

D. Primary hepatocytes from TSC22D4$^{hep-/-}$ mice were transduced either with vector control, TSC22D4-WT or -D2+TSC. After 48 hours, the cells were collected in Trizol to analyze the indicated gene expressions at the mRNA level by qRT-PCR.

E. Primary hepatocytes from WT or TSC22D4$^{hep-/-}$ mice (AV-transduced) were used as in (A). The cells were starved in phenol-free media for 8 h followed by treatment with gluconeogenic inducers (forskolin [100 µM], glucagon [100 nM] in the absence or presence of insulin [100 nM] and/or Akt inhibitor (Akti 1/2) [5 µM] for 12 h. The medium was collected to measure the glucose levels via Amplex Red Kit. Glucose concentration was normalized to the KO cells with vector control. (Data generated together with Dr. Ekim-Üstünel). **Statistical Analysis (A, C, D):** Two-way ANOVA with Tukey's Multiple Comparisons Test. */#: $p<0.05$, **/## $p<0.01$, ***/### $p<0.001$, ****/####: $p<0.0001$. *: comparison between different cell populations. #: Akti 1/2 effect in forskolin treated cells in A, insulin effect within each cell population in E.

receptor gamma coactivator 1-beta (PGC1β), medium-chain acyl-CoA dehydrogenase (MCAD) and very long-chain acyl-CoA dehydrogenase (VLCAD), are affected by the interaction status of TSC22D4 and Akt1 (Fig. 13d). Interestingly, PGC1β, which stimulates fatty acid oxidation and mitochondrial biogenesis, showed increased mRNA levels in D2+TSC expressing cells compared to WT-TSC22D4 and vector control cells. MCAD expression also significantly increased in D2+TSC expressing cells compared to vector control cells. In addition, Lipin1, a fatty acid oxidation regulator, also showed a significant increase in D2+TSC overexpressing cells compared to WT-TSC22D4 (Fig. 13d). Overall, these data indicate that D2+TSC and Akt1 interaction plays also role in regulating cellular energy metabolism.

Insulin-induced glucose production capacity of D2+TSC did not change upon Akt inhibition

To further elucidate the function of TSC22D4-Akt1 interaction in glucose metabolism, we evaluated glucose production capacity of TSC22D4 alleles in TSC22D4$^{hep-/-}$ cells expressing AV-empty vector control, WT-TSC22D4 and D2+TSC. Primary hepatocytes from WT mice were used as control. In the glucose secretion assay, we supplied the cells with various stimulants (e.g. glucagon, pyruvate, lactate, forskolin, etc.) to induce gluconeogenesis in the absence or presence of insulin [100 nM] and/or Akt inhibitor Akti 1/2 [5 µM] (Fig. 13e). As a result, insulin successfully suppressed glucose production and secretion into the media for all the groups, except for D2+TSC overexpressing cells. WT-TSC22D4 overexpressing cells secreted more glucose in the media in starved conditions compared to empty vector control or D2+TSC overexpressing cells.

Interestingly, when the cells were treated with Akti 1/2, secreted glucose levels remained the same in the transduced TSC22D4$^{hep-/-}$ cells, whereas WT control cells produced more glucose than the cells only stimulated with insulin. Akt inhibition did not reverse the insulin-mediated inhibition of gluconeogenesis in the TSC22D4$^{hep-/-}$ cells. These findings support the hypothesis that the chronic loss of hepatic TSC22D4 deletion might have caused an alternative compensatory mechanism to suppress gluconeogenesis.

11.1.2. *In vivo* analysis: Introduction of AAVs expressing TSC22D4 alleles into TSC22D4$^{hep-/-}$ mice

Hepatic TSC22D4-Akt1 interaction improves glucose and lipid metabolism

To test the function of TSC22D4-Akt1 interaction *in vivo*, we introduced TSC22D4$^{hep-/-}$ mice with adeno-associated viruses (AAV) carrying vector control, Flag-WT-TSC22D4, -ΔD2 or -D2+TSC alleles specifically in their livers (cohorts established and run by Dr. Ekim Üstünel). In summary, we first fed them with 6 weeks of chow diet followed by 7 weeks of a high fat/high sucrose diet (HF/HSD) challenge. We performedIntraperitoneal (i.p) insulin tolerance test (ITT) and glucose tolerance test (GTT) at different time points. Miceexpressing D2+TSC performed better in ITTs and GTTs than WT-TSC22D4 when they were in a chow diet or HF/HSD. After 7 weeks of HF/HSD, WT-TSC22D4 expressing mice showed increased insulin levels and insulin

resistance compared to D2+TSC and ΔD2 expressing mice. Liver triglyceride levels increased in WT-TSC22D4 overexpressing mice after 7 weeks of HF/HSD compared to ΔD2 and D2+TSC expressing mice in agreement with Dr. Wollf´s publication [54]. In another cohort, we challenged the mice with 12 weeks of HF/HSD. D2+TSC expressing mice showed better glucose handling compared to WT-TSC22D4 and ΔD2 expressing mice. Interestingly, ΔD2 expressing mice showed higher blood glucose levels than WT-TSC22D4 overexpressing mice when exposed to longer HF/HSD (Demir et al, [59], [61]).

To evaluate lipid metabolism, we performed morphometric lipid quantification by analyzing hematoxylin and eosin (H&E) stained liver sections. For the 1st mice cohort fed with 6 weeks of chow diet followed by 7 weeks of HF/HSD, hepatic overexpression of WT-TSC22D4 caused an increased number of lipid droplets in the liver compared to ΔD2 and D2+TSC overexpressing livers (Fig. 14a). Since the accumulation of lipid droplets is a hallmark of insulin resistance and liver diseases [67], these data support the previous findings [52] that TSC22D4 leads to insulin resistance.

In lipid droplet analysis of the second AAV cohort, which includes 12 week HF/HSD mice, WT-TSC22D4 and ΔD2 overexpressing livers showed significantly increased numbers of lipid droplets compared to vector control (Fig. 14b). D2+TSC expressing livers, on the other hand, showed similar levels of lipid droplet density with vector control. There was no difference among the lipid metabolites such as serum ALT, AST, HDL, LDL, and TG levels in all the groups.

Additionally, I analyzed genes responsible for fatty acid metabolism in the liver lysates of AAVs expressing mice by Western Blotting. Expression levels of Acetyl-CoA carboxylase (Acc1), fatty acid synthase (Fasn), and stearoyl-CoA desaturase-1 (Scd1) were decreased in the D2+TSC compared to the vector control and WT-TSC22D4 expressing mice (Fig. 14c). Interestingly, ΔD2 expressing cells also showed decreased levels of Scd1 at the protein level.

TSC22D4 and Akt1 interact in vivo: Overexpression immunoprecipitations (IPs)

To verify TSC22D4-Akt1 interaction levels of different TSC22D4 mutants *in vivo*, I performed Flag-IP with the liver lysates of AAV injected mice and analyzed the endogenous Akt1 levels in the IPs in the absence or presence of nutrients (i.e. insulin) as we previously observed in Hepa1-6 cells. Consequently, TSC22D4 strongly interacted with Akt1, but not with Akt2, in starved mice (lanes 3-5) compared to the mice injected with insulin 10 minutes before the sacrifice (lanes 6-7) (Fig. 15a). Therefore, we confirmed the enriched TSC22D4-Akt1 interaction in the WT-TSC22D4 overexpressing TSC22D4$^{hep-/-}$ mice compared to the empty vector expressing mice (lanes 1-2) and the weakened interaction upon insulin injection *in vivo*.

Then, we evaluated Akt1 interaction levels in the liver lysates of empty vector control, WT-TSC22D4 and ΔD2 overexpressing TSC22D4$^{hep-/-}$ mice. In the IPs, ΔD2 expressing mice tended to show less enrichment for Akt1 interaction than WT-TSC22D4 on average of the livers (Fig. 15b). Furthermore, pAkt levels increased in

ΔD2 expressing cells (lane 7-8) compared to WT-TSC22D4 livers (lane 11-12) when stimulated with insulin (Fig. 15c).

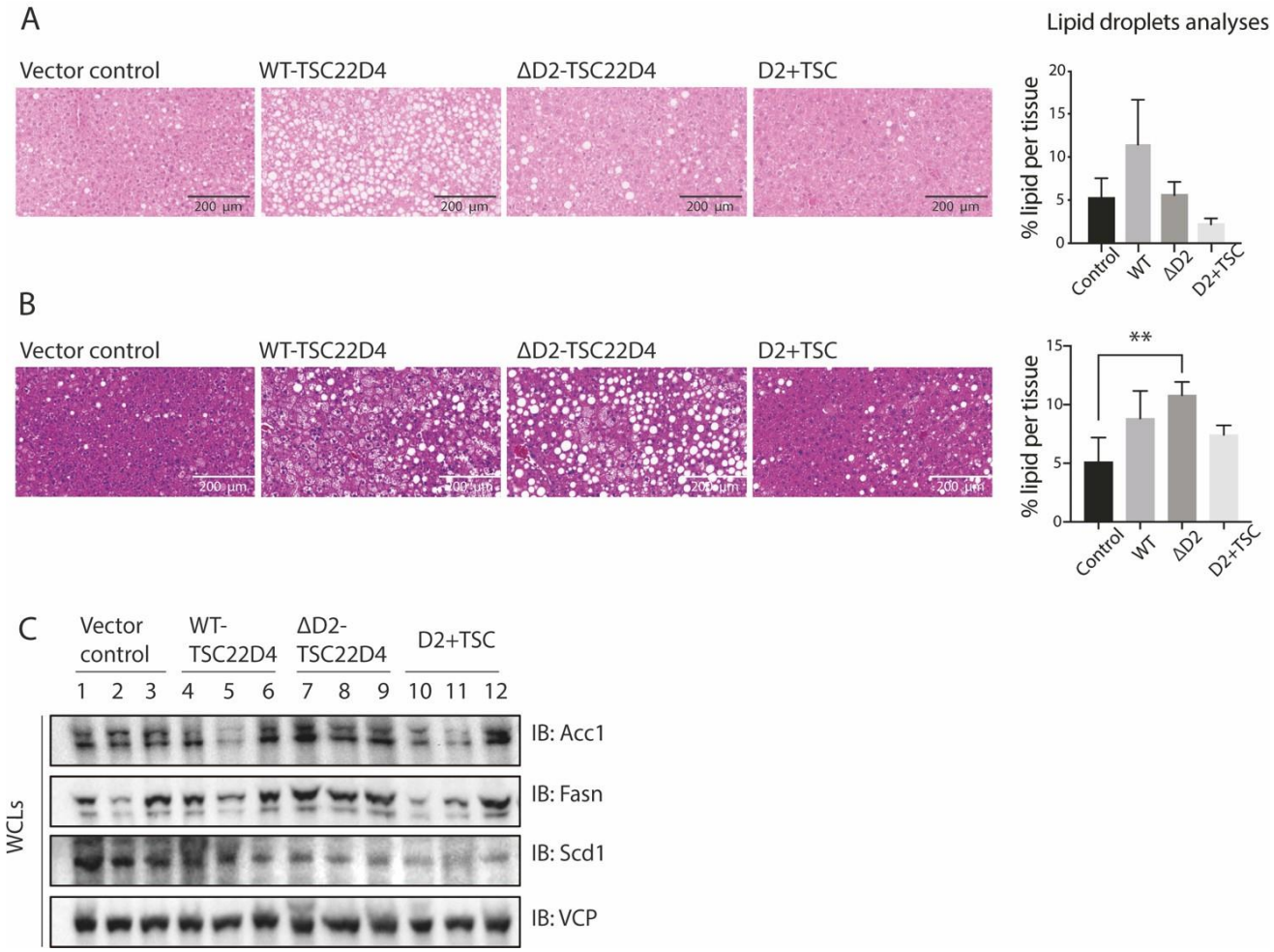

Figure 14: TSC22D4-Akt1 interaction controls liver lipid metabolism.

A, B. Hematoxylin and eosin (H&E) staining of liver sections of AAVs expressing TSC22D4$^{hep-/-}$ mice. Right panel: Quantification of lipid droplets. Statistical Analysis: One-way ANOVA followed by Dunnet's Multiple Comparisons Test **: $p<0.01$. **C.** Liver lysates of AAVs expressing TSC22D4$^{hep-/-}$ mice were analyzed for lipogenic gene expressions with the indicated antibodies at the protein level.

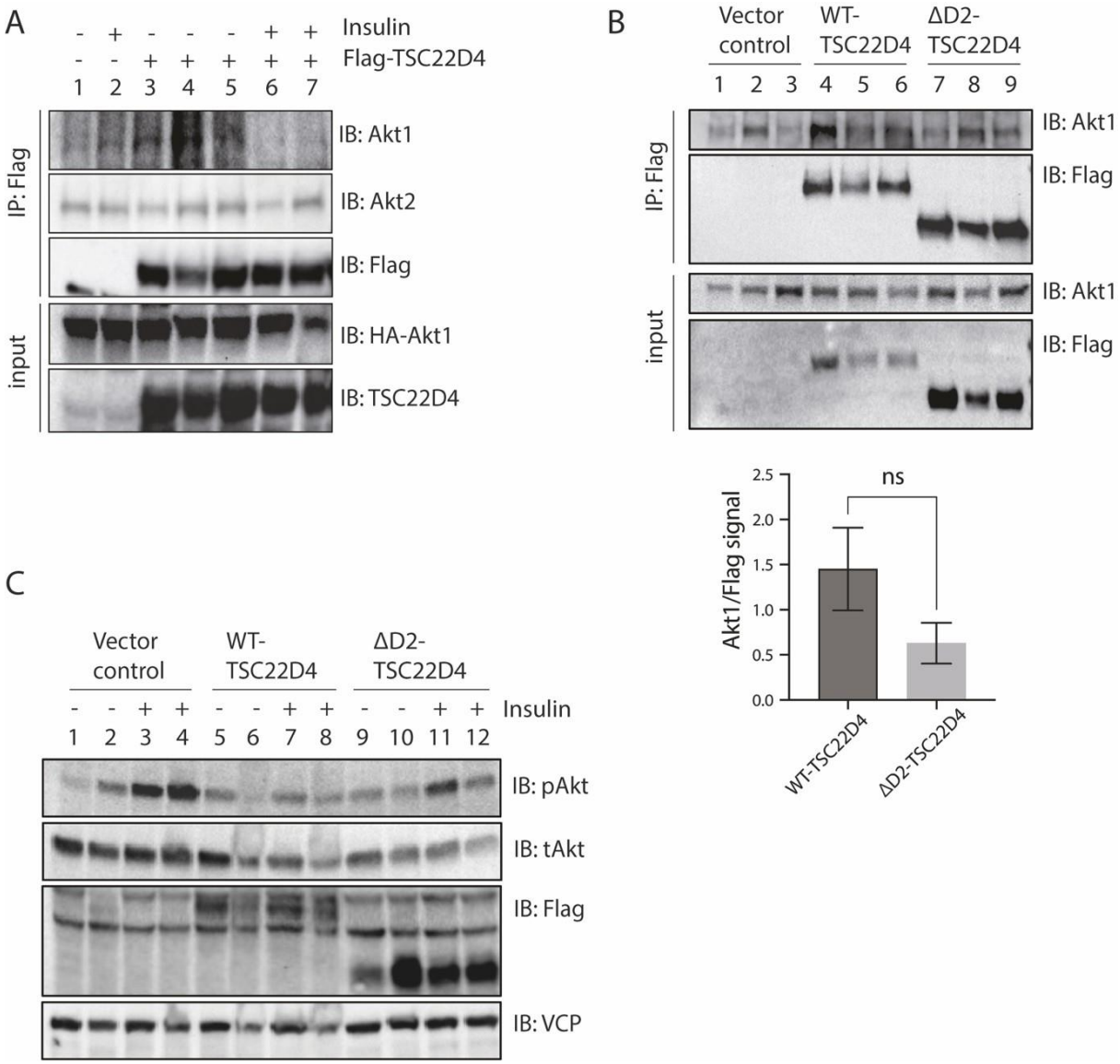

Figure 15**: **TSC22D4-Akt1 interaction in the liver of TSC22D4$^{hep-/-}$ mice expressing TSC22D4 alleles.

A. Flag-TSC22D4 was immunoprecipitated with Flag affinity gel (IP: Flag) from liver lysates of 6 hours starved and insulin injected mice (1.3U/kg for 10 min). IP Flag and whole liver lysates (input) were immunoblotted (IB) with the indicated antibodies. **B.** Flag-TSC22D4 was immunoprecipitated (IP: Flag) in the liver lysates of AAVs expressing TSC22D4$^{hep-/-}$ mice and immunoblotted (IB) with the indicated antibodies. Lower panel: Quantification of Akt1 enrichment in the IPs normalized to Flag signal. **C**. Liver lysates of vector control, WT-TSC22D4 or ΔD2-TSC22D4 were immunoblotted (IB) with the indicated antibodies.

D2+TSC and Akt1 interaction might play a role in proliferation of liver cells in db/db mice

Since D2+TSC decreased hepatic lipid accumulation in HF/HSD fed mice in the AAV experiments (Fig. 14a-b), we hypothesized that the D2+TSC mutant might also improve lipid content in db/db mice which shows a diabetes phenotype with elevated triglyceride and lipid levels. To this end, we overexpressed AAVs expressing vector control vs. D2+TSC in db/db mice specifically in their hepatocytes. We did not observe significant differences in liver mass or body mass between the vector control and D2+TSC overexpressing mice (Fig. 16a). There was no difference among the main gluconeogenic (PGC1α, PEPCK and G6P) and lipogenic (Fasn, Scd1, Acly, and Acc1) gene expressions between D2+TSC and vector control mice at mRNA levels (Fig. 16b). We also did not see any difference between the groups regarding lipid accumulation and triglyceride levels in the liver (Fig. 16c). Interestingly, we observed elevated pAkt levels in the liver lysates with D2+TSC expression (Fig. 16d).

The Akt signaling pathway contributes to a wide range of critical signaling events in the cell. Since we could not detect any significant changes in glucose and lipid metabolism in vector vs. D2+TSC expressing mice, we explored if D2+TSC expression affects a distinct function of Akt. Proliferation is one of the cellular processes that Akt contributes to. Therefore, we examined a proliferation marker, Ki67, in stained liver sections and compared its density per tissue in D2+TSC and control livers (Fig. 16e). D2+TSC expressing livers showed less Ki67 density than the control livers. We also evaluated Ki67 expression in mRNA levels and confirmed that hepatic Ki67 mRNA was significantly decreased in D2+TSC expressing livers (Fig. 16e, right panel). Overall, D2+TSC expression diminished the proliferating cells in livers of db/db mice, indicating an impediment in cell regeneration. Constitutive binding of D2+TSC to Akt suppressed Akt function on cell growth and proliferation.

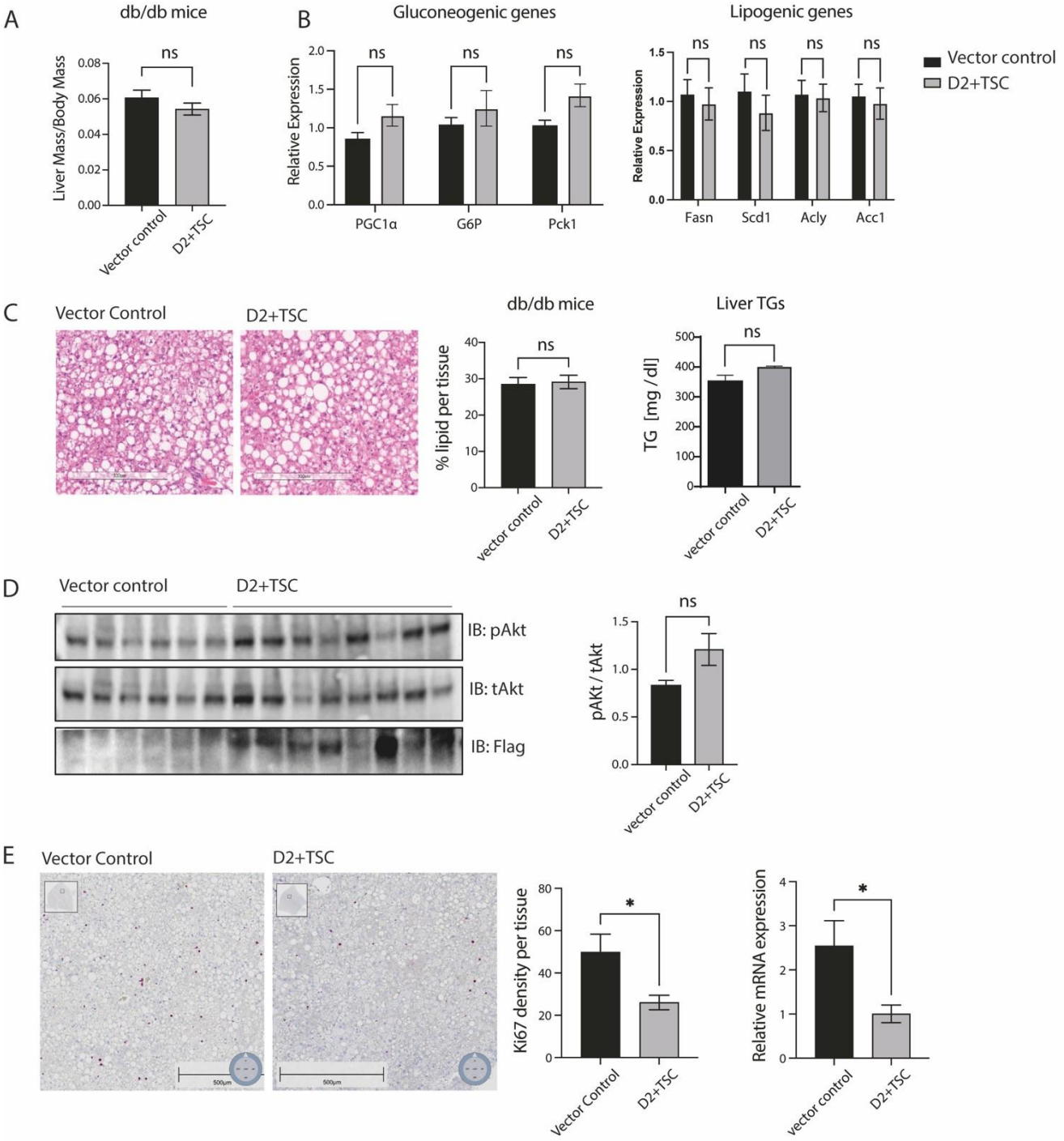

***Figure 16: A strong Akt1 interaction might regulate other cell processes in db/db mice*.**

A. Analysis of liver and body mass of db/db mice expressing AAVs with vector control or D2+TSC. **B.** mRNA expression of the main gluconeogenic and lipogenic genes analyzed by qRT-PCR in the livers of vector control and D2+TSC expressing db/db mice. **C**. Lipid droplet analysis of Hematoxylin and eosin (H&E) stained livers of AAVs expressing db/db mice. Right panel: Quantification of lipid droplets and quantification of liver triglyceride levels of liver lysates. **D.** Liver lysates of db/db mice expressing vector control or D2+TSC were analyzed with the indicated antibodies at the protein level. Right panel: Quantification of pAkt enrichment, normalized to tAkt levels. **E.** Liver sections of db/db mice were analyzed with Ki67 staining. Right panel: quantification of Ki67 density per tissue and qRT-PCR analysis for Ki67 mRNA expression.

7. Discussion

Akt is a crucial signaling protein regulating essential cellular processes including glucose and metabolism, glycogen and lipid synthesis, cell cycle, proliferation and survival. Dysregulated Akt action in the insulin signaling pathway is one of the main outcomes of insulin resistance and type 2 diabetes. Thus, by identifying molecular mechanisms causing deregulations in Akt signaling will help develop novel therapies against these particular reasons that leads type 2 diabetes. In my Ph.D. project, I identified TSC22D4 as a novel Akt1-interacting protein. By mapping TSC22D4, I identified the smallest polypeptide sequence that is required and sufficient for Akt interaction. I employed Akt-interaction deficient mutant (i.e. ΔD2) and constitutively Akt-interacting mutant (i.e. D2+TSC) in functional assays to assess the role of TSC22D1-Akt1 interaction in glucose and lipid metabolism.

As a key modulator in the insulin signaling pathway, Akt regulates lipid metabolism through mTORC1/S6K1 signaling axis. mTORC1 stimulates ribosomal protein S6 kinase 1 (S6K1) to promote lipogenesis via sterol response element binding protein 1c (SREBP1c) transcription factor [68], [69]. In the co-IP assays, D2 domain alone was sufficient for Akt1 interaction, whereas TSC Box failed to interact with Akt1 (Fig. 9b). Unexpectedly, basal pAkt levels were significantly low in both D2 domain and TSC Box expressing cells compared to vector control. In addition, pS6K1 levels in the TSC Box expressing cells were significantly increased upon insulin stimulation compared to D2 domain and vector control expressing cells. Since TSC Box is required for protein dimerization (Fig. 7d), it might modulate Akt function and lipogenesis due to its dimerization ability with other proteins (e.g. TSC22 family members, Fig. 7c), independent of Akt1 interaction. Of note, TSC22D4 does not interact with Akt1 directly based on the *in vitro* binding assays [59]. Thus, a mediator protein might promote TSC22D4-Akt1 interaction within a protein complex. Other TSC22 family members, which interact with Akt1 and contain the conserved TSC Box (Fig. 7a-b), might play role in mediating TSC22D4-Akt interaction as well. It is also conceivable that the mediator protein can be a regulator of Akt1 such as PDK1 or component(s) of mTORC2.

To understand the function of TSC22D4-Akt1 interaction, we produced adenoviruses (AVs) and adeno-associated viruses (AAVs) to employ primary hepatocytes (*in vitro)* and mice *(in vivo)*. For the interaction-deficient mutant, we generated ΔD2 instead of ΔTSC because the D2 domain alone was sufficientfor Akt1 interaction (Fig. 6c-d, Fig. 9b), whereas TSC Box was only required for protein dimerization (Fig. 7d, Fig. 9b). In parallel, as an Akt-interacting mutant, we produced D2+TSC instead of producing D2 alone, to ensure the strong interaction ability of TSC22D4 to Akt1.

In the experiments performed in primary hepatocytes of TSC22D4$^{hep-/-}$ mice, D2+TSC expressing cells showed decreased basal pAkt protein levels (Fig. 12b). Furthermore, the levels of the downstream effectors regulating distinct cellular metabolisms (i.e., FoxO1, GSK3β, pS6) were also lower in D2+TSC expressing cells.

Thus, a constant Akt interaction of TSC22D4 regulates not only glucose metabolism as we observed *in vivo* [59], but also lipogenic pathway via mTORC1/S6K1/SREBP1c axis. mTORC1 promotes SREBP1c function by inhibiting Lipin1, a regulator of fatty acid oxidation (FAO) and mitochondrial oxidative phosphorylation (OXPHOS) [70]. Notably, D2+TSC expressing primary hepatocytes showed significant elevation of Lipin1 levels in comparison to WT-TSC22D4 and vector control at the mRNA level (Fig. 13d).

Activated SREBP1c induces lipogenic genes such as aceyl-CoA carboxylase (Acc1), fatty acid synthase (Fasn) and stearoyl-CoA desaturase (Scd1) to promote fatty acid synthesis. Livers lysates of the AAV-transduced mice, fed with HF/HSD for 12 weeks, showed decreased protein levels of Acc1, Fasn and Scd1 in D2+TSC expressing mice compared to the other groups (Fig. 14c). In addition, lipid droplet intensities in D2+TSC expressing livers were lower in comparison to the other groups (Fig. 14a-b, right panels). Thus, in parallel with the previous findings of primary hepatocytes, hepatic D2+TSC overexpression resulted in reduced lipogenic gene expressions and reduced lipid accumulation in the liver. Although the lipid droplet intensity in the livers of ΔD2 expressing mice tended to be higher than D2+TSC (Fig. 14a-b, right panels), Scd1 expression at the protein level diminished in ΔD2 expressing mice (Fig. 14c). By employing AAVs to the TSC22D4$^{hep-/-}$ mice, we targeted specifically hepatocytes for overexpressing the TSC22D4 alleles. The other cell types in the liver such as hepatic stellate cells or Kupffer cells could have stimulated alternative mechanisms to suppress Scd1 expression at the protein level in ΔD2 expressing mice livers. Alternatively, since deletion of the D2 domain, resulted in losing several phosphorylation sites in TSC22D4 [61], it is possible that TSC22D4 changed its conformation and was unable to regulate the lipogenic program through Scd1 axis.

As a central regulator of energy homeostasis, AMP-activated protein kinase (AMPK) might have also interfered with the regulation of the lipid program. In a healthy state, AMPK inhibits anabolic pathways including lipogenesis and glycogenolysis, while it promotes catabolic events such as fatty acid oxidation and glycolysis [71]. Based on preliminary data performed in Hepa1-6 cells, rotenone/antimycin treatment resulted in a stronger TSC22D4-Akt interaction and increased AMPK phosphorylation. Interestingly, in the co-IP assays in WT vs. AMPK double knockout (KO) U2O2 cells, TSC22D4-Akt1 interaction acted similarly in WT and the KO cells in the presence of nutrients (i.e. glucose/insulin) or mitochondrial inhibitors (i.e. rotenone/antimycin) [59]. Thus, TSC22D4-Akt1 interaction is regulated independently of AMPK function. Nevertheless, these data strengthen our hypothesis that reduced lipogenic gene expressions and lipid accumulation in D2+TSC expressing mice might have resulted from the strong and constant interaction of D2+TSC with Akt1.

To understand the function of TSC22D4-Akt1 interaction on glucose metabolism, we transduced primary hepatocytes of TSC22D4$^{hep-/-}$ mice with TSC22D4 alleles and measured the glucose production capacity of the cells upon forskolin/glucagon treatment. Upon constant Akt interaction (with D2+TSC mutant), the cells produced less glucose compared to WT-TSC22D4 and empty vector control (Fig. 13e) and insulin failed to suppress gluconeogenesis. Based on our initial observations, we would have expected higher glucose levels in

D2+TSC expressing cells due to the constant inhibition of Akt (Fig. 8b-c), and, therefore, enhanced gluconeogenesis. However, among the main gluconeogenic genes, PGC1α was the only effector that showed elevated expression levels (Fig. 13a), indicating the global gluconeogenic transcriptional program remained relatively dormant. Notably, upon Akt inhibition, AV-transduced hepatocytes of TSC22D4$^{hep-/-}$ mice did not reverse the insulin effect by producing more glucose, as opposed to WT control cells. It is possible that the TSC22D4$^{hep-/-}$ mice might have developed a compensatory mechanism for inhibition of insulin-induced gluconeogenesis independent of Akt function. Nevertheless, insulin-induced PGC1α expression was elevated in D2+TSC expressing cells upon Akt inhibition, indicating D2+TSC regulates PGC1α expression via Akt axis.

Based on my Ph.D. studies and previous publications [52], [54], [58], we proposed a working model explaining the TSC22D4-Akt1 interaction [59]. In a healthy state, TSC22D4 indirectly interacts with Akt1 upon starvation and the interaction is impaired in the presence of high glucose and insulin levels. During chronic hyperglycemia and hyperinsulinemia, TSC22D4 fails to interact with Akt1 and exacerbates the pathogenesis of insulin resistance and type 2 diabetes. Although TSC22D4 knockdown improves glucose and lipid metabolism, a strong and constant Akt interaction of TSC22D4 (via D2+TSC mutant) ameliorates insulin resistance.

8. Conclusion and Outlook

In my Ph.D. project, I investigated the molecular mechanisms underlying the development of insulin resistance and type 2 diabetes. By identifying TSC22D4 as a novel regulator of Akt, we contributed to revealing distinct molecular mechanisms that will help to establish novel therapies to target insulin resistance in the near future. Modifying TSC22D4-Akt1 interaction would pave the way for the development of effective treatments.

As a key regulator in cell metabolism and survival, phosphorylation of the activation sites is required for Akt to contribute to its function. We identified TSC22D4 as a determinant of Akt function in distinct metabolic conditions, however, how exactly TSC22D4 modulates Akt and how it interferes with Akt´s phosphorylation is still yet-to-be-identified. Since TSC22D4 does not interact with Akt directly [59], the mediator proteins involved should be determined to reveal the mechanism behind the TSC22D4-Akt1 interaction. For identifying the binding partners of Akt in the close proximity of TSC22D4, high throughput tools such as crosslinking mass spectrometry (MS) can be used alongside the well-established tools like co-immunoprecipitation (co-IP), yeast-two hybrid assay or proximity labeling techniques. Crosslinking MS serves as an advantageous platformto detect even weak or transient interactions without the requirement of tagging proteins [72], [73]. Since we showed that TSC22D4 interacts with Akt1 via its D2 domain, which is located in the intrinsically disordered region of the protein, it is possible that the TSC22D4-Akt1 interaction is rather transient depending on the environmental factors.

Out of 15 novel phosphorylation sites identified on TSC22D4, 6 of them are located in the D2 domain (206-318 aa) [61]. To understand the role of these phosphorylation sites on Akt interaction, we created TSC22D4-Alanine mutants, where we substituted Serine (S) or Threonine (T) residues with Alanine (A) amino acids individually or in combinations. Based on preliminary *in vitro* analyses in Hepa1-6 cells, we observed that the phospho-deficient mutant of TSC22D4-T252/S254/S258A caused a noticeable shift at the protein level, indicating loss of phosphorylation at multiple sites. Thus, these S and T residues can be considered as candidates which play a role in TSC222D4 action. In the near future, the Akt interaction status of the TSC22D4-Alanine mutants can be evaluated by co-IP assays to conclude how TSC22D4 modulates Akt function in detail. Analysis of TSC22D4-Alanine mutants might also help identify kinase(s) modulating TSC22D4 function. Further, it can be assessed if the kinase(s) are directly interacting with TSC22D4 or Akt1 with co-IP or in vitro binding assays in cells.

Since Akt regulates not only cell metabolism but also cell survival, further functional assays can be performed to determine TSC22D4 action on Akt function. In db/db mice, we observed overexpression of D2+TSC decreased proliferating cells in the liver (Fig. 16). Function of the strong interaction of TSC22D4-Akt1 can be studied by employing the D2+TSC allele in cells to perform proliferation assays. In addition to using cell

proliferation markers (e.g. Ki67), the metabolic activity of the cells can be observed to determine the change in the number of cells. Therefore, the translational potential of TSC22D4-Akt1 interaction can also be studied in other complex diseases such as cancer.

9. Materials & Methods

9.1. Animal experiments

9.1.1. Endogenous TSC22D4 co-immunoprecipitation from liver lysates

Liver lysates of WT mice (control diet, high-fat diet (HFD), high fat/high sucrose diet (HF/HSD)) and db/db mice (chow diet) were prepared to analyze endogenous interaction of TSC22D4-Akt1. Frozen and pulverized liver samples were ground using Dounce homogenizer with ice cold CHAPS lysis buffer containing 10 mM KPO_4 (pH 7.2), 1 mM EDTA, 5 mM EGTA, 10 mM $MgCl_2$, 50 mM β-Glycerophosphate, 0.3% CHAPS, Complete Protease Inhibitor Cocktail (Roche, #11836145001) and PhosSTOP EASYpack phosphatase inhibitor (Roche, #4906837001). Protein concentrations were measured by Bradford assay (BioRad, #5000006) using a biophotometer (Eppendorf). Liver lysates were incubated with TSC22D4 antibody (Pineda, homemade antibody, 1mg/ml) at 4°C overnight on a rotating rack. The next day, protein A/G beads were conjugated to protein-antibody complex via 2 hours of incubation at 4°C on a rotating rack. The lysates were washed 3 times with CHAPS lysis buffer and added 70 μl of 4x sample buffer. As a negative control for the TSC22D4 antibody, normal rabbit IgG (CST, #2729S) was used.

Liver lysates of WT mice and db/db mice (fasted 18h vs refed 1h) were prepared to analyze the endogenous interaction of TSC22D4-Akt1 as described above. Liver samples of WT and db/db mice for this study were kind gift from Dr. Ana Jimena Alfaro (Helmholtz Munich).

Db/db mice were used to analyze the effects of the D2+TSC construct. Db/db mice were injected with AAVs expressing either empty vector control or the D2+TSC allele. Liver lysates were prepared using CHAPS lysis buffer to analyze the targets in the insulin signaling pathway at the protein level. Endogenous TSC22D4 IP was performed as described above.

9.1.2. Flag-TSC22D4 immunoprecipitation from liver lysates

Liver lysates of hepatocyte-specific TSC22D4 KO ($TSC22D4^{hep-/-}$) mice injected with AAVs expressing Flag-tagged empty vector control, WT-TSC22D4, ΔD2-TSC22D4 or D2+TSC were used to analyze interaction levels of Akt with different TSC22D4 alleles. Frozen and pulverized liver samples were ground with Dounce homogenizer with ice cold CHAPS lysis buffer. Protein concentrations were determined with Bradford assay (BioRad, #5000006). For Flag immunoprecipitation, anti-Flag affinity gel (Sigma, #A2220) was used. Prior to use, the beads were washed with lysis buffer via centrifugation at 4000 rpm for 2 minutes. Then, cell lysates were incubated with the beads overnight at 4°C on a rotator. The next day, the beads were washed 3 times with 1 ml ice-cold lysis buffer with centrifugation. 4x laemmli buffer was added to the samples which then were boiled at 95°C for 5 minutes.

9.2. Primary hepatocyte experiments

9.2.1. Primary hepatocyte isolation and treatments

Primary hepatocytes of WT mice ($TSC22D4^{flox/flox}$) and $TSC22D4^{hep-/-}$ mice were used to analyze the phosphorylation status of Akt and its downstream targets. Primary hepatocytes were isolated by Dr. Gretchen Wollf as described before [54]. To investigate if glucose and insulin stimulation affects signaling molecules in the insulin pathway, primary hepatocytes were seeded to collagen-coated 6-well plates ($1x10^6$ cells per well) in William´s medium (Pan Biotec, #P04-29510) supplemented with 2 mM L-Glutamine,

100 nM Dexamethasone, 10% FBS and 1 Pen/Strep. After 4 hours, the cells were washed 2 times with PBS to get rid of the cells which do not attach to the surface. After 36 hours of incubation, the cells were starved with DMEM media (Life Tech, #A1443001) supplemented with 5 mM D-Glucose, 2 mM L-Glutamine, 0.5% FBS and 1% Pen/Strep overnight. The next day, the cells either remained starved or stimulated with glucose [20 mM] for 30 minutes and insulin [100 nM] for another 30 minutes prior to cell lysis. The cells were collected in 180 μl 1.5x sample buffer, boiled at 95^{o}C for 5 minutes and kept at -20^{o}C until used for Western Blotting.

9.2.2. Primary hepatocytes transduced with Adenoviruses

Gene expression analyses

To analyze the effects of TSC22D4-Akt interaction on gluconeogenesis, primary hepatocytes from TSC22D4$^{hep-/-}$ mice were transduced mice with AVs expressing TSC22D4 alleles: empty vector control, WT- TSC22D4, ΔD2-TSC22D4 or D2+TSC constructs (at a multiplicity of infection of 10). 36 hours post-transfection, the cells were starved overnight and stimulated either with DMSO vehicle control or Forskolin ([10 µM], 4,5 hours) in the absence or presence of an Akt inhibitor (Akti1/2, 5 μM, Tocris, #5773). The cells were collected with QIAzol to be analyzed further at the mRNA level.

Gluconeogenesis assay

Primary hepatocytes were seeded in 24-well plates (200.000 cells/well) in collagen monolayer in Williams E Medium (Pan Biotec, #P04-29510) containing 100 nM Dexamethasone, 10% FBS and 1% PenStrep. The next day, the cells were transduced with AVs expressing TSC22D4 alleles at a multiplicity of infection of 10 as described above. After 36 hours post-transfection, the medium was changed to phenol-free DMEM supplemented with 0.5% FBS, 5mM glucose and 4 mM glutamine for starvation for 8 hours. Then, the cells were washed 2 times with PBS and added 200 μl of DMEM supplemented with 4 mM glutamine, 2 mM pyruvate, 20 mM lactate (basal medium) plus 100 nM glucagon, 100 nM Dexamethasone and 100 μM Forskolin for stimulation and another group with 100 nM glucagon, 100 nM Dexamethasone, 100 μM Forskolin and 100 nM insulin. After 12 hours of incubation, the medium was collected and centrifuged at 6000 rpm for 2 minutes at room temperature. The supernatant was collected and stored at -20^{o}C until glucose determination assay (Amplex Red glucose assay kit, Life Tech, #A22189). The cells that remained in the 24 well plates were added QIAzol to be analyzed further at the mRNA level.

9.3. Recombinant viruses

9.3.1. Adeno-associated virus (AAV) production

For generating AAVs with cDNAs of TSC22D4 alleles (WT, ΔD2 or D2+TSC) were amplified with the following primer pairs followed by Nhe1 and Xba1 digestion and subcloning into the pdsAAV-LP1 plasmid: TSC22D4-AAV-F with NheI: gatgctagcgtgtgctggaattctg, TSC22D4-AAV-R with XbaI: gcatctagactcgagtcagatggaggg. The successful clones were sequenced for confirmation with the following primers: pdsAAV-TSC-F: ctgataggcacctattggtc, pdsAAV-TSC-R: ccacaactagaatgcagtg. Once the sequence was confirmed, the plasmids were purified using the Mega Prep kit (Qiagen, #12381) according to the manufacturer's instructions and sent to Vigene Biosciences (Maryland, USA) for AAVs generation and purification.

9.3.2. Adenovirus production

Cloning of adenoviruses

Adenovirus (AV) expressing vector control, WT-TSC22D4, ΔD2-TSC22D4 (206-318 aa) and D2+TSC (206-378 aa) alleles under control of the CMV promoter were initially cloned into pENTR plasmid (kan^+ resistant) to be recombined into adenoviral pAd/BLOCK-iT™ DEST vector (amp^+ resistant) using the modified BLOCK-iT™ Adenoviral RNAi expression system (Invitrogen, #K494100). pAd/BLOCK-iT DEST vector contains the adenovirus serotype 5 DNA, but lacks the E1 and E3 genes required for viral replication. The viral vectors containing TSC22D4 cDNA alleles were linearized by restriction digest using the enzyme *Pac*I. After phenol-chloroform extraction, they were transfected into HEK239A cells (~70% confluent, seeded in 6-well plates in DMEM supplemented with 10% FBS) using Lipofectamine 2000 (Invitrogen, #11668019) according to the manufacturer's instructions. 24 hours post-transfection, the medium was replaced with fresh media containing antibiotics (Pen/Strep). 48 hours post-transfection, the cells were transferred to 10 cm plates containing 10 ml medium (DMEM supplemented with 10%FBS and 1% PenStrep). HEK293A cells express the viral E1 and E3 genes necessary for a viral outbreak, allowing the virus to expand in this cell line. Viral plaques appeared 6 to 10 days after transfection and cells started to detach from the cell culture dish. Once about 70% of cells were round and floating, they were collected and centrifuged at 2000 rpm at 4°C for 5 minutes. The pellet was resuspended in 500 μl PBS, and kept at -80°C. An empty adenovirus was already present in the lab, therefore used as a negative control in overexpression experiments.

Virus harvest using the Freeze-Thaw method

Cells infected with adenoviruses were harvested in DMEM supplemented with 10% FBS and 1% PenStrep. The medium was collected from twenty 15 cm culture dishes and centrifuged for at 2000 rpm for 10 min. The supernatant was discarded and the cell pellet was resuspended in 4 ml PBS-TOSH buffer. The tubes containing the virus were snap-frozen in liquid nitrogen and subsequently thawed by harsh vortexing. To release the virus from the cells, the freeze-thaw cycle was repeated three times. After cell lysis, the mixture was centrifuged at 4500 rpm at 4°C for 10 min. The crude supernatant was stored at -80°C.

Caesium chloride gradient

Virus lysates from twenty 15 cm culture dishes were thawed on ice. PBS-TOSH was added to a final volume of 20 ml. Gradients were prepared in ultracentrifuge tubes (Beckmann Polyallomer 25 mm x 89 mm) and were balanced after the addition of each solution. First, 9 ml of 4 M caesium chloride were added to the tubes, then 9 ml of 2.2 M caesium chloride was added and 20 ml of viral lysate was carefully added on top. The gradients were centrifuged at 24000 rpm at 4°C in a Beckmann ultracentrifuge XL-70 for 2 hours using an SW28 swing bucket rotor. After centrifugation, a distinct band corresponding to the purified adenovirus was visible between the 4 M and 2.2 M caesium chloride layers. The band was carefully removed by piercing the tube with a 5 ml syringe and a 1.2 mm needle. The obtained virus (~3 ml) was mixed with an equal volume of saturated caesium chloride solution and transferred into a 12 mL centrifuge tube (Beckmann Polyallomer 14mm x 89 mm). 2 ml of the 4 M cesium chloride and 2 ml of the 2.2 M cesium chloride solution were used to overlay the gradient. The tubes were centrifuged at 35000 rpm at 4°C in a SW40 Ti swing bucket rotor for 3 hours. A distinct viral band was visible between the 4 M and 2.2 M cesium chloride layers. The purplish/pinkish virus band was visible (~700 µl) and removed using a 2 ml syringe and 1.2 mm needle. To remove cesium chloride from the viral solution, viruses were transferred to a dialysis membrane (Spectra/Por® Biotech, MWCO 15,000, 10 mm diameter) and dialyzed against 1 L PBS containing 10 % glycerol 2 times (1 and 24 hours) at 4°C. After dialysis, aliquots of 20–100 µl were prepared and stored at -80°C until further use.

Virus titration

The Tissue Culture Infectious Dose 50 ($TCID_{50}$) assay was used to titrate adenovirus. HEK293A cells were harvested in DMEM medium supplemented with 2% FBS and 1% penicillin/streptomycin and transferred to 96 well plates. 10^5 cells in a volume of 100 µl cells were added to each well and two plates (technical duplicates) were required for each titration. After seeding, cells were incubated for 2 hours so that they could attach. Serial dilutions of the viruses were prepared in the same medium as above. 100 µl of each dilution step (10^{-7}-10^{-14}) were added to ten wells, and 100 µl of medium without virus were added to negative control wells. The cells were incubated for ten days to determine the viral titer. It was possible to detect plaque formation in the cell monolayer using a microscope. Each well in which at least one plaque could have been detected was considered a positive well. The titer was determined using the following formula:

Ta= viruses per 100 µl =$10^{1+(s-0.5)}$

s = the sum of all positive wells starting from the 10^{-1} dilution, whereby 10 positive wells correspond to the value 1.

T= viruses per 1 ml = Ta * 10 (ifu/ml)

9.4. Cell lines and cell culture maintenance

Hepatoma 1-6 (Hepa1-6) cells (ATCC, CRL-1830) cells were used for transient transfection experiments. The cells were maintained in Dulbecco's modified Eagle's medium (DMEM, Gibco, #41966029) supplemented with 10% heat-inactivated fetal bovine serum (FBS, Life Technologies, #16000044). Human embryonic kidney 293A cells (HEK293A, Thermo Fischer Scientific, #R70507) cells were used to generate adenoviruses. All the cell lines were maintained in a humidified 37°C incubator containing 5% CO_2.

9.5. Creating deletion mutants

9.5.1. Site-directed mutagenesis

Wild type TSC22D4, wild type Akt1 and deletion mutants of TSC22D4 expression constructs were created using either pcDNA3 or pENTR plasmid backbone (Table 1). Expression constructs for Flag-tagged WT-TSC22D4, the deletion mutants of TSC22D4 and hemagglutinin (HA)-tagged WT-Akt1 obtained by site-directed mutagenesis experiments with standard PCR-based methods (Q5 site-directed mutagenesis kit, NEB, #E0554S) using corresponding primer sets:

DELETION MUTANTS		
TSC22D4 MUTANTS	**FORWARD PRIMER**	**REVERSE PRIMER**
TSC22D4-ΔD2	GACTTGGTGAAGTCCCAC	CTGAGCACTATCTCCAGT
TSC22D4-ΔTSC	CCCTCTGCACCCAATGGGC	CATGGCTTGTTCAATCTTGTTGT
TRUNCATION MUTANTS		
D2+TSC	GGAGATAGTGCTCAGACCCTG	GGCCGCTGGCTTGTCATCGTC
D2 Domain	CCCTCTGCACCCAATGGGC	CATGGCTTGTTCAATCTTGTTGT
TSC Box	GACTTGGTGAAGTCCCACCTCATG	GGCCGCTGGCTTGTCATCGTC
SMALL PEPTIDES		
D2-ΔN	AGCCTGGTCCATAAGTCTCC	GGCCGCTGGCTTGTCATC
D2-ΔC	TCTGCACCCAATGGGCC	GGCATCGAAGTAGAGGGC
D2-ΔC-ΔC	TCTGCACCCAATGGGCC	AACTAACTCCATCCTCAGCCG
D2-ΔC-ΔN (SM)	ACCCCTCCACTGTCACGG	GGCCGCTGGCTTGTCATC
D2-ΔC-ΔN	CGGAGAAGAGATGGAGCAGTT	GGCCGCTGGCTTGTCATC

Exponential amplification of the region of interest was performed with the following reactions in corresponding cycling conditions. The online NEB primer design software was used for the annealing temperature (Ta) of the mutagenic primers (https://tmcalculator.neb.com).

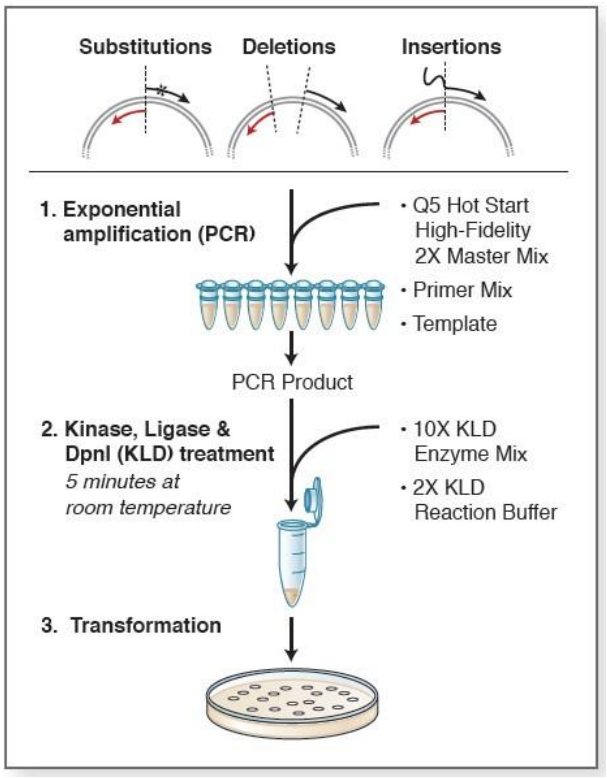

1.Exponential amplification (PCR)

	25 µl RXN	FINAL CONC.
Q5 Hot Start High-Fidelity 2X Master Mix	12.5 µl	1X
10 µM F + R Primer	2.5 µl	0.5 µM
Template DNA (1–25 ng/µl) (25 ng/µl TSC22D4 #806)	1 µl	1-25 ng
Nuclease-free water	9.0 µl	

2. KLD Reaction

STEP	VOLUME	FINAL CONC.
PCR Product	1 µl	
2X KLD Reaction Buffer	5 µl	1X
10X KLD Enzyme Mix	1 µl	1X
Nuclease-free Water	3 µl	

For the 3rd step transformation, E.Coli chemically-competent cells (NEB, 5α competent cells) were used. 5 µl of KLD product was mixed with 50 µl of competent cells and incubated for 30 minutes on ice. Then, the cells were exposed to heat-shock treatment at 42°C for 30 seconds followed by a 5 minute incubation on ice. Then, the cells were added to 950 µl of SOC medium and incubated on a shaker at 37°C for 1 hour. After incubation, the bacteria were spread on LB plates supplemented with appropriate antibiotics and incubated overnight at 37°C.

9.5.2. Plasmid preparation

Small scale plasmid preparation (Mini-Prep)

Miniprep growing cultures were prepared using a single colony to inoculate 3 ml LB-medium supplemented with the appropriate concentration of a specific antibiotic. Cultures were incubated overnight at 37°C under vigorous shaking. The next day, plasmid preparation was performed using Plasmid Miniprep Kit (Qiagen, #27104) with 2 ml of bacterial culture. To confirm the sequence of the plasmids, we sent the minipreps to LGC Genomics (LGC, Biosearch Technologies) and analyzed the sequences with the software DNA Baser Assembler v5.

Large scale plasmid preparation (Maxi Prep)

After confirming the correct plasmid sequence expressing our deletion mutant, we prepared the plasmids on a large scale. 1 ml of bacterial culture remained from Mini Prep preparations was added to 10 ml of LB medium and used as a starter culture for ~6 hours at 37°C under vigorous shaking. Then, 200 ml LB medium was

inoculated with the pre-culture and incubated overnight at 37°C under vigorous shaking. The next day, the large scale bacterial preparation was performed using Maxi Prep Kit (Qiagen, #12163). The plasmid DNA was resuspended in 200-300 µl H_2O and the concentration was measured by spectral photometry. Plasmid DNA was stored at -20°C.

9.6. Plasmid DNA transfection and RNAi interference

Plasmids expressing TSC22D4 and Akt1 mutants were transiently co-transfected to Hepa1-6 cells using Lipofectamine 2000 (Invitrogen, #11668019) according to the manufacturer's instructions. For starvation experiments: 30 hours post-transfection, the cells were starved with RPMI medium (Gibco, #11879020) overnight and the next day cells were pre-stimulated with glucose [20 mM] for 30 minutes and with insulin [100 nM] for an additional 30 minutes followed by cell lysis. For experiments that did not involve starvation, cells were lysed 48 hours post-transfection.

Transient siRNA transfections [50 nM] of Hepa1-6 cells were performed by using non-targeting scramble control (Qiagen, #SI00780521) or siRNAs targeting mouse TSC22D4 (Qiagen, #1027418) with Lipofectamine RNAiMAX (Invitrogen, #13778150). 72 hours post-transfection, cells were harvested to obtain RNA and complementary DNA (cDNA) to be analyzed with qRT-PCR. Additionally, the cells were analyzed with immunohistochemistry using TSC22D4 (ProteinTech, #55017-1-AP) to assess the efficiency of the knockdown.

9.7. RNA isolation, cDNA preparation and RT-qPCR

Total RNA was isolated from Hepa1-6 cells or primary cells using QIAzol and RNeasy kit (Qiagen, #74106) according to the manufacturer's instructions. 200 ng RNA was used for cDNA synthesis and the QuantiTect reverse transcription kit (Qiagen, #205311) was followed according to the manufacturer's instructions. Samples were incubated in PCR cyclers at 42°C for 30 minutes followed by 95°C for 3 minutes. Quantitative reverse transcription polymerase chain reaction (RT-qPCR) was performed with ABI StepOnePlus sequence detector (Applied Biosystems) using TaqMan gene expression assay (Thermo Fischer Scientific, #4370048) with following probes: TBP (Mm 00446973_m1), TSC22D4 (Mm 00470231_m1), Fasn (Mm00662319_m1), Acc1 (Mm01304279_m1), Acly (Mm00652520_m1), Scd1 (Mm00772290_m1), Gck (Mm00439129_m1), Pepck (Mm00440636_m1), Pgc1α (Mm00447183_m1). Amplification of specific transcripts was confirmed by melting curve profiles (cooling the sample to 68°C and heating slowly to 95°C with fluorescence measurement) at the end of each PCR.

9.8. Cell lysis and Co-immunoprecipitation (Co-IP)

Cells were lysed in ice-cold CHAPS lysis buffer. Lysed cells were centrifuged at 12000 rpm for 5 minutes at 4°C and supernatants were collected. Protein concentrations were measured with Bradford assay (BioRad, #5000006). Anti-Flag affinity gel (Sigma, #A2220) or HA agarose beads (Sigma, #A2095) were used for immunoprecipitation. Before use, the beads were washed with lysis buffer via centrifugation at 4000 rpm for 2 minutes. Cell lysates were incubated with the beads for 2 hours at 4°C on a rotator for immunoprecipitation. The beads were washed 3 times with 1 ml ice-cold lysis buffer with centrifugation steps. 4xlaemmli buffer was added to the samples, which were then boiled at 95°C for 5 minutes.

9.9. Western blot analysis

Protein extracts and immunoprecipitates were run on 10% (BioRad, #4561036) or any kDa (BioRad, #4569036) precast protein gels in sodium dodecyl sulfate (SDS) buffer followed by electrophoretic transfer of proteins to

nitrocellulose membrane (BioRad, #2895). After blocking in 5% nonfat dried milk (Roth, #T145) diluted in tris-buffered saline and 1% tween 20 (TBS-T) for 1 hour at RT, the membranes were incubated with primary antibodies specific for TSC22D4 (home-made, by PINEDA Antibody Service), Flag (#A8592, Sigma), HA (#2999, CST), Myc (#2040, CST), p-Akt (S473) (#4060, CST), p-Akt (T308) (#13038, CST), Akt (#9272 ,CST), Akt1 (#2938, CST), Akt2 (#3063, CST), p-GSK3 beta (S9) (#05-643, Upstate), GSK3 beta (#05-412, Upstate), p-Foxo1 (S256) (#9461, CST), Foxo1 (#2880, CST), p-p70S6K1 (#9234, CST), p70S6K1 (#9209, CST), pS6 (#2271, 2215), S6 (#2217, CST), VCP (ab11433, Abcam). Primary antibodies were incubated in 3% BSA overnight at 4°C on a rocker. After 3 times washing with TBS-T for 10 minutes, membranes were incubated with HRP-conjugated secondary antibodies targeting rabbit or mouse IgG for 1 hour at RT. HRP-conjugated veriblot (Abcam, #131366) or rabbit light chain (Cell signaling, #93702) was used as a secondary antibody to avoid background noise in endogenous co-IP experiments. Immunoblots were developed using ECL western blotting substrate (Sigma, #GERPN2209 or Amersham, #GERPN2236).

9.10. Tissue lipid extraction

Lipids were extracted from frozen and pulverized liver tissue using chloroform: methanol (2:1). One spoon of the pulverized liver was transferred into a 2 ml tube containing 1.5 ml chloroform/methanol and a steel bead. The tissue was homogenized using a tissue lyzer for 30 seconds at a frequency of 30 Hz three times. For the lipid extraction, samples were incubated on a rotating wheel at room temperature for 20 minutes. Samples were centrifuged at 13000 rpm for 30 min at room temperature, and 1 ml of the supernatants were transferred to fresh tubes. The organic layer was mixed with 200 µl 0.9% sodium chloride and the aqueous solution was discarded. The solution was centrifuged at 2000 rpm for 5 min. 750 µl of the lower organic layerwas transferred to a fresh tube and stored at -80 °C. For lipid resuspension, 40 µl of triton-X 100:chloroform (1:1) was pipetted into new tubes and 200 µl of the organic lipid sample was added. The reagents were mixed and the solvent was evaporated using a speed vac. The residue containing the hydrophobic contents of the liver was resuspended in 2 ml water and stored at -20°C until further use. Cholesterol and triglyceride levels were determined using commercial kits (Randox, #CH200; Human, #10724, respectively). Before lipid extraction, the weight of the aliquoted liver was measured, and the end values were normalized to the initialaliquoted liver weight (mg).

9.11. Immunofluorescence (IF) and Immunohistochemistry (IHC)

9.11.1. Cells

For siRNA experiments (siTSC22D4 or siNC), Hepa1-6 cells were seeded on collagen-coated (10 $\mu g/cm^2$) glass coverslips in 24-well plates and maintained in DMEM with 10% FBS. Following the siRNA transfection protocol, the cells were washed with phosphate-buffered saline (PBS, Gibco, #10010023) and fixed with 4% Histofix (Roti, #P087) for 15 minutes at RT in humid chambers. After 2 washes with PBS each for 5 minutes, cells were permeabilized in 0.1% Triton-X (Gerbu, #2999) in PBS for 5 minutes at RT. After washing with PBS, cells were incubated in a blocking solution (10% horse serum in PBS) for 1 hour at RT. Following the incubation, cells were washed 3 times with PBS and incubated with primary antibody (TSC22D4, homemade Pineda) in 5% horse serum in PBS overnight at 4°C. After washing with PBS, cells were incubated with secondary antibody (Alexa 568 goat anti-rabbit IgG (H+L), #A11011) in 5% horse serum in PBS for 2 hours at RT. The coverslips were mounted onto glass slides with mounting media containing DAPI (Invitrogen, #P36935). The cells were analyzed with a Zeiss fluorescent microscope with 40x magnification and imaged with Zen software.

Flag-WT-TSC22D4 and HA-Akt1 transfected Hepa1-6 cells were seeded (5000 cells/well) into 4-well chamber slides (Thermo Fisher Scientific, #154526). The cells were fixed, blocked, stained and mounted as described above. Primary antibodies anti-Flag (Sigma, #F1804) and anti-HA (Santa Cruz, #Sc7392)); and secondary antibodies Alexa Fluor® 488 goat anti-mouse (Invitrogen, #A11029) and Alexa Fluor® 568 goat anti-rabbit (Invitrogen, #A11011) were diluted in 5% horse serum in PBS.

For the IF experiments where we used anabolic stimulations, Flag-TSC22D4 transfected Hepa1-6 cells were seeded into 4 well chamber slides. After overnight starvation, the cells were either stimulated with glucose [20 mM] for 30 minutes and with insulin [100 nM] for another 30 minutes, or rotenone and antimycin [1 mM] for 1 hour. Negative controls for the immunostaining experiments were performed by omitting primary antibodies.

For endogenous Akt1 staining, the cells were seeded into 4 well chambers and stained in starved, glucose/insulin and rotenone/antimycin stimulated conditions. As described above, the cells were incubated in a blocking solution, followed by incubation with primary antibody (anti-Akt1, Cell Signaling, #2938) and secondary antibody (Alexa Fluor® 568 goat anti-rabbit). Cells then were mounted and imaged as described above.

9.11.2. Lipid droplet analysis

Quantification of lipid amount was morphometrically determined on H&E stained liver sections following a previously published protocol [Feuchtinger, 2015 #76]. The H&E stained tissue sections were scanned with an AxioScan.Z1 digital slide scanner (Zeiss, Jena, Germany) equipped with a 20x magnification objective and evaluated using digital image analysis (Definiens Developer XD 2; Definiens AG, Germany). The calculated parameter was the percentage of surface areas considered as lipid droplets, divided by the surface area of the entire analyzed liver tissue for each sample.

Paraffin sectioning of formaldehyde (formalin) fixed livers and H&E staining was performed by the Center for model system and comparative pathology (CMCP) lab at Heidelberg University. Lipid droplet analysis was performed in the pathology department at Helmholtz Zentrum München.

9.11.3. Ki67 analysis

Ki67 staining was performed to analyze dividing cells in vector control and D2+TSC overexpressing mice livers. Paraffin sectioning of formaldehyde (formalin) fixed livers and Ki67 staining was performed by the Center for model system and comparative pathology (CMCP) lab at Heidelberg University. Quantification of Ki67 positive cells were measured by the pathology department at Helmholtz Zentrum München.

9.11.4. Proximity ligation assay (PLA)

PLA was performed in Hepa1-6 cells, grown in chamber slides, for *in situ* detection of TSC22D4-Akt1 interaction according to the manufacturer´s instructions (Sigma, DUO092002).

9.12. Software and data analysis

Adobe Illustrator and IBS (Illustrator for biological sequences) programs were used to create figures and cartoons of deletion mutants. ImageJ was used to analyze immunofluorescence results and quantify signaling intensities. ImageLab was used to analyze and prepare western blot results and quantify signal intensities. For statistical analyses, Graphpad was used to perform appropriate statistical tests as specified in the figures (significance level 0.05).

10. References

1. World Health, O., *Global report on diabetes*. 2016, Geneva, Switzerland: World Health Organization. 86 pages : illustrations (colour).
2. Atkinson, M.A., G.S. Eisenbarth, and A.W. Michels, *Type 1 diabetes.* Lancet, 2014. **383**(9911): p. 69-82.
3. Cerf, M.E., *Beta cell dysfunction and insulin resistance.* Front Endocrinol (Lausanne), 2013. **4**: p. 37.
4. Jumpertz, R., et al., *Assessment of non-insulin-mediated glucose uptake: association with body fat and glycemic status.* Metabolism, 2010. **59**(10): p. 1396-401.
5. Rojas, J.M. and M.W. Schwartz, *Control of hepatic glucose metabolism by islet and brain.* Diabetes Obes Metab, 2014. **16 Suppl 1**: p. 33-40.
6. Demir, S., et al., *Emerging Targets in Type 2 Diabetes and Diabetic Complications.* Adv Sci (Weinh), 2021. **8**(18): p. e2100275.
7. Ahlqvist, E., et al., *Novel subgroups of adult-onset diabetes and their association with outcomes: a data-driven cluster analysis of six variables.* Lancet Diabetes Endocrinol, 2018. **6**(5): p. 361-369.
8. Balakrishnan, S., S. Dhavamani, and C. Prahalathan, *beta-Cell specific transcription factors in the context of diabetes mellitus and beta-cell regeneration.* Mech Dev, 2020. **163**: p. 103634.
9. Adeva-Andany, M.M., et al., *Liver glucose metabolism in humans.* Biosci Rep, 2016. **36**(6).
10. Rui, L., *Energy metabolism in the liver.* Compr Physiol, 2014. **4**(1): p. 177-97.
11. Guertin, D.A., et al., *Ablation in mice of the mTORC components raptor, rictor, or mLST8 reveals that mTORC2 is required for signaling to Akt-FOXO and PKCalpha, but not S6K1.* Dev Cell, 2006. **11**(6): p. 859-71.
12. Huang, X., et al., *The PI3K/AKT pathway in obesity and type 2 diabetes.* Int J Biol Sci, 2018. **14**(11): p. 1483-1496.
13. Pauta, M., et al., *Akt-mediated foxo1 inhibition is required for liver regeneration.* Hepatology, 2016. **63**(5): p. 1660-74.
14. Haggblad Sahlberg, S., et al., *Different functions of AKT1 and AKT2 in molecular pathways, cell migration and metabolism in colon cancer cells.* Int J Oncol, 2017. **50**(1): p. 5-14.
15. Martelli, A.M., et al., *The emerging multiple roles of nuclear Akt.* Biochim Biophys Acta, 2012. **1823**(12): p. 2168-78.
16. Gonzalez, E. and T.E. McGraw, *The Akt kinases: isoform specificity in metabolism and cancer.* Cell Cycle, 2009. **8**(16): p. 2502-8.
17. Manning, B.D. and A. Toker, *AKT/PKB Signaling: Navigating the Network.* Cell, 2017. **169**(3): p. 381-405.
18. Rayasam, G.V., et al., *Glycogen synthase kinase 3: more than a namesake.* Br J Pharmacol, 2009. **156**(6): p. 885-98.
19. Danielpour, D. and K. Song, *Cross-talk between IGF-I and TGF-beta signaling pathways.* Cytokine Growth Factor Rev, 2006. **17**(1-2): p. 59-74.
20. Franke, T.F., *Intracellular signaling by Akt: bound to be specific.* Sci Signal, 2008. **1**(24): p. pe29.
21. Du, K. and P.N. Tsichlis, *Regulation of the Akt kinase by interacting proteins.* Oncogene, 2005. **24**(50): p. 7401-9.
22. Jahn, T., et al., *Role for the adaptor protein Grb10 in the activation of Akt.* Mol Cell Biol, 2002. **22**(4): p. 979-91.

23. Yuan, Z.Q., et al., *ArgBP2γ interacts with Akt and p21-activated kinase-1 and promotes cell survival.* J Biol Chem, 2016. **291**(43): p. 22845.
24. Du, K., et al., *TRB3: a tribbles homolog that inhibits Akt/PKB activation by insulin in liver.* Science, 2003. **300**(5625): p. 1574-7.
25. Cheng, K.K., et al., *APPL1 potentiates insulin-mediated inhibition of hepatic glucose production and alleviates diabetes via Akt activation in mice.* Cell Metab, 2009. **9**(5): p. 417-27.
26. Saito, T., et al., *The interaction of Akt with APPL1 is required for insulin-stimulated Glut4 translocation.* J Biol Chem, 2007. **282**(44): p. 32280-7.
27. Oates, M.E., et al., *D²P²: database of disordered protein predictions.* Nucleic Acids Res, 2013. **41**(Database issue): p. D508-16.
28. Bondos, S.E., A.K. Dunker, and V.N. Uversky, *Intrinsically disordered proteins play diverse roles in cell signaling.* Cell Commun Signal, 2022. **20**(1): p. 20.
29. Hendus-Altenburger, R., et al., *A phosphorylation-motif for tuneable helix stabilisation in intrinsically disordered proteins - Lessons from the sodium proton exchanger 1 (NHE1).* Cell Signal, 2017. **37**: p. 40-51.
30. Hilser, V.J. and E.B. Thompson, *Intrinsic disorder as a mechanism to optimize allosteric coupling in proteins.* Proc Natl Acad Sci U S A, 2007. **104**(20): p. 8311-5.
31. Liu, Z. and Y. Huang, *Advantages of proteins being disordered.* Protein Sci, 2014. **23**(5): p. 539-50.
32. *UniProt: the universal protein knowledgebase in 2021.* Nucleic Acids Res, 2021. **49**(D1): p. D480-d489.
33. Kester, H.A., et al., *Transforming growth factor-beta-stimulated clone-22 is a member of a family of leucine zipper proteins that can homo- and heterodimerize and has transcriptional repressor activity.* J Biol Chem, 1999. **274**(39): p. 27439-47.
34. Shibanuma, M., T. Kuroki, and K. Nose, *Isolation of a gene encoding a putative leucine zipper structure that is induced by transforming growth factor beta 1 and other growth factors.* J Biol Chem, 1992. **267**(15): p. 10219-24.
35. Fiol, D.F., S.K. Mak, and D. Kültz, *Specific TSC22 domain transcripts are hypertonically induced and alternatively spliced to protect mouse kidney cells during osmotic stress.* Febs j, 2007. **274**(1): p. 109-24.
36. Dragotto, J., et al., *The interplay between TGF-β-stimulated TSC22 domain family proteins regulates cell-cycle dynamics in medulloblastoma cells.* J Cell Physiol, 2019. **234**(10): p. 18349-18360.
37. Kester, H.A., et al., *Expression of TGF-beta stimulated clone-22 (TSC-22) in mouse development and TGF-beta signalling.* Dev Dyn, 2000. **218**(4): p. 563-72.
38. Choi, S.J., et al., *Tsc-22 enhances TGF-beta signaling by associating with Smad4 and induces erythroid cell differentiation.* Mol Cell Biochem, 2005. **271**(1-2): p. 23-8.
39. Yasukawa, T., et al., *NRBP1-Containing CRL2/CRL4A Regulates Amyloid β Production by Targeting BRI2 and BRI3 for Degradation.* Cell Rep, 2020. **30**(10): p. 3478-3491.e6.
40. Canterini, S., et al., *Multiple TSC22D4 iso-/phospho-glycoforms display idiosyncratic subcellular localizations and interacting protein partners.* Febs j, 2013. **280**(5): p. 1320-9.
41. Zhang, X., et al., *Promotion of cellular senescence by THG-1/TSC22D4 knockout through activation of JUNB.* Biochem Biophys Res Commun, 2020. **522**(4): p. 897-902.
42. Canterini, S., F. Mangia, and M.T. Fiorenza, *Thg-1 pit gene expression in granule cells of the developing mouse brain and in their synaptic targets, mature Purkinje, and mitral cells.* Dev Dyn, 2005. **234**(3): p. 689-97.

43. Canterini, S., et al., *Subcellular TSC22D4 localization in cerebellum granule neurons of the mouse depends on development and differentiation.* Cerebellum, 2012. **11**(1): p. 28-40.
44. Canterini, S., et al., *THG-1pit moves to nucleus at the onset of cerebellar granule neurons apoptosis.* Mol Cell Neurosci, 2009. **40**(2): p. 249-57.
45. Liang, F., et al., *TSC22D2 interacts with PKM2 and inhibits cell growth in colorectal cancer.* Int J Oncol, 2016. **49**(3): p. 1046-56.
46. Li, Q., et al., *Yeast two-hybrid screening identified WDR77 as a novel interacting partner of TSC22D2.* Tumour Biol, 2016. **37**(9): p. 12503-12512.
47. Tran, S.T.P., et al., *Generation of non-standard macrocyclic peptides specifically binding TSC-22 homologous gene-1.* Biochem Biophys Res Commun, 2019. **516**(2): p. 445-450.
48. Ayroldi, E., et al., *Modulation of T-cell activation by the glucocorticoid-induced leucine zipper factor via inhibition of nuclear factor kappaB.* Blood, 2001. **98**(3): p. 743-53.
49. Ayroldi, E., et al., *GILZ mediates the antiproliferative activity of glucocorticoids by negative regulation of Ras signaling.* J Clin Invest, 2007. **117**(6): p. 1605-15.
50. Ayroldi, E., et al., *Glucocorticoid-induced leucine zipper inhibits the Raf-extracellular signal-regulated kinase pathway by binding to Raf-1.* Mol Cell Biol, 2002. **22**(22): p. 7929-41.
51. Ayroldi, E., et al., *L-GILZ binds p53 and MDM2 and suppresses tumor growth through p53 activation in human cancer cells.* Cell Death Differ, 2015. **22**(1): p. 118-30.
52. Ekim Üstünel, B., et al., *Control of diabetic hyperglycaemia and insulin resistance through TSC22D4.* Nat Commun, 2016. **7**: p. 13267.
53. Jones, A., et al., *TSC22D4 is a molecular output of hepatic wasting metabolism.* EMBO Mol Med, 2013. **5**(2): p. 294-308.
54. Wolff, G., et al., *Hepatocyte-specific activity of TSC22D4 triggers progressive NAFLD by impairing mitochondrial function.* Mol Metab, 2022. **60**: p. 101487.
55. Anstee, Q.M. and R.D. Goldin, *Mouse models in non-alcoholic fatty liver disease and steatohepatitis research.* Int J Exp Pathol, 2006. **87**(1): p. 1-16.
56. Loft, A., et al., *Liver-fibrosis-activated transcriptional networks govern hepatocyte reprogramming and intra-hepatic communication.* Cell Metab, 2021. **33**(8): p. 1685-1700.e9.
57. Dewidar, B., et al., *TGF-β in Hepatic Stellate Cell Activation and Liver Fibrogenesis-Updated 2019.* Cells, 2019. **8**(11).
58. Sakurai, M., et al., *TSC22D4 promotes TGFβ1-induced activation of hepatic stellate cells.* Biochem Biophys Res Commun, 2022. **618**: p. 46-53.
59. Demir, S., et al., *TSC22D4 interacts with Akt1 to regulate glucose metabolism.* Science Advances, 2022.
60. Yang, Z.H., et al., *Diet high in fat and sucrose induces rapid onset of obesity-related metabolic syndrome partly through rapid response of genes involved in lipogenesis, insulin signalling and inflammation in mice.* Diabetol Metab Syndr, 2012. **4**(1): p. 32.
61. Demir, S., et al., *TSC22D4 interacts with Akt1 in response to metabolic and stress signals.* bioRxiv, 2021: p. 2021.12.20.473554.
62. van der Lee, R., et al., *Classification of intrinsically disordered regions and proteins.* Chem Rev, 2014. **114**(13): p. 6589-631.
63. Lipok, M., et al., *Identification of a peptide antagonist of the FGF1-FGFR1 signaling axis by phage display selection.* FEBS Open Bio, 2019. **9**(5): p. 914-924.
64. Petersen, M.C. and G.I. Shulman, *Mechanisms of Insulin Action and Insulin Resistance.* Physiol Rev, 2018. **98**(4): p. 2133-2223.
65. Fernandez-Marcos, P.J. and J. Auwerx, *Regulation of PGC-1α, a nodal regulator of mitochondrial biogenesis.* Am J Clin Nutr, 2011. **93**(4): p. 884s-90.

66. Scarpulla, R.C., *Metabolic control of mitochondrial biogenesis through the PGC-1 family regulatory network.* Biochim Biophys Acta, 2011. **1813**(7): p. 1269-78.
67. Seebacher, F., et al., *Hepatic lipid droplet homeostasis and fatty liver disease.* Semin Cell Dev Biol, 2020. **108**: p. 72-81.
68. Liu, X., et al., *The role of AMPK/mTOR/S6K1 signaling axis in mediating the physiological process of exercise-induced insulin sensitization in skeletal muscle of C57BL/6 mice.* Biochim Biophys Acta, 2012. **1822**(11): p. 1716-26.
69. Um, S.H., D. D'Alessio, and G. Thomas, *Nutrient overload, insulin resistance, and ribosomal protein S6 kinase 1, S6K1.* Cell Metab, 2006. **3**(6): p. 393-402.
70. Finck, B.N. and D.P. Kelly, *PGC-1 coactivators: inducible regulators of energy metabolism in health and disease.* J Clin Invest, 2006. **116**(3): p. 615-22.
71. Kim, J., et al., *AMPK activators: mechanisms of action and physiological activities.* Exp Mol Med, 2016. **48**(4): p. e224.
72. Lenz, S., et al., *Reliable identification of protein-protein interactions by crosslinking mass spectrometry.* Nat Commun, 2021. **12**(1): p. 3564.
73. Rao, V.S., et al., *Protein-protein interaction detection: methods and analysis.* Int J Proteomics, 2014. **2014**: p. 147648.
74. Feuchtinger, A., et al., *Image analysis of immunohistochemistry is superior to visual scoring as shown for patient outcome of esophageal adenocarcinoma.* Histochem Cell Biol, 2015. **143**(1): p. 1-9.
75. Sachs, S., et al., *Plasma proteome profiles treatment efficacy of incretin dual agonism in diet-induced obese female and male mice.* Diabetes Obes Metab, 2021. **23**(1): p. 195-207.

11. Appendices

Review Article

REVIEW

ADVANCED SCIENCE Open Access

www.advancedscience.com

Emerging Targets in Type 2 Diabetes and Diabetic Complications

*Sevgican Demir, Peter P. Nawroth, Stephan Herzig, and Bilgen Ekim Üstünel**

Type 2 diabetes is a metabolic, chronic disorder characterized by insulin resistance and elevated blood glucose levels. Although a large drug portfolio exists to keep the blood glucose levels under control, these medications are not without side effects. More importantly, once diagnosed diabetes is rarely reversible. Dysfunctions in the kidney, retina, cardiovascular system, neurons, and liver represent the common complications of diabetes, which again lack effective therapies that can reverse organ injury. Overall, the molecular mechanisms of how type 2 diabetes develops and leads to irreparable organ damage remain elusive. This review particularly focuses on novel targets that may play role in pathogenesis of type 2 diabetes. Further research on these targets may eventually pave the way to novel therapies for the treatment—or even the prevention—of type 2 diabetes along with its complications.

1. Introduction

Diabetes mellitus is a chronic, metabolic disorder characterized by abnormally high blood glucose levels known as hyperglycemia. The Greek word diabetes means *to* siphon or to pass through and the Latin word mellitus means sweet, referring to high sugar levels in the urines of patients with diabetes. The earliest mention of diabetes dates back to 1552 BC written on an Egyptian papyrus, making it one of the oldest diseases described in human history. Initial attempts for treating diabetes mainly focused on herbal extracts and dietary interventions. Patients with diabetes had very poor prognosis with very low quality of life and particularly it used to be a death sentence for children. It was not until the discovery of insulin in 1921 by Frederik G. Banting and Charles Best at the University of Toronto, when life-saving treatments started to take off.[1,2] Later in 1923, Banting and John Macleod received the Nobel Prize in Physiology or Medicine for their discovery of insulin. Banting shared his winnings with his assistant Best, Macleod, on the other hand, shared it with James Collip, with whose help insulin was successfully purified.

We can describe diabetes as a disease of insulin insufficiency or impaired insulin action. Mainly, two main types of diabetes exist: type 1 and type 2. Type 1 diabetes develops at early stages of life due to an auto-immune disorder where the cells of the immune system attack the insulin producing β cells of the pancreas. Type 2 diabetes, however, develops later in life, due to systemic dysfunctions in metabolic homeostasis. Genetic background plays a critical role in predisposing individuals to type 2 diabetes, where unhealthy eating habits and sedentary life style act as powerful triggers.[3,4] Unlike type 1 diabetes, type 2 diabetes is relatively heterogeneous and very complex, involving too many pathophysiological mechanisms that not only affect pancreas but also the metabolic organs, making effective treatment very challenging.

In 2018, Groop and colleagues stratified patients with type 2 diabetes into five different subgroups based on six variables: age at diagnosis, body-mass index (BMI), insulin resistance, beta cell function, Hb1Ac levels, and glutamate decarboxylase antibodies. Each cluster represented a specific subset of patients with differing risk for particular diabetic complications, which were: 1) severe autoimmune diabetes; 2) severe insulin-deficient diabetes; 3) severe insulin-resistant diabetes; 4) mild obesity-related diabetes; and 5) mild age-related diabetes.[5] Similar to type 2 diabetes patients, individuals that are not yet diagnosed but are at a high risk of developing it, were also stratified into six different subgroups that could predict the complications such as diabetic kidney disease without rapid progression to overt type 2 diabetes.[6] These findings indicate that the pathophysiological variation between individuals already exists before type 2 diabetes develops. These findings by independent groups once again provide the evidence for heterogeneity and complexity of

S. Demir, Prof. P. P. Nawroth, Prof. S. Herzig, Dr. B. Ekim Üstünel
Institute for Diabetes and Cancer (IDC)
Helmholtz Center Munich
Ingolstädter Landstr. 1, Neuherberg 85764, Germany
E-mail: bilgen.ekimuestuenel@med.uni-heidelberg.de

S. Demir, Prof. P. P. Nawroth, Prof. S. Herzig, Dr. B. Ekim Üstünel
Joint Heidelberg - IDC Translational Diabetes Program
Internal Medicine 1
Heidelberg University Hospital
Im Neuenheimer Feld 410, Heidelberg 69120, Germany

S. Demir, Prof. P. P. Nawroth, Prof. S. Herzig, Dr. B. Ekim Üstünel
DZD
Deutsches Zentrum für Diabetesforschung
Ingolstädter Landstraße 1, Neuherberg 85764, Germany

S. Demir, Prof. P. P. Nawroth, Prof. S. Herzig, Dr. B. Ekim Üstünel
Department of Internal Medicine 1 and Clinical Chemistry
Heidelberg University Hospital
Im Neuenheimer Feld 410, Heidelberg 69120, Germany

The ORCID identification number(s) for the author(s) of this article can be found under https://doi.org/10.1002/advs.202100275

DOI: 10.1002/advs.202100275

type 2 diabetes most likely due to aberrant regulation of different signaling pathways in different target tissues. For instance, it is possible that in severe autoimmune diabetes, defective immune system is responsible for development of type 2 diabetes, whereas in mild age-related diabetes, pathways that play role in aging and cell senescence in β-cells might play a role. Dissecting these tissue-specific signaling pathways and identifying novel targets that contribute to type 2 diabetes will definitely, in the future, improve the current taxonomy of diabetes and contribute to precision medicine.

Although the precise definition of sub-clusters is still a matter of debate and it may take some time to establish protocols and categorize the patients, such stratification will certainly contribute to identify patients that are at risk for developing type 2 diabetes and diabetic complications, which will lead to personalized diabetes therapies, which unfortunately do not exist yet.

Diabetes is a global endemic. In 2019, 463 million of adults (20–79 years old) were living with diabetes; and again–only in–2019, diabetes caused 4.2 million deaths. The number of patients with diabetes is increasing at a very high rate, estimated to reach 700 million by 2045. Diabetes is not only about high blood glucose levels. Patients with diabetes also suffer from a number of complications, which are sometimes already present when diabetes is diagnosed such as diabetic retinopathy; or they develop later during the course of the disease.[7,8] These complications involve dysfunctions in many vital organs all over the body; mainly kidney, cardiovascular system, retina, and the nervous system. Fibrosis of the liver and fibrosis of the lungs as well as cognitive dysfunction are also emerging as novel pathologies that develop secondary to diabetes.

In this review, we will introduce the novel targets/concepts that play role in pathogenesis of type 2 diabetes and the diabetic complications both in the context of peripheral organs and β-cells of the pancreas. We will initially focus on insulin and glucagon signaling pathways which are deregulated in type 2 diabetes. We will discuss insulin resistance in metabolic organs liver, skeletal muscle, and adipose tissue separately due to the tissue specific mechanisms. Then, we will discuss the role of β-cell dysfunction in pathogenesis of type 2 diabetes.

Finally, we will give an overview of the state-of-the-art in our current understanding of diabetic complications in peripheral organs including the kidney, cardiovascular system, retina, nerve, and liver.

For this review article, we particularly focused on publications that emerged after 2016. Due to immense number of articles, we specifically chose the targets that showed compelling in vivo evidence regarding their potential role in development of type 2 diabetes and its late complications, summarized in **Table 1**.

2. Insulin and Insulin Signaling Pathway

Insulin (literally meaning island in Latin) is a peptide hormone produced and secreted by the β-cells of the pancreas upon elevated blood glucose levels. Insulin acts on metabolic organs such as liver, skeletal muscle, and adipose tissue to promote storage of glucose in the form of glycogen and/or lipids, lowering blood glucose levels. Insulin also crosses the blood-brain-barrier regulating key functions in the central nervous system such as food intake, peripheral metabolism, memory, and cognition.[9]

When bound by insulin, insulin receptor (IR), a receptor tyrosine kinase, homodimerizes, and autophosphorylates to recruit and phosphorylate its mediator proteins insulin substrate 1 and 2 (IRS1/2) on tyrosine residues (**Figure 1**).[10] IRS1/2 in turn recruits the lipid kinase phosphatidylinositol 3-kinase (PI3K) to the cell membrane, which phosphorylates the lipid phosphatidylinositol (3,4)-bisphosphate (PIP_2) and converts it to phosphatidylinositol (3,4,5)-trisphosphate (PIP_3). PIP_3 in turn recruits 3-phosphoinositide-dependent protein kinase 1 (PDK1) and protein kinase B (PKB)/Akt to the cell membrane where PDK1 and mechanistic target of rapamycin complex 2 (mTORC2) phosphorylate Akt on T308 and S473, respectively.[10] Double phosphorylation of Akt leads to its full activation, which phosphorylates a wide range of targets including glycogen synthase kinase 3 β (GSK3β), forkhead box protein O1 (FoxO1), and tuberous sclerosis complex 2 (TSC2) to promote glycogen and lipid synthesis, protein translation, cell growth, and glucose uptake (Figure 1).[10] When cells are simulated with insulin, activated Akt phosphorylates TSC2 on several residues to impair the function of TSC complex, leading to mTORC1 activation and subsequent phosphorylation of mTORC1 downstream targets including p70 ribosomal protein S6 kinase 1 (S6K1) and 4E binding protein (4E-BP1). The non-canonical IκB kinases IKKϵ and TANK-binding kinase 1 (TBK1) directly phosphorylate mTOR within its kinase domain and promote mTORC1 signaling to its downstream targets.[11,12] Indeed amlexanox, an inhibitor of IKKϵ/TBK1 kinases, alleviates obesity related metabolic dysfunctions such as liver steatosis and adipose tissue inflammation while promoting weight loss and insulin sensitivity not only in mice but also in a subset of obese type 2 diabetes patients.[13] When bound by insulin, IR also recruits and phosphorylates Shc adaptor proteins p46 and p52, which in turn navigate the insulin signaling toward RAS dependent ERK activation to promote cell proliferation.[14] $p66^{Shc}$, another isoform of Shc proteins, on the other hand, plays role in metabolic regulation and energy expenditure in metabolic tissues such as liver, muscle, and brown adipose tissue.[15–17] Yet whether $p66^{Shc}$ alleviates or exacerbates metabolic disorders remains elusive as almost all of the in vivo studies depend on $p66^{Shc}$ whole body knockouts. It will be critical in the future to create the tissue-specific $p66^{Shc}$ knockout mouse models to dissect its role in glucose and lipid homeostasis in corresponding organs.[18]

Very recent findings indicate that IR also translocate to nucleus where it directly engages at transcriptionally active promoters together with DNA polymerase II (Figure 1).[19] Target promoters that IR binds to include genes that regulate lipid metabolism and protein synthesis as well disease related genes implicated in diabetes, neurodegeneration, and cancer. Parallel to its role at the cytoplasm, IR localization to nucleus elevates upon insulin stimulation and its nuclear re-localization is impaired in insulin resistant ob/ob mouse livers.[19]

3. Type 2 Diabetes: At the Crossroads of Insulin Resistance and Glucagon Action

Type 2 diabetes is a very heterogenous and complex disease that develops due to aberrant regulation of many signaling pathways. In this section, we will describe how insulin resistance develops in metabolic organs and what glucagon does in return.

Table 1. List of novel targets with emerging implications in type 2 diabetes.

Section described	Target	Effect/Potential role	Reference
Insulin signaling pathway	Amlexanox inhibition of TBK1/IKKe	Alleviates obesity related metabolic dysfunctions	[13]
	p66Shc	Glucose and lipid homeostasis	[18]
	Nuclear insulin receptor (IR)	Glucose and lipid metabolism, protein synthesis	[19]
Insulin resistance in liver	IQGAP1	Induces insulin resistance and glucose intolerance	[22]
	TSC22D4	Promotes insulin resistance and glucose intolerance	[27]
	CHOP	Apoptotic cell death due to chronic unfolded protein response	[36]
	Vitamin D receptor (VDR)	Blunts ER stress and UPR	[37]
	Them2/PC-TP	Reduce ER stress and enhances hepatic insulin resistance	[38]
	Cx43	Plays role in ER stress dissemination to adjacent cells	[39]
	Differential expression of IRS1 and IRS2	Plays role on distinction of gluconeogenic and lipogenic program	[40–41]
Insulin resistance in skeletal muscle	Glut4 specific motifs	Modulates Glut4 trafficking	[44]
	Non-canonical PI3K-Rac1-PAK1 signaling	An alternative axis for GSC translocation upon insulin engagement	[46]
	ApoJ	A novel hepatokine regulating muscle glucose and lipid metabolism	[48]
	LRP2	Required for insulin-induced IR internalization	[48]
	Lkb1	Skeletal muscle protein homeostasis	[49]
	β-AR agonist 5'HOD	Promotes anabolic functions in muscle	[52]
	Quercetin	Suppresses muscle atrophy	[53]
	Myostatin	Suppresses muscle growth	[54–56]
Insulin resistance in adipose tissue	CCL2	Macrophage infiltration into adipose tissue insulin resistance	[57]
	ANT2	Increases adipose tissue hypoxia	[64]
	LTB4/LTB4R1	Leukocyte infiltration into adipose tissue and cytokine production	[66]
	miR-155	Exacerbates insulin resistance	[67]
	Sphk1	Promotes inflammation in adipose tissue and glucose intolerance	[68]
	DES1	Causes insulin resistance	[69]
Glucagon signaling	Klf9	Regulates PGC1alpha	[81]
	β-arrestin 2	Regulates GcgR	[88]
	SRI-37330	Promotes glucose handling in T1D and T2D	[89]
	GLP-1R/GcgR	Regulates hyperglycemic effects of glucagon action	[91]
Role of β-cells in T2D	Inceptor	Inhibits INSR and IGFR1	[103]
	PLCDX3	Promotes GSIS and insulin content	[104]
	NGF	Promotes glucose induced insulin secretion in β-cells	[110]
	TrkA	Promotes insulin granule exocytosis	[110]
	Tcf7l2	Regulates glucose handling and beta cell function	[111]
Diabetic complications	Methylglyoxal modifications	Increase upon hyperglycemic flux and impaired detoxification	[122–126]
Diabetic kidney disease	Angiotensin II	Induces ROS production and activates TGFβ1 signaling	[142]
	SMPDL3b	Impaires insulin/Akt signaling in podocytes	[152]
	JAML	Promotes excessive lipid accumulation and renal lipotoxicity	[154]
	VEGF-B	Elevates glomerular lipid content and causes insulin resistance	[128]
	Ketone Bodies	Blunt hyperactivated mTORC1 signaling and attenuate renal damage	[161]
Cardiovascular complications	QKI-7	Promotes mRNA degradation of essential genes for EC function	[176]
	Endothelin B receptor	Increases NO levels to protect against the proatherogenic insults	[177]
	Sarcolipin	Causes diabetic heart failure	[178]
	HDAC4	Protects from diabetic heart failure	[179]
	Exophers	Maintain a healthy heart function	[180]

(*Continued*)

Table 1. (Continued).

Section described	Target	Effect/Potential role	Reference
Diabetic retinopathy	Sema4d	Biomarker for anti-VEGF-1 therapy	[183]
	Ang1	Promotes TGFβ and PDGF signaling	[184]
	Ang2	Promote blood retina barrier permeability	[185]
	circRNA-cPWWP2A	Impair miR-579 function and upregulate Ang1/Occludin/SIRT1 expression	[186]
	circRNA-cZNF532	Regulates pericyte function and vascularization	[187]
	Prostaglandin E2 and its receptor	Induces L1β and inflammasome NLRP3-ASC signaling	[190]
	Ceramide 6	Impairs JNK function and prevents apoptosis	[191]
	DHA and EPA	Plays protective role in pathogenesis of diabetic retinopathy	[192]
	12-HETE or 15S-HETE	Exacerbate the progression of diabetic retinopathy	[192]
	Linagliptin	Shows anti-angiogenic effects	[193]
Diabetic neuropathy	Na(v) 1.8	Increases hyperalgesia	[197]
	HCN2	Increases hyperalgesia	[198]
	CXCL12/CXCR4	Promotes initiation of mechanical allodynia	[199]
	Notch1 or TLR4	Alleviates mechanical allodynia and thermal hyperalgesia thresholds	[204]
Liver fibrosis	circRNA-SCAR	Inhibits mitochondrial ROS output and fibroblast activation	[207]
	AMPK-Caspase signaling	Inhibits inflammation and liver damage by controlling apoptosis	[208]
	TAZ	Promotes the expression of pro-fibrogenic genes and proliferation	[210]
Other complications of T2D	RAGE	DNA damage repair pathway and lung fibrosis	[213–214]

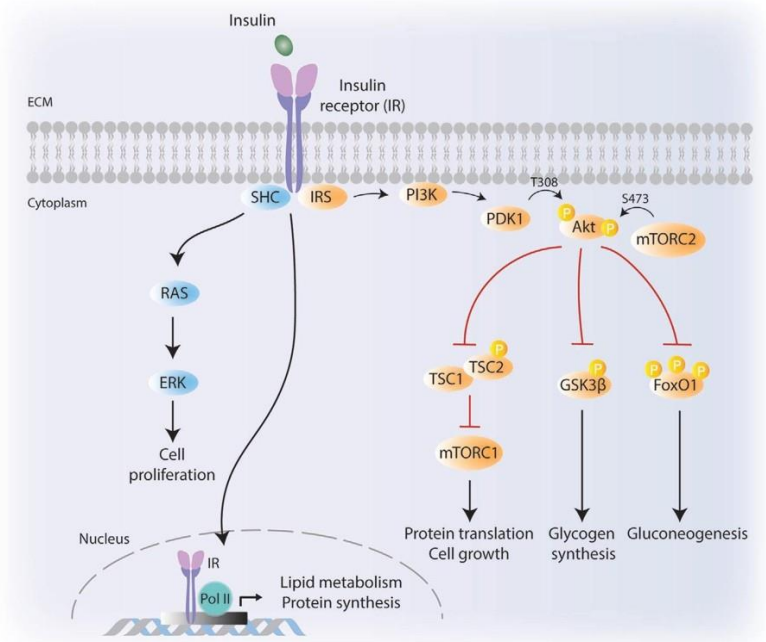

Figure 1. Canonical insulin signaling pathway. Binding of insulin to insulin receptor (IR) triggers phosphorylation of IRS, which in turn phosphorylates PI3K. Activated PI3K recruits PDK1 to the cell membrane. Akt is phosphorylated by PDK1 (on T308) and mTORC2 (on S473). Activated Akt targets a wide range of downstream targets including TSC2, GSK3β, and FoxO1 to regulate essential metabolic events. Insulin binding to its receptor also activates SHC adaptor proteins which target RAS and ERK to promote cell proliferation. Activated IR can also translocate to cell nucleus to induce the expression of genes that play role in lipid metabolism and protein synthesis. ECM, extracellular matrix.

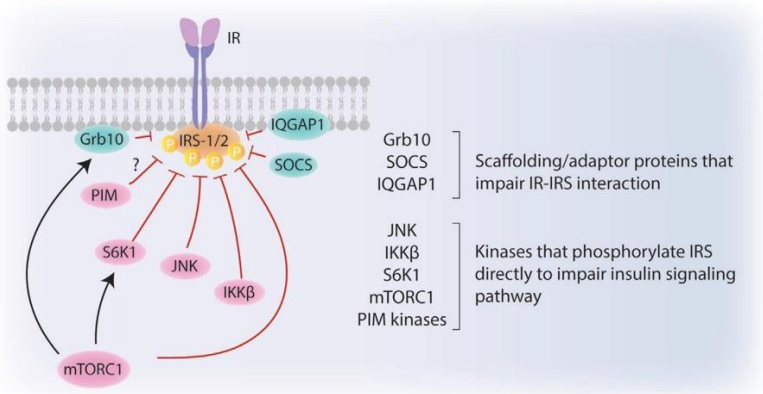

Figure 2. Insulin resistance at IRS-1/2. Insulin receptor substrate-1/2 (IRS-1/2) is a critical target that can be phosphorylated by various kinases to regulate its interaction with insulin receptor (IR). As Grb10, SOCS, or IQGAP1 proteins impair IR-IRS1/2 interaction; JNK, IKKβ, S6K1, mTORC1, and PIM kinases phosphorylate IRS-1/2 to promote its proteasomal degradation.

3.1. Insulin Resistance in Liver

Under conditions of over nutrition, high blood glucose levels oblige pancreas to produce and secrete more insulin. Constitutive activation of insulin signaling pathway at target tissues due to increased and sustained insulin levels, initiates several negative feedback loops, putting brakes on the initial steps of insulin signaling, contributing to pathological condition known as insulin resistance.

One of the well described negative feedback loops takes place in response to overnutrition-induced constitutive mTORC1 activation which leads to inhibitory phosphorylations on IRS-1 by S6K1.[20] mTORC1 itself also phosphorylates IRS1 to promote its proteasome-dependent degradation.[21]

IRS-1, indeed, acts as a critical target where independent signaling pathways merge on to establish an insulin resistant state (**Figure 2**). The effects of S/T phosphorylations on IRS1 function are multifactorial: First, these phosphorylations might impair the IRS1–IR interaction and impair IR induced IRS1 tyrosine phosphorylations. Indeed, hepatocyte specific deletion of IQGAP1 scaffolding protein, which enables IR and IRS-1 to interact, induces insulin resistance and glucose intolerance in vivo.[22] Second, S/T phosphorylations on IRS1 also promote its ubiquitin dependent proteasomal degradation.[21] Hyperactivated mTORC1 signaling also contributes to insulin resistance by phosphorylating and stabilizing Grb10 adaptor protein, which impairs IR-IRS1 interaction.[23–25] Similarly, suppression of cytokine signaling (SOCS) scaffolding proteins impair the IR-IRS-1 interaction and promote degradation of IRS-1.[26]

Recently our lab has identified transforming growth factor-β stimulated clone 22 D4 (TSC22D4) as a novel regulator of insulin resistance and hyperglycemia in mouse models of type 2 diabetes. Interestingly hepatic TSC22D4 expression positively correlates with insulin resistance in obese patients and liver specific TSC22D4 knockdown in diabetic mice improves glucose homeostasis and insulin resistance.[27]

In addition, inflammatory signals initiated by tumor necrosis factor α (TNFα), interleukin (IL)-1ß, and IL6 cytokines merge on inhibitor of nuclear factor kappa-B kinase subunit beta (IKKß) and jun N-terminal kinase (JNK) signaling pathways to induce inhibitory phosphorylations on IRS-1.[28,29] PIM kinases are also emerging as novel kinases responsible for IRS1 S1101 phosphorylation, yet the implications of these in metabolic regulation still remains elusive.[30]

Chronic accumulation of unfolded proteins results in inflammatory responses in the cells leading to metabolic diseases such as type 2 diabetes and obesity. Endoplasmic reticulum (ER) is essentially responsible for protein synthesis and protein folding. In response to accumulation of unfolded or misfolded proteins in ER lumen, ER stress leads to unfolded protein response (UPR) to prevent additional injury to the cell.[31–33] In liver, ER stress results in insulin resistance by impairing regulation of gluconeogenesis and lipogenesis. Each of the UPR proteins has distinct effects on metabolic gene regulation. cAMP-responsive element binding protein hepatocyte specific, for instance stimulates gluconeogenesis. X-binding protein 1 (XBP1), on the other hand, suppresses FoxO1 activation hence indirectly promotes sterol regulatory element binding protein 1c (SREBP1c) to activate lipogenesis. Protein kinase RNA-like endoplasmic reticulum kinase (PERK)–eukaryotic initiation factor 2 (eIf2α) branch also activates SREBP1c, and additionally promotes activating transcription factor 4 (ATF4), which in turn stimulates hepatic lipogenesis.[34] Fibroblast growth factor 21 (Fgf21) expression is also upregulated upon ER stress via PERK-eiF2α-ATF4 branch of UPR.[33] Fgf21 counteracts ER stress; and by inhibiting lipogenic program, it stimulates glucose uptake in the cells and alleviates hyperglycemia. Chronic UPR may also result in apoptotic cell death via upregulation of C/EBP homologous protein (CHOP) which is regulated by ATF4 in liver.[35] CHOP reduces B-cell lymphoma 2 (Bcl2) anti-apoptotic mitochondrial protein expression leading to cytochrome c release and caspase-3 activation.[36]

Very recent findings have shown that vitamin D receptor (VDR) blunts ER stress and UPR in the liver. VDR deficiency in VDR KO heterozygous mice not only increased UPR action and induced apoptosis but also promoted activation of pro-inflammatory cytokines such as Interleukin (IL)-1β, IL-6, and TNFα.[37]

Elevated amount of saturated free fatty acids (SFA) in the ER membrane promotes ER stress, insulin resistance, and eventually excessive hepatic gluconeogenesis. Thioesterase superfamily member 2 (Them2) is a mitochondria-associated long-chain fatty acyl-CoA and it forms a complex with phosphatidylcholine transfer protein (PC-TP) to promote β-acid oxidation upon acute ER stress. Them2/PC-TP complex regulates conversion of SFAs to saturated phospholipids to reduce ER membrane fluidity and ER stress. Them2/PC-TP complex also enhances Ca^{2+} flux into cytosol which leads to hepatic insulin resistance and gluconeogenesis.[38]

Cell-cell communication is critical for maintaining systemic metabolism of cells. Gap junctions (GJ) are essential channels that maintain cell-cell communication by allowing ions, signaling molecules, and metabolites to enter the adjacent cells. GJ are consisted of connexons, which are formed by six connexin (Cx) subunits. Very recently, connexin 43 (Cx43) emerged as one of the key regulators of ER-stress induced cell-cell coupling in hepatocytes in response to obesity. Chronic ER stress promotes expression of Cx43 and, therefore, Cx43-mediated intercellular trafficking disseminates ER stress toward adjacent cells ("bystander cells"). Since hepatic ER stress and dysfunction play role in regulating stress signals associated to insulin resistance and diabetes, systemic glucose homeostasis become disrupted also in the bystander cells. Indeed, liver specific deletion of Cx43 protects mice from diet induced-ER stress, insulin resistance, and hepatosteatosis.[39]

3.2. Selective Insulin Resistance

In healthy individuals, fasting increases glucagon secretion from pancreas, which activates gluconeogenic program in metabolic organs, mainly liver and kidney. Gluconeogenesis is the process of de novo glucose synthesis from non-carbohydrate precursors, including amino acids, pyruvate, lactate, glycerol as well as the intermediates of the Krebs cycle. Sustained gluconeogenesis represents one of the hallmarks of insulin resistance and type 2 diabetes in which liver keeps maintaining gluconeogenic activity despite high glucose levels in the blood, exacerbating hyperglycemic state.

In healthy individuals, to lower blood glucose levels, insulin suppresses gluconeogenesis while promoting lipogenesis. In type 2 diabetes, however, insulin action fails to suppress gluconeogenesis, yet it keeps activating lipogenesis, pairing two deadly weapons of metabolic syndrome: "hyperglycemia" and "hyperlipidemia". This pathogenic paradox, known as selective insulin resistance, represents one of the key questions in metabolic syndrome (**Figure 3**). Recent studies indicate that differential expression of IRS1 and IRS2 in periportal (PP) and perivenous (PV) zones of the liver creates this distinction between gluconeogenic and lipogenic program. IRS2 localizes in PP and PV whereas IRS1 localizes mainly in PV area, which is responsible for lipogenesis. While hyperinsulinemia-via negative feedback loops-leads to a decrease in IRS2 expression in PP and PV zones and relieve the inhibition of gluconeogenesis, it fails to downregulate IRS1 expression in the PV zone, where lipogenic processes still take place.[40] Indeed, IRS2 expression is epigenetically repressed in the livers of obese humans with type 2 diabetes.[41] Selective insulin resistance is an emerging topic in metabolic syndrome. Understanding exact molecular mechanisms underlying this pathological paradox will be of great benefit in search for novel treatments for metabolic diseases.

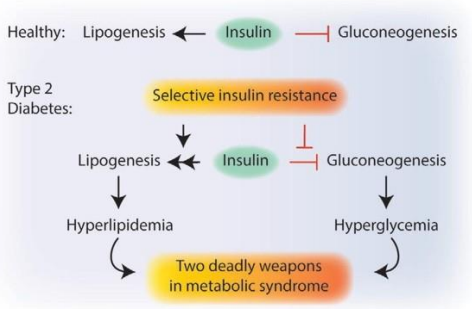

Figure 3. Selective insulin resistance. In healthy individuals, insulin promotes lipogenesis while suppressing hepatic gluconeogenesis to lower the blood glucose levels. In type 2 diabetes, distorted insulin action promotes lipogenesis yet fails to inhibit gluconeogenesis. This phenomenon is known as selective insulin resistance.

3.3. Insulin Resistance in Skeletal Muscle

In addition to liver, skeletal muscle also plays a vital role in reducing blood glucose levels by promoting its uptake upon insulin stimulation.[42] In skeletal muscle, glucose transporter 4 (GLUT4) is identified as the most abundant glucose transporter isoform. Although a small portion of GLUT4 can be found on the cellular membrane, around 80% of GLUT4 is located in GLUT4 storage vesicles (GSV). In the presence of insulin or upon exercise, GLUT4 translocates from GSVs to muscle cell surface to promote glucose uptake.[42,43] Upon glucose uptake, skeletal muscle cells either direct the glucose to glycolysis or use it for glycogen synthesis depending on their metabolic needs.

GLUT4 contains specific motifs in the amino cytoplasmic domain (FQQI) and in carboxyl cytoplasmic domain (LL and TELEY) which modulate GLUT4 trafficking from GSVs. Although the roles of certain proteins (GGA, retromer, AP1, etc.) that are interacting with these specific motifs in this trafficking are well known, there are still gaps to complete for GLUT4 translocation machinery including GSV regulations.[44]

In type 2 diabetes, reduction in insulin's ability to stimulate glucose uptake from peripheral tissues occurs due to the disruption of GLUT4 translocation to the cell surface.[45] Muscle GLUT4 emerges as a specific target upon insulin action because exercise-modulated GLUT4 translocation remains unchanged in type 2 diabetes.[44] Since exercise—induced glucose uptake remains preserved in insulin resistant—skeletal muscle, exercise

is suggested as a key therapy against metabolic diseases such as type 2 diabetes. Although PI3K-Akt signaling axis is one of the major pathways activated upon insulin engagement, defects in Akt phosphorylation on both phosphorylation sites (S-473 and Thr-308) showed only minor effects toward phosphorylation of Akt downstream targets.[44] Other than the canonical PI3K-Akt-Rab axis, non-canonical PI3K-Ras-related C3 botulinum toxin substrate 1 (Rac1) – p21-activated kinase (Pak1) actin remodeling pathway emerges as an alternative axis for GSV translocation upon insulin engagement.[46]

Accumulation of plasma free fatty acid also causes insulin resistance in skeletal muscle.[47] Palmitic acid and stearic acid are some examples of saturated long chain fatty acids (FAs) causing mitochondrial dysfunction and insulin resistance. In mitochondrial dysfunction, not only mitochondrial density decreases in insulin resistant people but also rate of ATP synthesis and oxygen consumption decrease. Elevated reactive oxygen species (ROS) levels resulting from accumulation of FA-derived metabolites (i.e., diacylglycerol and ceramides), impair mitochondrial biogenesis and activate stress kinases impairing glucose uptake and insulin tolerance.[47]

Hepatokines, liver derived hormones, are essential for liver-muscle trafficking; and Apolipoprotein J (ApoJ) emerges as a novel hepatokine targeting muscle glucose metabolism and insulin sensitivity via low density lipoprotein-related protein 2 (LRP2).[48] LRP2 is required for insulin-induced insulin receptor internalization in skeletal muscle. Muscle specific LRP2 deficiency or hepatic specific ApoJ deficiency promotes glucose intolerance and insulin resistance. ApoJ KO mice have defective insulin signaling with reduced phosphorylation on its canonical targets such as insulin receptor, IRS1/2, Akt and Akt substrate of 160 kDa (AS160) in skeletal muscle. FGF21 and selenoprotein B are other examples of hepatokines directly affecting glucose and lipid metabolism in liver, muscle, and adipose tissue. LRP2 also binds to selenoprotein B and promotes its uptake in kidney.[48]

Liver kinase B1 (*Lkb1*) suppresses amino acid induced gluconeogenesis in the liver. Hepatocyte specific *Lkb1* deletion showed increased levels of hepatic amino acid catabolism, inducing gluconeogenesis. Although *Lkb1* deficiency increased levels of amino acids in liver, it decreased the levels of amino acids in plasma. This metabolic impairment disrupts protein homeostasis in skeletal muscle and contributes to metabolic disorders such as cachexia and sarcopenia.[49]

Cachexia is a metabolic syndrome that involves extreme body weight loss and muscle wasting. Usually cachexia emerges as a complication of certain diseases such as cancer, AIDS, or chronic kidney disease.[50] In very rare cases, cachexia also represents itself as a complication of diabetes also known as diabetic neuropathic cachexia (DNC). The underlying molecular mechanisms that lead to DNC remain elusive. Unlike DNC, sarcopenia is more prevalent among patients with type 2 diabetes. Sarcopenia involves age-related loss in muscle mass and function due to impaired protein metabolism, mitochondrial dysfunction, and cell death, causing inflammation and impairing skeletal muscle's ability to uptake glucose. Hence, sarcopenia has a bidirectional relationship with type 2 diabetes, that is, while it promotes pathogenesis of type 2 diabetes it might as well emerge due to insulin resistance, oxidative stress, and vascular complications.[51]

One of the mechanisms that enhances muscle hypertrophy and stimulate skeletal muscle metabolism is via activation of the β-adrenergic receptor (β-AR) signaling pathway and cAMP production. The use of β-AR agonists such as formoterol, however, has been challenging due to its extensive burden in cardiovascular system. Nevertheless, very recently a novel β-AR agonist called 5-hydroxybenzothiazolone-derived (5'HOD) has been described which showed superior selectivity for muscle tissue and promoted anabolic functions in the muscle without inducing any side effects in the cardiovascular parameters.[52]

The increased levels of pro-inflammatory cytokines such as IL-6, monocyte chemoattractant protein 1 (MCP-1), and TNFα contributes to sarcopenia by inducing muscle wasting. Recent findings show that quercetin, a flavonoid with anti-oxidant and anti-inflammatory features, successfully counteracts the muscle atrophy induced by TNFα. Quercetin suppresses the expression of atrophic factors MAFbx/atrogin-1 and Muscle RING Finger-1 (MuRF1) while promoting the function of heme oxygenase -1 (HO-1) and Nrf-2.[53]

Ectopic accumulation of lipids in the skeletal muscle also induces inflammation, oxidative stress, and lipotoxicity, impairing insulin-dependent glucose uptake and mitochondrial function, overall contributing to insulin resistance. A critical upstream regulator of these cellular functions is a protein called myostatin, which is upregulated under conditions of metabolic syndrome. Myostatin impairs Akt and AMPK function to downregulate muscle growth. Inhibition of myostatin function in mice increased muscle mass and improved insulin sensitivity.[54–56]

3.4. Insulin Resistance in Adipose Tissue

Adipose tissue is spread all over the body with different types and unique features regulating metabolic activities. While brown adipose tissue (BAT) maintains lipogenic program upon changing thermogenic activities, lipids are stored mainly in white adipose tissue (WAT) which has two subtypes: the visceral WAT (vWAT) and the subcutaneous WAT (scWAT). In metabolic disorders, vWAT secretes IL-6 and plasminogen-activator inhibitor (PAI-1) into portal system. On the other hand, scWAT expresses leptin and adiponectin and secrete the adipokines into systemic circulation for maintaining metabolic homeostasis.[57]

The trafficking between adipocyte-hepatocyte differs in fasted and fed state of the cells. In the fasted state, adipocytes produce glycerol and release nonesterified fatty acids (NEFA) into circulation. In hepatocytes, while glycerol promotes gluconeogenesis directly; NEFAs are processed through β-oxidation to produce acetyl CoA, which in turn activates pyruvate carboxylase to stimulate gluconeogenesis.[43] On the other hand, upon insulin binding (fed state), insulin-IR-Akt axis activates mTORC1 which stimulates SREBP1c in liver inducing de novo lipogenesis (DNL).[57] Liver packs triglycerides into very low-density lipoproteins (VLDL) and secretes them into circulation to be taken up by skeletal muscle and adipocytes via CD36 and lipoprotein lipase (LPL) action.[43] Consequently, insulin stimulation suppresses NEFA and glycerol release from WAT into the circulation.[43]

Additional to overnutrition, aging also promotes senescence in type 2 diabetes associated organs, and type 2 diabetes patients experience relatively rapid aging.[58] Secreted pro-inflammatory cytokines and changing metabolites upon aging result in low-grade inflammation that manifests itself with hyperglycemia, dyslipidemia, and other metabolic problems.[59] Therefore, aging and type 2 diabetes share particular characteristics in expressing high levels of pro-inflammatory cytokines; for example, IL-6. Senescence-associated secretory phenotype (SASP) which is shared in both type 2 diabetes and aging is particularly related to oxidative and ER stress. Together with the state of low-grade inflammation, the senescent cells eventually become both the cause and the consequence of systemic changes associated in diabetes. Interestingly, leukocyte telomere length (LTL) which is a marker of senescence has been proposed to be used as a marker for type 2 diabetes since some diabetic complications are associated with telomere length.[58]

As in skeletal muscle, mitochondrial dysfunction occurs in adipocytes leading to ER stress, hypoxia, and fibrosis. Because of metabolic imbalance in adipocytes, various cytokines (e.g., IL-1, IL-12) and chemokines (IL-8) attract immune cells to the peripheral tissues. Synthesized proinflammatory mediators (e.g., TNFα and IL-6) disrupt tissue functions and cause metaflammation, which is a state of chronic and low-grade inflammation. Excessive nutrient consumption causes metaflammation since the cytokine expression and immune cell infiltration accumulates over time.[60–62]

One of the earlier events that may lead to inflammation is the hypoxic conditions that emerge due to the enlargement of adipose tissue and adipocyte size.[63] One of the targets that promote adipose tissue hypoxia is adenine nucleotide translocase 2 (ANT2) which increases adipose tissue oxygen demand. Interestingly, adipocyte specific ANT2 KO mice not only had lower levels of adipocyte hypoxia but also showed improved glucose metabolism and insulin sensitivity.[64,65]

TNFα, which plays role in metabolic alterations in cancer, cachexia, and dyslipidemia, emerges as one of the main mediators that have negative correlations on insulin resistance. TNFα neutralization in fat tissue improves insulin sensitivity and glucose handling in obese and diabetic mouse models.[62]

Infiltration of immune cells, such as macrophages into adipose tissue is one of the characteristics of metaflammation. CC-motif chemokine ligand 2 (CCL2) is a chemokine expressed in adipocytes and it promotes macrophage infiltration into adipose tissue in obesity-induced insulin resistance. Leptin also contributes to macrophage infiltration by increasing circulation of proinflammatory mediators upon food intake. Additionally, leptin acts as insulin sensitizer in liver and skeletal muscle and regulates β cell activity in pancreas.[57]

Not only macrophages but also B2 lymphocytes are enriched in obese adipose tissue. B2 cell deficient mice are protected against diet induced insulin resistance. Very interestingly, adoptive transfer of B2 cells from high fat diet (HFD) fed mice to the B-cell deficient null mice rendered the latter to insulin resistance. B2 cell recruitment to the adipose tissue and its activation was mediated by chemokine leukotriene B4 (LTB4), which binds to LTB4 Receptor 1 on B cells. LTB4/LTB4R1 engagement promotes further leukocyte infiltration into adipose tissue and promotes cytokine production.[66]

The macrophages that reside in adipose tissue of obese mice secrete miRNA-containing exosomes, which induce insulin resistance and glucose intolerance when administered to lean mice. Conversely, transfer of these vesicles from lean mice to obese mice improved insulin resistance. One of miRNAs overexpressed in macrophages of obese mice is miR-155, which targets PPARγ and knockout of miR-155 in mice improves both glucose handling and insulin sensitivity.[67]

Sphingosine kinase 1 (Sphk1) regulates sphingolipid metabolism which is essential for cell recognition, stress responses, inflammation, and apoptosis. Sphk1 deficiency decreases inflammation in adipose tissue and protects obese mice from diabetes. Additionally, Sphk1 promotes glucose sensitivity and promotes β-cell survival in diet-induced obese mice.[68] Ceramides are also sphingolipids that excessively accumulate in the adipose tissue due to obesity, impair glucose uptake and exacerbate insulin resistance. The enzyme dihydroceramide desaturase 1 (DES1) plays a role in ceramide synthesis by introducing a conserved double bond into molecules. Interestingly, both whole body and tissue specific (liver and/or adipose tissue) DES1 deficiency improves insulin resistance in mice, suggesting DES1 as a novel target against imbalanced glucose handling and metabolic disorders.[69]

4. Glucagon Signaling

When Banting and Best discovered insulin, they also noted that the pancreatic extracts contained hyperglycemic properties as well. In 1922, Kimball and Murlin successfully isolated the fraction that had only hyperglycemic effect and named it glucagon.[70] In 1948, Sutherland and de Duve showed that, it is the alpha cells of the pancreatic islets that produce glucagon.[70] Although skeletal muscle, heart, kidney, stomach, and small intestine are among the organs that express the glucagon receptor, glucagon exerts its metabolic effects mainly by liver. Glucagon receptor is a seven transmembrane receptor that belongs to G-protein coupled receptor family. Binding of glucagon to hepatic glucagon receptor activates adenylate cyclase (AC) 5 and AC 6 increasing cellular cAMP levels, which act as a second messenger to activate protein kinase A (PKA) signaling (**Figure 4**).[71,72] cAMP action in liver is very critical during fasting state to ensure glucose-dependent tissues such as brain and red blood cells have sufficient glucose supply provided by liver.

One of the well-characterized substrates of PKA is cAMP responsive element binding protein (CREB). CREB acts a transcription factor (binding to promoter regions of genes) that plays key role in gluconeogenesis such as pyruvate carboxylase (PC), phosphoenolpyruvat-carboxykinase (PEPCK), glucose-6-phosphatase (G6Pase), and peroxisome proliferator-activated receptor-gamma coactivator-1alpha (PGC1α) (Figure 4).[73–80] Recently, Krüppel like factor 9 (Klf9) was identified as a novel upstream regulator of PGC1α. Glucocorticoids (i.e., dexamethasone) and fasting upregulates Klf9 gene expression and Klf9 itself binds to the promoter region of PGC1α and acts a transcriptional activator. Interestingly liver specific Klf9 deficiency alleviates dexamethasone-induced hyperglycemia, potentially revealing one of the mechanisms explaining how glucocorticoids might promote diabetes.[81]

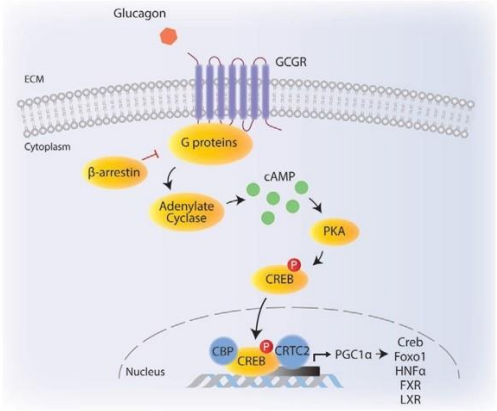

Figure 4. Glucagon signaling. Upon glucagon binding, GCGR activates adenylate cyclase that increases cAMP levels in the cytoplasm. cAMP activates PKA which phosphorylates CREB and leads to its translocation to nucleus. CREB forms a complex with CBP and CRTC2 to regulate gluconeogenic gene expression and fatty acid oxidation via targets such as PGC1α, FoxO1, hepatic HNF4α, FXR, and LXR. ECM: Extracellular matrix.

4.1. Glucagon Signaling in Diabetes

Unlike in healthy individuals where glucagon levels elevate under conditions of hypoglycemia, some patients with diabetes present increased blood glucagon levels despite hyperglycemia. Persistent exposure to glucagon creates an excessive burden on liver due to ongoing gluconeogenesis and glycogenolysis, which in turn exacerbates hyperglycemia and eventually creating a vicious cycle, contributing to pathological condition known as insulin resistance.

Indeed, approaches antagonizing glucagon signaling as well as studies in glucagon receptor knockout mice lead to promising results in which blood glucose levels decreased while glucose tolerance and insulin sensitivity improved.[82–85] For instance, inhibition of glucagon receptor (GCGR) via overexpression of β-arrestin 2 alleviated metabolic defects in HFD fed mice.[86] β-arrestins bind to GCGRs when GCGRs undergo multiple phosphorylation events by glucagon receptor kinases (GRKs) and inhibition of GCGR signaling via β-arrestins involve at least two mechanisms. β-arrestins can either impair the interaction between GCGR and G proteins or promote the internalization of GCGRs via clathrin-mediated endocytosis leading to a desensitization mode (Figure 4).[87] The barcode hypothesis of GCGR refers to the long-standing idea that specific phosphorylation events on GCGR direct the interaction with corresponding β-arrestins, induce different conformational changes on β-arrestins and dictate which signaling molecules they will recruit to initiate corresponding signaling pathways. Recent studies with atomic-level simulations and site-directed spectroscopy showed that the barcode hypothesis might indeed be a valid one and point out that it is not the number of phosphorylation events per se but the position of phosphorylated residues that act as barcodes.[88]

Although anti-glucagon approaches in several independent labs alleviated diabetic symptoms in mouse models, developing therapies that target glucagon has been challenging due to its lipogenic potential. Very recently, a high throughput screening of 300.000 compounds led to the discovery of SRI-37330, an orally bioavailable small molecule. SRI-37330 treatment ameliorated diabetes both in type 1 and type 2 diabetes mouse models. SRI-37330 impaired thioredoxin-interacting protein (TXNIP) function in pancreas, which in turn impaired glucagon secretion from the alpha cells, contributed to lower blood glucose levels.[89] Unlike glucagon receptor antagonists, SRI-37330 did not have any lipogenic effect.[90] In fact, if anything, SRI-37330 reversed hepatic fat accumulation, facilitating its potential use in treatment of type 2 diabetes and fatty liver disease.

Interestingly, glucagon shares the same precursor molecule, which is proglucagon, with glucagon like peptides 1 and 2 (GLP1 and GLP2). Yet, due to tissue specific posttranslational modifications, alpha cells of the pancreas secrete glucagon, whereas L cells of the intestine secrete GLP1 and GLP2. GLP1 represents one of the most characterized incretin hormones, which is secreted postprandially and acts both on central nervous system and peripheral tissues to induce satiety, reduce food intake, and promote insulin secretion from pancreas. Several GLP-1 receptor (GLP-1R) agonists are prescribed to patients with obesity and type 2 diabetes. Yet, like any other medication, GLP-1R agonists are also not without side effects such as nausea, preventing patients from receiving it at higher doses. Combined therapies in the form of rationally designed unimolecular GLP-1 and GCGR agonism, on the other hand, have a much greater efficacy in reducing body weight and Hb1Ac levels compared to GLP-1R agonists only. Co-agonism of GLP1 and glucagon receptors proves to be sufficient to buffer the hyperglycemic effects of glucagon action. Several unimolecular GLP-1R/ GCGR agonists are currently tested in phases 1 and 2 clinical studies with promising outcomes.[91]

In addition to GLP1 and GLP2 hormones, the intestine also contributes to metabolic homeostasis via the microbiota it houses. The gut microbiota is not only an important modulator of gut permeability, but also a critical regulator of glucose and lipid metabolism, with potential implications in pathogenesis of type 2 diabetes and its late complications.[92–94] Many cause-effect relationships regarding microbiome's potential role type 2 diabetes are derived from rodent models. Clinical studies in humans, also show that there is a clear correlation between different aspects of gut microbiome and metabolic health. Yet, further studies are needed to address whether alterations in gut microbiome in humans is a cause of type 2 diabetes or is an outcome of it.[93,95–98]

5. Role of β-cells in Type 2 Diabetes

β-cells, located in Langerhans islet of pancreas, are connected to each other by gap junctions and surrounded by other hormone secreting cells such as α (alpha) and δ (delta) cells. Thanks to the vascularized structure of the islets, pancreas can maintain islet function by regulating trafficking of secreted growth factors and rapid release of insulin to bloodstream when β-cells sense nutrients. Having appropriate number of functional insulin secreting β-cells (known as β-cell mass) is one of the essential components of insulin secretion. Insulin is secreted via vesicles (insulin secretory granules) and insulin secretion is tightly

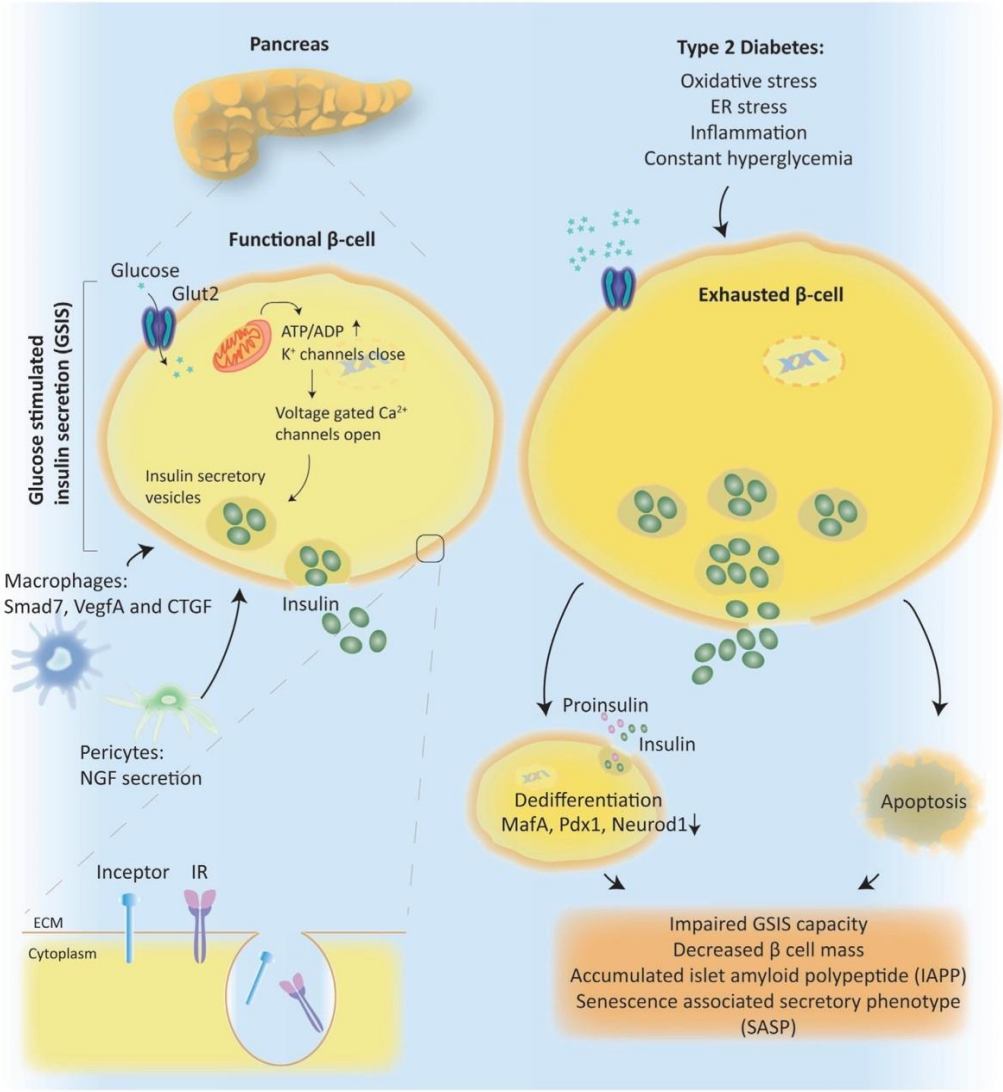

Figure 5. Role of β-cells in type 2 Diabetes. B-cells, located in Langerhans islet of pancreas, maintain islet function by regulating insulin release upon glucose stimulation. Glucose stimulated insulin secretion (GSIS), β-cell mass and function are also promoted by different transcription factors regulated via pancreatic macrophages and pericytes. Inceptor, insulin inhibitory receptor, promotes insulin receptor (IR) internalization via clathrin-mediated endocytosis. Exhausted β-cells in type 2 diabetes increase their number and size to secrete more insulin to blood stream. Challenged β cells can either dedifferentiate or undergo apoptosis. Dysfunctional β cells cause cytotoxic effects exacerbating type 2 diabetes symptoms.

mediated by regulatory signals. β-cells can sense key regulators such as free fatty acids, amino acids, and hormones such as GLP1 and glucose dependent insulinotropic polypeptide, and most importantly circulating glucose concentration. Glut2 is a transmembrane protein that is abundantly located on β-cell surface and senses the circulating blood glucose levels. Glut2 dependent glucose uptake leads to closure of ATP-sensitive potassium channels on the membrane (K_{ATP} channels), and opens voltage-gated calcium channels in return, which leads to secretion of insulin via granules (**Figure 5**).[99]

In type 1 diabetes, β-cells are destroyed by autoimmune mechanism leading to apoptosis and causing insulin deficiency.

Hence, type 1 diabetes patients need lifelong external insulin treatment. In type 2 diabetes, however, initially β-cells are functional and can still secrete insulin upon high blood glucose concentrations. As the metabolic tissues develop insulin resistance over time, β-cells increase their number and size to secrete more insulin, which puts excessive burden on β-cell function. Over time, β-cells become exhausted, lose their function, stop proliferating which overall decreases β-cell mass.[100] Constant hyperglycemic state also causes extra burden on β-cells due to glucotoxicity, which exacerbates β-cell malfunctioning.[101]

In type 2 diabetes, pancreatic islets have around 60% decrease in β-cell mass and present impaired glucose stimulated insulin secretion (GSIS) capacity. Diabetic islets also contain increased levels of islet amyloid polypeptide (IAPP) compared to non-diabetic pancreatic islets. Accumulated IAPP has cytotoxic effects and exacerbates β-cell failure by inducing pro-inflammatory cytokines such as IL-1β, TNFα, and IL-6.[101,102]

Insulin and insulin growth factor 1 (IGF1) signaling also play a critical role in function and proliferation of β-cells. Recently, scientists discovered an inhibitor of insulin receptor (IR) and IGF1 receptor (IGFR), which they named insulin inhibitory receptor, that is, "inceptor." Similar to IR and IGF1R, inceptor is also a transmembrane protein located at the cell membrane. Inceptor interacts with IR and IGF1R and promotes endocytosis-mediated internalization of these receptors leading to their desensitization. Indeed, β-cell specific inceptor knockout mice showed increased IR/IGF1R activation in pancreas, promoted β-cell proliferation and improved glucose homeostasis.[103]

PLCXD3, a member of the phosphoinositide-specific phospholipases (PI-PLC) family, also emerges as a novel regulator of genes that play role in insulin signaling pathway. Experiments performed in INS-1 cells showed that PLCXD3 depletion reduces GSIS and insulin content, and downregulates the expression of genes that play role in insulin synthesis and insulin signaling such as insulin, neuronal differentiation 1 (NEUROD1), GLUT2, glucokinase (GCK), IR, IRS2, and AKT. Indeed, human diabetic islets have reduced PLCXD3 expression, which correlates positively with insulin and GLP1R expression and negatively with donors' BMI index and HbA1c levels.[104]

Under stress conditions, mature β-cells also lose their differentiated phenotype and dedifferentiate to a precursor-like state which leads to loss of functional β-cell mass in type 2 diabetes. Additionally, oxidative stress, ER stresses, inflammation, and hypoxic environment stimulates dedifferentiation of β-cells. Factors that lead to dedifferentiation include loss of key β-cell transcription factors MafA, Pdx1, and Neurod1 as well as other targets such as Glut2 and Gck.[105]

In addition to dedifferentiation, β-cell senescence and aging also accelerate in type 2 diabetes. Senescence can be characterized with loss of β-cell markers and detection of β-galactosidase and $p16^{INK4A}$ expression, which exacerbate the inflammatory state.[106] This phenomenon is known as senescence associated secretory phenotype (SASP). When senescent cells secrete various modulators such as growth factors, cytokines and chemokines, SASP enforces cells to be in cell cycle arrest and activates immune response. SASP is mainly modulated by NF-κB, C/EBP and p53 transcription factors.[107] Moreover, removal of senescent cells (senolysis), by using transgenic INK- ATTAC mouse model or oral senolytic molecule (ABT263), decreases the rate of SASP and improves glucose handling and β-cell function.[108]

Resident macrophages, located in mouse pancreatic islets, also play role in tissue homeostasis by promoting β-cell mass and β-cell function via various signaling molecules such as Smad7, vascular endothelial growth factor A (VegfA), and connective tissue growth factor (CTGF).[109] In addition to macrophages, pericytes are also important players in pancreatic islets maintaining islet blood flow and regulating β-cell function. Dysfunctions in pericytes lead to impaired β-cell function and insulin secretion in diabetes.[109] For instance, upon high glucose stimulation, pericytes secrete nerve growth factor (NGF), which binds to its receptor TrkA located on the β-cells. Activation and phosphorylation of TrkA, in return, stimulates insulin secretion from the β-cells. Disruption of NGF or TrkA impairs glucose handling and insulin secretion in mice.[110] In addition to NGF/TrkA signaling axis, transcription factor 7 Like 2 (Tcf7l2) emerges as another factor that mediates pericyte dependent β-cell regulation. Loss of Tcf7l2 in pancreatic pericytes impairs β-cell function and exacerbates glucose intolerance in mice.[111]

Overall, loss of β-cell mass and function is key to the development of full-blown type 2 diabetes. Indeed, several of the type 2 diabetes treatments target β-cells to induce insulin secretion such as sulfonylureas, dipeptidyl peptidase 4 inhibitors (DPP4i) as well as drugs that act as GLP-1R and GPR40 agonists.[112]

6. Diabetic Complications

"Science, has been built upon many errors; but they are errors which it was good to fall into, for they led to the truth" said once the ingenious and talented French novelist Jules Verne, who himself developed type 2 diabetes in his fifties and unfortunately suffered miserably due to the diabetic complications in his late years.[113]

Diabetes is hardly a disease of mere elevation in blood glucose levels. In most cases, it brings along a plethora of complications in peripheral tissues such as kidneys, cardiovascular system, retina, the nervous system, and liver. Although the symptoms and the indications of these pathologies are quite well characterized, the underlying molecular mechanisms remain elusive. Hence, the existing therapies are not always as effective. The usual suspect leading to diabetic complications would be hyperglycemia; yet studies indicate that strict blood glucose control does not always prevent the progress of these pathologies let alone reversing it.[114,115] Large interventions trails such as UKPDS, VADT, ACCORD, and ADVANCED with glucose-lowering approaches presented evidence for statistically significant reductions in relative risks for developing some of the diabetic complications, the rate of absolute risks however remained relatively small, such as a reduction of 0.28% for microvascular complications or 0.04% reduction in diabetic kidney disease in the UKPDS study.[115,116] Multifactorial interventions targeting hypertension, dyslipidemia, and microalbuminuria, along with hyperglycemia, on the other hand, were much more effective in reducing diabetic complications in Steno-2 study.[117,118] In addition to strict glycemic control, insulin sensitizers were also associated with a reduction in diabetic complications but only with a 1.5% of absolute risk ratio for cardiovascular mortality and with a 1.8% absolute risk ratio for cardiovascular events in the case

of pioglitazone.[119] These data also raise the question how much hyperglycemia and insulin resistance play role in development of diabetic complications and whether they are just epiphenomena, that is, they might be symptoms of type 2 diabetes but might not necessarily contribute to its pathogenesis. In addition to hyperglycemia, deregulation of other cellular activities such as generation of the reactive metabolites may contribute to development of diabetic late complications.

According to Brownlee hypothesis a.k.a unifying hypothesis, hyperglycemia elevates ROS levels, which modify and impair the glycolytic enzyme glyceraldehyde 3-phosphate dehydrogenase (GAPDH). Inhibition of glycolysis via inhibition of GAPDH diverts the upstream metabolites from glycolysis to glucose overutilization pathways, which are the following: 1) the polyol pathway; 2) the protein kinase C (PKC) pathway; 3) advanced glycation end product (AGE) formation pathway; and 4) the hexosamine pathway.[120] These pathways lead to mitochondrial dysfunction and elevate ROS levels even further, contributing to disease progression and represent the root cause of diabetic complications.[120] A major drawback of this hypothesis is the fact that ROS have a very short half-life and spatially very limited actions. Although there are some studies that show patients with diabetes have elevated ROS, ROS levels do not necessarily change between patients with and without diabetic complications.[121] Although mitochondrial impairment is relevant in terms of pathogenesis of diabetes and diabetic complications, the evidence for ROS-induced mitochondrial dysfunction that leads to diabetic complications also remains elusive.

As both experimental and clinical approaches fail to provide solid and consistent evidence to support Brownlee hypothesis, researchers are investigating alternative pathways or metabolites that might play role in diabetic complications. Methylglyoxal (MG) represents one of these reactive metabolites; the levels of which increase upon hyperglycemic flux and impaired detoxification. One of the enzymes that play role in MG detoxification is Glyoxalase 1 (Glo1). Glo1 knockout flies have elevated levels of MG, which induces type 2 diabetes like phenotype such as insulin resistance, obesity, and hyperglycemia.[122] Similarly, Glo1 knockout together with diet-induced obesity elevates MG levels and induces type 2 diabetes like symptoms in zebrafish.[123] In support of these findings, MG is also sufficient to induce retinopathy like lesions in rat models without inducing hyperglycemia,[124] suggesting that accumulation of MG is creating a shortcut to develop diabetes-like phenotype in the absence of hyperglycemia.

In addition to Glo1, MG can also be metabolized either by aldo–keto reductases (AKR) to hydroxyacetone or by aldehyde dehydrogenase (ALDH) to pyruvate. Compensatory MG detoxification by increased AKR and ALDH activities is more relevant in mammals, as unlike in *Drosophila* and zebrafish, loss of Glo1 do not elevate MG levels in mice.[125,126]

6.1. Diabetic Kidney Disease

Diabetic kidney disease (DKD) (a.k.a diabetic nephropathy) develops as a microvascular complication of type 1 or type 2 diabetes with a prevalence rate of 30–40%. Diabetic kidney disease accounts for 30–47% of the end-stage renal disease (ESRD) cases, being one of the major causes of diabetes related deaths. A better control of blood glucose levels correlates with a decrease in diabetic kidney disease progression. Yet, patients with diabetes still develop kidney disease despite tight control of blood glucose levels; suggesting additional insults such as oxidative stress and lipotoxicity might play a critical role as well.[127,128] Alternatively, hyperglycemic memory might explain why patients with strict blood glucose control still develop diabetic kidney disease.[129,130] The theory of metabolic memory initially emerged after large clinical trials that continued with a follow-up period such as the DCCT trial with its follow-up EDIC study for type 1 diabetes or the UKPDS trial for type 2 diabetes.[131–134] During the clinical trials, patients with diabetes received either standard or very intensive treatment. Once the trial ended, all patients switched to very intensive treatment and had similar HbA1c levels from then on. Nevertheless, the follow up studies showed that despite similar Hb1Ac levels, patients that had received standard treatment were at a higher risk of developing microvascular complications compared to patients that received intensive treatment before.[131–135]

The exact underlying mechanisms that lead to metabolic memory remain elusive. Nevertheless, the experimental studies in the laboratories show that irreversible genetic, epigenetic, cellular, and tissue-level alterations that occur during episodes of hyperglycemia might lead to metabolic memory.[136–139]

Kidney's function in filtration, ion homeostasis, and blood pressure rely heavily on its specialized anatomical structure and the multiple cell types it contains. Cell types that reside in kidney include podocytes, epithelial cells, and mesangial cells. Diabetic kidney disease involves both functional and morphological changes in the kidney tissue such as impaired podocyte function and its detachment from glomerular basement membrane (GBM). GBM itself also thickens due to ectopic accumulation of extracellular matrix components such as collagen type IV and VI as well as laminin and fibronectin. Together with mesangial matrix expansion, GBM thickening leads to glomerular sclerosis and tubule-interstitial fibrosis, overall damaging kidney function, which presents itself as albuminuria and deteriorated glomerular filtration rate (GFR). Below, we will briefly describe the molecular mechanisms that underlie these morphological and functional changes in the kidney during diabetes.

Transforming growth factor-beta 1 (TGFβ1) plays a key role in development of fibrogenesis in the kidney by promoting extracellular matrix (ECM) deposition, impairing ECM degradation, enhancing crosslinking between collagen and elastin fibers, and activating proximal tubular and endothelial cell de-differentiation (Figure 5).[140] Hyperglycemia and insulin resistance increase the expression of Angiotensin II, which induces ROS production and activates TGFβ1 signaling.[141,142] Aberrant Janus kinase–signal transducer and activator of transcription (JAK-STAT) signaling also acts as an upstream regulator of TGFβ1 signaling. Increased ROS levels due to hyperglycemia activate JAK2, which in turn increases the expression of TGFβ1. Indeed, Baricinitib, a small molecule selective inhibitor of JAK1/2 effectively reduced albuminuria in type 2 diabetes patients in a phase 2 clinical trial study.[143–145] Other stimuli that activate TGFβ1 include mechanical stretch, AGEs and thrombospondin-1. Smad2/3 complex, protein kinase C (PKC), p38 mitogen-activated protein kinases (MAPK), interleukin like kinase (ILK) and Wnt/beta-catenin signaling are among the downstream targets that mediate profibrogenic effects of TGFβ1 (**Figure 6**).[146–149] Although evidence

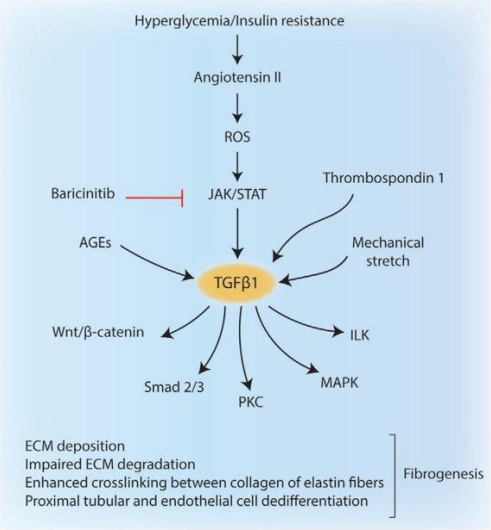

Figure 6. Diabetic kidney disease. Hyperglycemia and insulin resistance increase angiotensin II expression which activates TGFβ1 via ROS and JAK/STAT signaling. Baricinitib, selective inhibitor of JAK1/2, can reduce albuminuria in type 2 diabetes patients. TGFβ1 can also be activated via AGEs, mechanical stretch and thrombospondin 1. Activated TGFβ1 stimulates a wide range of targets including Wnt/β-catenin, Smad 2/3 complex, PKC, MAPK, and ILK to promote fibrogenesis in kidney.

suggest that TGFβ1 has an established role in pathophysiology of diabetic kidney disease, therapies that target active TGFβ1 unfortunately fail to show efficacy in clinical studies. Yet, targeting the latent form of TGFβ1 instead of the active one holds promise for the treatment of diabetic kidney disease in the future.[150]

Aberrant lipid signaling is another emerging topic in the context of diabetic kidney disease Sphingomyelin phosphodiesterase acid-like 3b (SMPDL3b) is a lipid draft enzyme, which is overexpressed in the kidneys of patients with type 2 diabetes.[151] High SMPDL3b expression reduces Ceramide 1 phosphate (C1P) levels in the plasma membrane and leads to impaired insulin/Akt signaling in podocytes. Interestingly podocyte specific SMPDL3b deletion increases C1P levels and protects db/db mice from diabetic kidney disease. Administration of C1P exogenously, on the other hand, reduces albuminuria, blunts mesangial expansion and restores Akt signaling; overall ameliorating diabetic injury. These promising findings pave the way to the use of active lipids such as C1P for the treatment of diabetic kidney disease and potentially other diabetic complications.[152]

Excessive lipid accumulation in the kidney and the accompanying lipotoxicity are unfolding as relatively new concepts that play a role in development of diabetic kidney disease as well.[153] Diabetic mice for instance overexpress junctional adhesion molecule-like protein (JAML) in their podocytes that activates the Sirtuin-1 (SIRT1) mediated Srebp1 signaling leading to excessive lipid accumulation and renal lipotoxicity. Podocyte specific deletion of JAML alleviates pathologies related to diabetic kidney disease such as lowering renal lipotoxicity impairing the progress of the disease.[154]

VEGF-B also emerges as a critical target that elevates glomerular lipid content and causes insulin resistance in podocytes. Inhibition of VEGF-B via pharmacological or genetic approaches ameliorates diabetic kidney disease in type 2 diabetes mouse models.[128]

The anti-diabetic SGLT2 inhibitors (SGLT2i) not only prove to be effective in reducing blood glucose levels but they also show decent efficacy in slowing down the progression of diabetic kidney disease.[155–160] A very recent study by Maegawa and colleagues showed that increased ketone body production might be one of the mechanisms how SGLT2i have a protective role in diabetic kidney disease. Improved ketone body production in the kidney blunts hyperactivated mTORC1 signaling and attenuates renal damage.[161] Enhanced mTORC1 signaling is a hallmark of diabetic kidney disease, which leads to podocyte and tubular damage by impairing autophagy, an essential cellular process for healthy podocyte function.[162–164]

In addition to increasing ketone body production, there are other potential mechanisms via which SGLT2i might have a renoprotective role. For instance, SGLT2 inhibitors initiate an anti-inflammatory state in the body by reducing leptin, IL-6, IL-1β levels in the serum, while increasing adiponectin levels.[165–167] In addition to these anti-inflammatory benefits, SGLTi also alleviate the burden on the kidney through many different mechanisms including inhibition of oxidative stress, lowering of blood pressure, and delaying the progress of kidney fibrosis.[168–171]

6.2. Cardiovascular Complications

Cardiovascular disease (CVD) is the most prevalent cause of mortality and morbidity among patients with diabetes. More than 30% of the type 2 diabetes patients suffer from cardiovascular complications and nearly half of type 2 diabetes related deaths occur due to CVD.[172] CVD covers a plethora of dysfunctions in the cardiovascular system including atherosclerosis, myocardial infarction, heart failure, and cardiomyopathy. Although the number of studies that explore the diabetes and CVD connection are increasing exponentially, the exact pathogenic mechanisms remain elusive. In this section, we will summarize the newly identified signaling molecules that might play role in development of type two diabetes-induced CVD.

Atherosclerosis the process of plaque formation inside the arteries and represents one of the most common form of CVD in patients with type 2 diabetes. Development of atherosclerosis is multifactorial and involves many different pathological stimuli and many different cell types. Hyperglycemia represents a great risk factor for atherosclerosis by promoting endothelial cell dysfunction, an early event during the development of atherosclerotic lesions. High blood glucose levels induce the production of AGEs that nonenzymatically attach to the proteins or lipids, altering their function. For instance, AGE-modified proteins or lipoproteins bind and activate the receptor for AGEs (RAGE), which increases VCAM-1 expression and enhances binding to monocytes that infiltrate into the ECM between the endothelial cells and smooth muscle cells (**Figure 7**).[173,174]

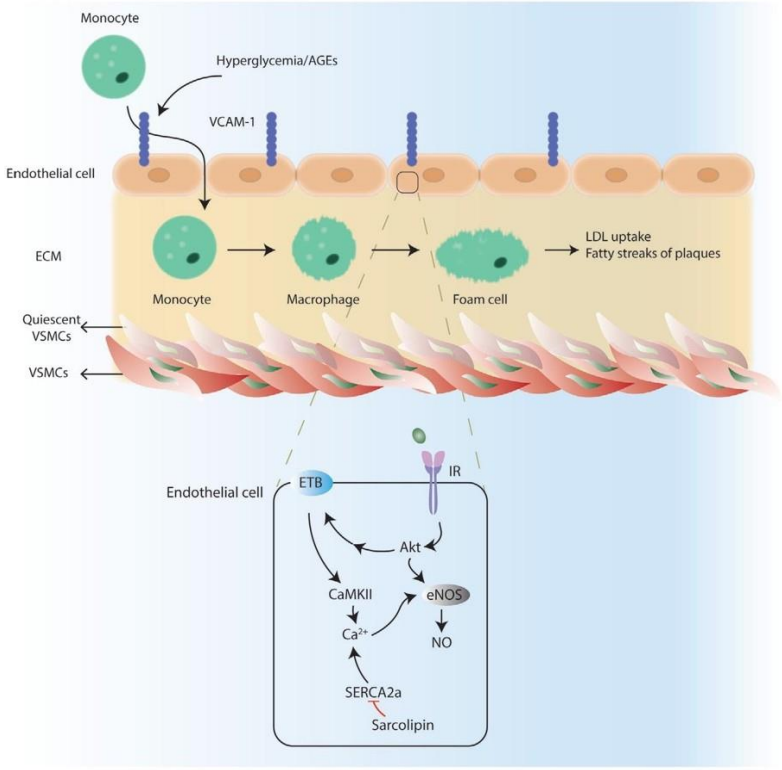

Figure 7. Cardiovascular complications. Hyperglycemia and AGEs cause endothelial cell dysfunction by increasing VCAM-1 expression on the cell membrane. Monocytes bind to VCAM-1 and infiltrate to ECM where monocytes differentiate into foam cells. Hyperglycemia also promotes quiescent vascular smooth muscle cell (qVSMC) activation which also contributes foam cell differentiation. In endothelial cells, eNOS can be regulated by Akt and CaMKII induced-Ca^{2+} levels via endothelin B receptor (ETB). Sarcolipin inhibits SERCA2a function which exacerbates Ca^{2+} dysregulation.

Hyperglycemia also activates the quiescent vascular smooth muscle cells (VSMC) that lie beneath the endothelial layer. When activated, VSMCs lose their contractility, gain proliferative, and migratory features along with enhanced inflammation and ECM production, altogether contributing to a proatherogenic phenotype.[175] Activated VSMCs also contribute to the differentiation of monocytes into the foam cells, which involves extensive take up of the low-density lipoproteins (LDL), leading to fatty streaks of the plaques at the artery walls (Figure 7).

Recently QKI-7, an RNA binding protein, emerged as a key regulator of hyperglycemia-induced vascular endothelial dysfunction. Patients with diabetes have increased QKI-7 expression in their vessels. Interestingly, QKI-7 binds and promotes mRNA degradation of its downstream targets CD144, Neuroligin 1 (NLGN1), and TNF-α-stimulated gene/protein 6 (TSG-6), all of which are essential for EC function. Indeed in vivo knock down QKI7 restored endothelial cell function in mice, suggesting a potential role for QKI-7 targeting in treatment of vascular complications of diabetes.[176] Nitric oxide (NO) plays a protective role in development of atherosclerosis by regulating the contraction of vessels, inhibiting leukocyte attachment and platelet aggregation. NO was the first soluble gas to be identified as a signaling molecule. The enzyme responsible for intracellular NO production is called nitric oxide synthase (eNOS), which is regulated by signaling pathways such as PI3K/Akt, PKA, and Ca^{2+}/calmodulin-dependent protein kinase II (CaMKII). Although insulin resistance represents a great risk factor for development of atherosclerosis, the underlying mechanisms remain controversial and/or elusive. Akt can directly phosphorylate eNOS on S1177 and promote its function. Recent findings also show that PI3K/Akt signaling induces the expression of endothelin B receptor, which activates CamKII and elevates Ca^{2+} levels. Elevated Ca^{2+} level activates eNOS, which in turn increases NO levels, adding an extra protection against the proatherogenic insults (Figure 7).[177]

Dysregulated calcium signaling is a hallmark of diabetic hearts as hyperglycemia and AGEs disrupt the healthy interplay between the sarcoplasmic/endoplasmic reticulum Ca^{2+}ATPase 2a (SERCA2a) mediated Ca^{2+} release and uptake by the sarcoplasmic reticulum. SERCA2a expression is indeed reduced in diabetic cardiomyocytes. Sarcolipin is one of the critical negative regulators of SERCA2a function. Increased sarcolipin expression

in diabetic cardiomyocytes blunts the expression of DNA methyl transferase 1 (DNMT1) and DNMT3a, overall causing demethylation of its own promoter and increasing its own transcription. Elevated sarcolipin suppresses SERCA2a activity and exacerbates Ca^{2+} dysregulation leading to diabetic heart failure (Figure 7).[178]

Class II histone deacetylase (HDACs) are essential regulators of epigenetic changes upon stress signals. Interestingly, unlike the other members of HDAC family, HDAC4 can regulate β-adrenergic signaling by responding to CaMKII and PKA signaling pathways. CaMKII phosphorylates HDAC4 at S467 and S632, and activates 14-3-3 mediated nuclear transport. PKA phosphorylates HDAC4 at S642 resulting in its proteolysis and cleavage of *N*-terminal of HDAC4 (HDAC4-NT). HDAC-NT fragment protects from diabetic heart failure via hexosamine biosynthetic pathway (HBP) and β-linked *N*-acetylglucosamine O-linked glycosylation (O-GlcNAcylation) of calcium sensor STIM1.[179]

Exophers represent a very novel concept in the field of cellular waste disposal. Exophers are specialized structures that cells pack with protein aggregates and defective organelles such as mitochondria and exude them to extracellular milieu where they can be taken up by other cells. After only a couple of years of their original discovery in *Caenorhabditis elegans*, scientists discovered exophers in mice as well. Mouse cardiomyocytes employ exophers to maintain a healthy heart function. The cardiac muscle requires tremendous amount of energy made possible by mitochondria, which undergo a fast turnover due to their heavy use. Possibly, the cardiomyocytes speed up the mitochondria turnover, by simply packing the exophers with dysfunctional mitochondria and exude them into extracellular matrix where macrophages recognize them via their phagocytic receptor Mertk and engulf.[180] Ablation of cardiac macrophages or Mertk deficiency leads to metabolic dysfunction in heart. Based on these exciting discoveries, it is very tempting to speculate that dysregulation of exopher-mediated mitochondria disposal might play a role not only in cardiomyopathy but also in other diabetic complications as well.

6.3. Diabetic Retinopathy

Diabetic retinopathy is a common complication of diabetes. Almost 20% of the patients have diabetic retinopathy at the time of diagnosis with diabetes and overall 40–45% of the patients develop retinopathy during the course of the disease. Diabetic retinopathy involves dysfunction in two main cell types of the retina: endothelial cells of the retinal microvasculature and the pericytes that lie beneath the endothelial cells to support and regulate endothelial cell function. Briefly, hyperglycemia, oxidative stress and AGEs, impair the tight junctions between the endothelial cells and induce detachment and apoptosis of pericytes.

Pericyte loss is one of the very early pathologies in diabetic retinopathy, which renders these cells an important target for early interventions to prevent the further progress of the disease. Hyperglycemia leads to detachment of pericytes from the endothelial cells, which eventually leads to apoptosis and increases the blood-retina barrier permeability. Signaling pathways that contribute to pericyte loss include Notch 1, Notch 3, hypoxia inducible factor 1 α (HIF1α), and VEGF-1 (**Figure 8**).[181,182]

Hyperactive VEGF-1 signaling contributes significantly to the progression of diabetic retinopathy by inducing highly unstructured, disorganized neovascularization of endothelial cells. Anti-VEGF-1 therapies have been very effective to delay the disease progression. Yet, not all patients respond to VEGF-1 treatment equally. Recent findings indicate that Semaphorin 4d (Sema4d) levels in the body fluids can successfully predict whether patients will respond to anti-VEGF1 therapy or not.[183] Non- or little responders of the anti-VEGF-1 therapy have elevated levels of Sema4d in the aqueous fluid of the eye. Sema4d not only acts as a biomarker but also plays a significant role in progression of diabetic retinopathy. Indeed, a combination therapy of anti-VEGF1 and anti-Sema4d might be a better alternative compared to only anti-VEGF1 treatments. Sema4d is a membrane bound protein whose expression elevated upon hypoxia in the retinal glial cells. Once shedded at the cell membrane by ADAM17, Sema4d binds to its receptor PlexinB1 at the surface of pericytes and endothelial cells, which activates downstream signaling of mDia1/Src pathway. Activation of Src contributes to phosphorylation and internalization of vascular endothelial cadherin (VE-Cadherin) which loosens the tight junctions and contributes to vascular leakage exacerbating the diabetic retinopathy (Figure 8).[183,184] Hence, Sema4d sets a nice example of how the crosstalk between retinal glial cells and the pericytes holds critical function to maintain a healthy vasculature in the eye.

Other upstream regulators of Src include Angiopoietin 1 (Ang1), which is expressed and secreted by pericytes and binds to its receptor Tie2 on endothelial cells. Activated Ang1/Tie2 signaling promotes TGFβ and platelet-derived growth factor (PDGF) signaling in endothelial cells, which stabilize the intercellular interactions. Ang1/Tie2 signaling also impairs Src function to promote the tightening of cell–cell junctions between epithelial cells blunting vascular hyperpermeability.[184] Ang2, on the other hand, acts as an antagonist to blunt the Ang1/Tie2 signaling and promote blood retina barrier permeability (Figure 8).[185]

Similar to glial cell–pericyte crosstalk, pericyte–endothelial cell crosstalk is also essential for a healthy retinal vasculature. One of the newly identified mediators of pericyte–endothelial cell crosstalk is the circular RNA called cPWWP2A. Circular RNAs are a group of non-coding RNAs with a closed loop structure and usually act as sponges to downregulate the action of their target microRNAs. High glucose levels upregulate the expression of cPWWP2A in pericytes, which acts as a sponge to impair miR-579 function and upregulate Ang1/Occludin/SIRT1 expression. cPWWP2A is also packed in exosomes and secreted into the pericyte medium to regulate the proliferation, migration, and tube formation of retinal endothelial cells.[186] Similar to cPWWP2A, cZNF532 is another novel circular RNA that plays role in controlling pericyte function and vascularization. cZNF532 acts as a sponge to downregulate miR-29a-3p, which in turn increases the expression of miR-29a-3p targets neuron-glial antigen 2 (NG2), lysyl oxidase like 2 (LOXL2), and cyclin-dependent kinase 2 (CDK2). Downregulation of cZNF532 impairs NG2, LOXL2, and CDK2 expression, which contribute to pericyte degeneration and vascular dysfunction.[187]

Chronic inflammation due to elevated levels of oxidized lipoproteins, free radicals and AGEs is also a hallmark of diabetic retinopathy. Proinflammatory cytokines that contribute to pathogenesis of diabetic retinopathy such as vascular leakage,

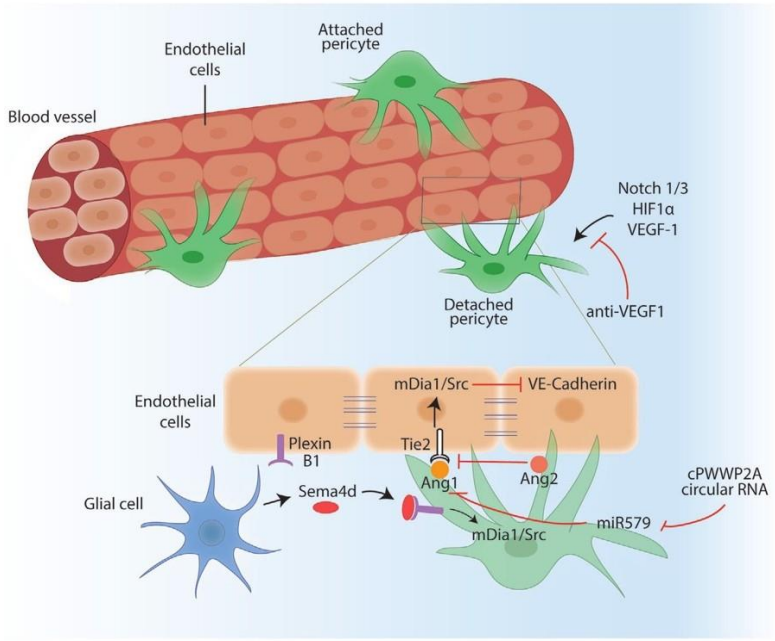

Figure 8. Diabetic retinopathy. Endothelial cells and pericytes are the two regulators of diabetic retinopathy. Hyperglycemia and oxidative stress cause pericyte detachment from the endothelial cells via Notch1/3, HIF1α, and VEGF-1 signaling pathways. Anti-VEGF-1 therapies are used to inhibit detachment of pericytes. Glial cells express Sema4d during hypoxia and upon Sema4d binding to its receptor Plexin B1 in pericytes, mDia/Src pathway gets activated. Activated Src promotes VE-cadherin internalization and loosens the tight junctions between endothelial cells. Ang1-Tie2 binding also impairs Src function, while Ang2 inhibits Ang1-Tie interaction. cPWWP2A circular RNA downregulates miR579, which in turn promotes Ang1 expression.

endothelial cell apoptosis and capillary degeneration including IL-6, IL-1β, IL-17A, MCP-1, and TNFα. Recent findings show that the prostaglandin E2 and its cognate EP2 receptor plays role in inducing the expression of not only IL1β but also the inflammasome NLR family pyrin domain containing 3 (NLRP3) signaling in diabetic retinopathy.[188–190]

Lipids are also emerging as secondary messengers that play role in progression of diabetic retinopathy. Ceramide 6, for instance, induces the expression of regulated in development and DNA damage responses 1 (REDD1), which impairs JNK function and prevents apoptosis.[191] Other lipids that might have a protective role in pathogenesis of diabetic retinopathy include decosahexaenoic acid (DHA) and eicosapentanoic acid (EPA); whereas 12-hydroxyeicosatrienoic acids (12-HETE) or 15S-HETE seem to exacerbate the progression of diabetic eye disease.[192]

Inhibitors of dipeptidyl peptidase 4 (DPP4i) are commonly used to treat type 2 diabetes. Linagliptin, sitagliptin, and diprotin A are the main DPP4i used against diabetic retinopathy. DPP4ii are regulated upon glucagon like peptide (GLP) 1 binding to GLP 1 receptor (GLP 1R) as well as other substance specific interactions such as high mobility group box 1 (HMGB 1) and stromal cell derived factor 1α (SDF 1 α). SDF 1α and VEGF work synergistically on neovascularization. In the oxygen induced retinopathy (OIR) model, a retinal neovascularization model, diprotin A induced aggravated permeability and promoted proangiogenic response leading to revascularization of avascular zone in retina. Interestingly, linagliptin acts more specific towards DPP 4 rather than other DPP family members and linagliptin treatments showed GLP1R independent anti angiogenic effects mediated by an inhibition of VEGFR signaling.[193]

6.4. Diabetic Neuropathy

Nearly half of diabetes patients experience complications in their autonomic and peripheral nervous system, known as diabetic neuropathy. In most cases, diabetic neuropathy affects the peripheral sensory nerve endings in hands and lower limbs causing pain, burning, tingling feeling as well as numbness. As the disease progresses, motor nerve endings at lower extremities get damaged, causing loss of balance and numb foot with loss of sensation. In addition to peripheral damage in the nerves, there are also cases where diabetic neuropathy develops at the proximal regions such as the thigh or pelvic and presents a proximal-to-distal gradient.[194–196]

Diabetes-induced activation of polyol pathway and concurrent depletion of NADPH and glutathione (GSH) lead to accumulation of MG and AGEs which impair nerve function. One of the targets of MG include the voltage-gated sodium channel Na(v)1.8 which leads to abnormally increased sensitivity to pain

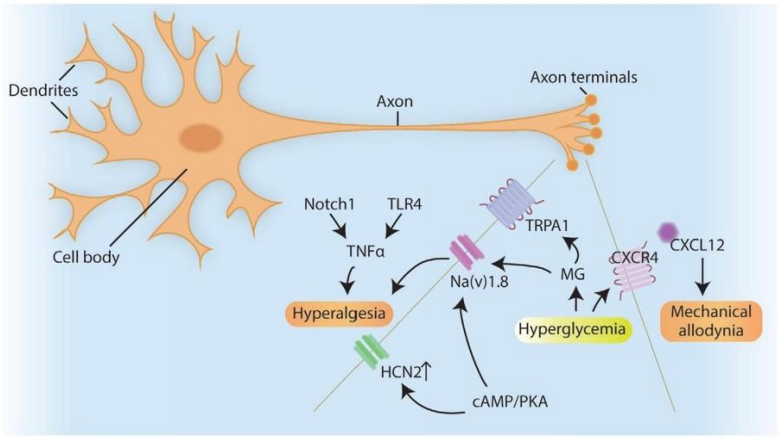

Figure 9. Diabetic neuropathy in axon terminals. Notch and TLR4 promotes the expression of TNFα which exacerbates hyperalgesia. Increased cAMP/PKA signaling leads to aberrant Na(v)1.8 channel and HCN2 channel function which also leads to hyperalgesia in diabetes. Hyperglycemia induced Methylglyoxal (MG) also modifies Na(v)1.8 and TRPA1 receptors and promotes hyperalgesia. CXCL12 and CXCR4 are novel targets that can initiate mechanical allodynia in diabetic neuropathy.

a.k.a hyperalgesia in diabetes.[197] Other upstream regulators of Na(v)1.8 include cAMP and PKA. cAMP also elevates the levels of hyperpolarization-activated cyclic nucleotide–gated 2 (HCN2) ion channels in nociceptive nerve fibers. Hyperactivated HCN2 in Na(v)1.8 positive neurons drive pain in mouse models of diabetic neuropathy and inhibition of HCN2 alleviates pain in both type 1 and type 2 diabetes mouse models (**Figure 9**).[198] In addition to hyperalgesia, diabetic neuropathy also involves mechanical allodynia and small fiber degeneration. Mechanical allodynia is a common phenomenon in diabetic neuropathy, which means induction of pain due to stimuli that under normal conditions do not provoke pain. Recent findings indicate the C-X-C motif chemokine 12 (CXCL12)/ C-X-C chemokine receptor type 4 (CXCR4) signaling axis might play a critical role in initiation of mechanical allodynia in diabetic neuropathy (Figure 9).[199]

MG modification of ligand-gated ion channel transient receptor potential cation channel, subfamily A, member 1 (TRPA1) also increases pain related hypersensitivity in diabetic neuropathy (Figure 9).[200] The neuronal oxidative/nitrosative stress also activates MAPK, JNK and nuclear factor "kappa-light-chain-enhancer" of activated B-cells (NFκB) pathways that further promote cytokine production and inflammation contributing to diabetic neuropathy. Recent advances in high throughput analysis such as microarrays and RNA-Seq indicated that pathways that regulate inflammation and lipid metabolism might play a critical role in development of diabetic neuropathy. Potential targets of such analyses include PPARγ, Apoliprotein E (ApoE), and leptin.[201] Genetic risk factors are also a component of diabetic neuropathy. Specific polymorphisms in proinflammatory and lipogenic genes such as APOE, SREBP-1, NF-κB, nitricoxidesynthase 3 (NOS3), Toll-like receptor 2 (TLR2) and TLR4, are associated with type 2 diabetes and diabetic neuropathy.[202,203] When activated TLR4 initiates a cascade of signaling events that promote the expression and secretion of TNFα creating a neuroinflammatory state. Inhibition of Notch1 or TLR4 reduces TNFα levels and alleviates mechanical allodynia while improving thermal hyperalgesia thresholds.[204]

Emerging evidence suggests lack of insulin and insulin resistance in sensory nerves might also play a role in development of diabetic neuropathy. Insulin acts as a neurotrophic hormone required to maintain normal nerve functions. Lack of insulin signaling in diabetes leads to mitochondrial dysfunction, impaired neurochemical synthesis and reduced regenerative capacity, all of which might contribute to development of diabetic neuropathy.[205]

A major component of the peripheral nervous system is the Schwann cells that surround the sensory axons for protection and survival. Hyperglycemia in diabetes not only impairs the sensory neurons but also the Schwann cell function which leads to myelin disruption, impaired axon conduction, and compromised regeneration in diabetic neuropathy via deregulation of different targets such as MAPK, p75 neurotrophin receptor (NTR), and β-nerve growth factor (NGF) as well as neurotrophic factor-3 (NT-3).[206]

6.5. Liver Fibrosis

Non-alcoholic steatohepatitis (NASH) and liver fibrosis are also emerging as late complications of diabetes. Under normal conditions, liver is great at handling acute stress conditions and regenerate when required. Apoptosis of damaged cells is a crucial part of this regeneration process, which needs to be under control for healthy liver function. Constant exposure to hyperglycemia, insulin resistance, and excessive lipid accumulation, on the other hand, induce a chronic inflammatory state where lipotoxicity and oxidative stress contribute to development of NASH from a relatively benign state of non-alcoholic fatty liver disease (NAFLD). Unlike NAFLD, NASH is hardly reversible which progresses further into fibrosis and eventually cirrhosis, when not managed

properly. Currently there are no FDA approved therapies to treat NASH and/or liver fibrosis, which represent the most common cause of liver transplants worldwide.

Mitochondrial non-coding RNAs are recently identified as contributing factors to NASH development. Steatohepatitis-associated circRNA ATP5B regulator (SCAR), which is located in mitochondria, inhibits mitochondrial ROS output and fibroblast activation.[207]

AMPK; a central regulator of cell metabolism, also plays a crucial role in maintaining hepatic homeostasis. NASH development suppresses the function of AMPK, which under normal conditions phosphorylates and inhibits caspase 6 activity. Down-regulation of AMPK during NASH leads to hyperactivation of Casp 6 causing excessive apoptosis in the liver tissue which exacerbates inflammation and liver injury.[208] One of the key mediators of liver inflammation and injury is JNK1. JNK1 induces the expression of pro-inflammatory cytokines and chemokines such as IL-6, MCP-1 via its targets c-jun and c-fos. Apoptosis signal-regulating kinase 1 (ASK1) represents one of the critical upstream activators JNK1. Ask1 homodimerization is indispensable for its activity, which is impaired by direct binding of Casp 8 and FADD like apoptosis regulator (CFLAR) protein. Interestingly hepatic CFLAR expression is reduced during metabolic syndrome and NASH. Adeno associated virus (AAV) mediated hepatic reconstitution of CFLAR improves glucose tolerance and alleviates liver fibrosis both in mice and monkeys, rendering it an attractive target for development of novel therapies against NASH.[209]

In addition to hepatocytes, hepatic stellate cells also play an important role in development of NASH and liver fibrosis. When stimulated by inflammatory cytokines or growth factors such as TGFβ1, stellate cells get activated and undergo epithelial to mesenchymal transition, gain fibroblastic features and start to proliferate. Upon activation, stellate cells also increase the production of extracellular matrix components such as collagen contributing to liver stiffness and fibrosis.

The crosstalk between hepatocytes and stellate cells exhibit a major factor that accelerates fibrotic process. TAZ protein, for instance, initiates a signaling cascade to activate the expression of secretory factor Indian Hedgehog (Ihh). Ihh secreted from hepatocytes binds to smoothened receptor on stellate cells and induces the expression of pro-fibrogenic genes and promotes proliferation. TAZ silencing in hepatocytes delays the progression of NASH and alleviates inflammation.[210]

6.6. Other Complications of Type 2 Diabetes

In addition to relatively well-characterized pathologies explained above, emerging data indicate restrictive lung diseases such as lung fibrosis might be a late complication of diabetes as well.[211,212] Since it is a relatively new concept, the number of studies that unravel the potential mechanisms are limited. Nevertheless, compelling evidence suggests that hyperglycemia/oxidative stress-induced DNA damage might play a role in diabetes-associated lung fibrosis. RAGE plays role in DNA damage repair pathway and AAV-mediated delivery of hyperactive phospho-mimetic RAGE reverses diabetes-associated fibrosis both in the lungs and kidneys of mice with diabetes.[213,214]

Between 13%–24% of patients with diabetes present cognitive dysfunction in many multiple forms such as dementia, impaired attention, poor verbal memory, and deficits in executive functioning. The insulin resistance in the brain might be one of the mechanisms that lead to impaired neural function. Other potential causes include neuroinflammation, deregulated iron metabolism, and accumulation of hyperphosphorylated tau protein, which creates protein aggregates. Indeed, there is a strong association between type 2 diabetes and Alzheimer's disease.[215]

7. Conclusion

Although diabetes mellitus is one of the earliest described diseases of the human history, there is still no cure for it. Currently the existing therapies for type 2 diabetes target reducing blood glucose levels and alleviating the symptoms of accompanying complications. Although there are cases where bariatric surgeries, intermittent fasting, or certain diets such as ketogenic diet improve type 2 diabetes; these interventions are either highly invasive or the diet regimens are hard to follow up in the long run, respectively.

Thus, main research efforts should aim for the development of novel preventive and therapeutic concepts. This will likely include the more thorough investigation of SGLT2 inhibitors and GLP1 receptor agonists, which show effective clinical outcomes not only in reducing blood glucose levels, but also in alleviating the diabetic complications particularly in cardiovascular system and kidney.[216,217] Furthermore, the clinical validation of unimolecular, dual agonists, islet cell replacement as well as novel RNA-based therapies for tailored diabetes treatment will certainly contribute to more efficacious therapies in type 2 diabetes and related complications.

Emerging insights into mechanisms of diabetic long-term complications that go beyond the simple glucose-centric view and incorporate as-yet unexplored organ complications will be the basis for intensified research efforts to prevent or even reverse long-term complications.

In addition to a better understanding of mechanisms playing role in pathogenesis of type 2 diabetes, patient stratifications based on these very pathogenic mechanisms will pave the way to more effective treatments for type 2 diabetes and its complications.

Major progress in these areas will eventually move us closer to our vision to make type 2 diabetes a livable and most importantly a curable disease in the future.

Acknowledgements

The authors would like to thank Dr. Thomas Fleming, Dr. Stefan Kopf, and Dr. Luke Harrison for their great assistance during the writing process of this manuscript. This study was funded by German Research Foundation (DFG) to B.E.Ü. (EK 108/1-1) and to Collaboration Research Center (CRC) 1118 for reactive metabolites as a cause of diabetic complications to S.H. and P.P.N.

Conflict of Interest

The authors declare no conflict of interest.

Keywords

type 2 diabetes, diabetic complications, insulin resistance, metabolism, signaling pathways

Received: January 22, 2021
Revised: May 7, 2021
Published online: July 28, 2021

[1] M. Karamanou, *World J. Diabetes* **2016**, *7*, 1.
[2] F. G. Banting, C. H. Best, *Indian J. Med. Res.* **2007**, *125*, 251.
[3] M. S. Udler, M. I. Mccarthy, J. C. Florez, A. Mahajan, *Endocr. Rev.* **2019**, *40*, 1500.
[4] Y. Zheng, S. H. Ley, F. B. Hu, *Nat. Rev. Endocrinol.* **2018**, *14*, 88.
[5] E. Ahlqvist, P. Storm, A. Käräjämäki, M. Martinell, M. Dorkhan, A. Carlsson, P. Vikman, R. B. Prasad, D. M. Aly, P. Almgren, Y. Wessman, N. Shaat, P. Spégel, H. Mulder, E. Lindholm, O. Melander, O. Hansson, U. Malmqvist, Å. Lernmark, K. Lahti, T. Forsén, T. Tuomi, A. H. Rosengren, L. Groop, *Lancet Diabetes Endocrinol.* **2018**, *6*, 361.
[6] R. Wagner, M. Heni, A. G. Tabák, J. Machann, F. Schick, E. Randrianarisoa, M. Hrabě De Angelis, A. L. Birkenfeld, N. Stefan, A. Peter, H.-U. Häring, A. Fritsche, *Nat. Med.* **2021**, *27*, 49.
[7] A. M. W. Spijkerman, J. M. Dekker, G. Nijpels, M. C. Adriaanse, P. J. Kostense, D. Ruwaard, C. D. A. Stehouwer, L. M. Bouter, R. J. Heine, *Diabetes Care* **2003**, *26*, 2604.
[8] E. Selvin, Y. Ning, M. W. Steffes, L. D. Bash, R. Klein, T. Y. Wong, B. C. Astor, A. R. Sharrett, F. L. Brancati, J. Coresh, *Diabetes* **2011**, *60*, 298.
[9] E. M. Rhea, W. A. Banks, *Front. Neurosci.* **2019**, *13*, 521.
[10] B. D. Manning, A. Toker, *Cell* **2017**, *169*, 381.
[11] B. Ekim, B. Magnuson, H. A. Acosta-Jaquez, J. A. Keller, E. P. Feener, D. C. Fingar, *Mol. Cell. Biol.* **2011**, *31*, 2787.
[12] C. Bodur, D. Kazyken, K. Huang, B. Ekim Ustunel, K. A. Siroky, A. S. Tooley, I. E. Gonzalez, D. H. Foley, H. A. Acosta-Jaquez, T. M. Barnes, G. K. Steinl, K. -. W. Cho, C. N. Lumeng, S. M. Riddle, M. G. Myers, D. C. Fingar, *EMBO J.* **2018**, *37*, 19.
[13] E. A. Oral, S. M. Reilly, A. V. Gomez, R. Meral, L. Butz, N. Ajluni, T. L. Chenevert, E. Korytnaya, A. H. Neidert, R. Hench, D. Rus, J. F. Horowitz, B. Poirier, P. Zhao, K. Lehmann, M. Jain, R. Yu, C. Liddle, M. Ahmadian, M. Downes, R. M. Evans, A. R. Saltiel, *Cell Metab.* **2017**, *26*, 157.
[14] T. Sasaoka, M. Kobayashi, *Endocr. J.* **2000**, *47*, 373.
[15] K. Hagopian, A. A. Tomilov, N. Tomilova, K. Kim, S. L. Taylor, A. K. Lam, G. A. Cortopassi, R. B. Mcdonald, J. J. Ramsey, *Metabolism* **2012**, *61*, 1703.
[16] K. Hagopian, A. A. Tomilov, K. Kim, G. A. Cortopassi, J. J. Ramsey, *PLoS One* **2015**, *10*, e0124204.
[17] A. Tomilov, A. Bettaieb, K. Kim, S. Sahdeo, N. Tomilova, A. Lam, K. Hagopian, M. Connell, J. Fong, D. Rowland, S. Griffey, J. Ramsey, F. Haj, G. Cortopassi, *Aging Cell* **2014**, *13*, 1049.
[18] S. Ciciliot, G. Fadini, *Int. J. Mol. Sci.* **2019**, *20*, 985.
[19] M. L. Hancock, R. C. Meyer, M. Mistry, R. S. Khetani, A. Wagschal, T. Shin, S. J. Ho Sui, A. M. Näär, J. G. Flanagan, *Cell* **2019**, *177*, 722.
[20] K. D. Copps, M. F. White, *Diabetologia* **2012**, *55*, 2565.
[21] Y. Yoneyama, T. Inamitsu, K. Chida, S.-I. Iemura, T. Natsume, T. Maeda, F. Hakuno, S.-I. Takahashi, *iScience* **2018**, *5*, 1.
[22] B. Chawla, A. C. Hedman, S. Sayedyahossein, H. H. Erdemir, Z. Li, D. B. Sacks, *J. Biol. Chem.* **2017**, *292*, 3273.
[23] A. M. Edick, O. Auclair, S. A. Burgos, *Am. J. Physiol. Endocrinol. Metab.* **2020**, *318*, E173.
[24] P. P. Hsu, S. A. Kang, J. Rameseder, Y. Zhang, K. A. Ottina, D. Lim, T. R. Peterson, Y. Choi, N. S. Gray, M. B. Yaffe, J. A. Marto, D. M. Sabatini, *Science* **2011**, *332*, 1317.
[25] L. Wang, B. Balas, C. Y. Christ-Roberts, R. Y. Kim, F. J. Ramos, C. K. Kikani, C. Li, C. Deng, S. Reyna, N. Musi, L. Q. Dong, R. A. Defronzo, F. Liu, *Mol. Cell. Biol.* **2007**, *27*, 6497.
[26] L. Cao, Z. Wang, W. Wan, *Front. Neurosci.* **2018**, *12*, 417.
[27] B. Ekim Üstünel, K. Friedrich, A. Maida, X. Wang, A. Krones-Herzig, O. Seibert, A. Sommerfeld, A. Jones, T. P. Sijmonsma, C. Sticht, N. Gretz, T. Fleming, P. P. Nawroth, W. Stremmel, A. J. Rose, M. Berriel-Diaz, M. Blüher, S. Herzig, *Nat. Commun.* **2016**, *7*, 13267.
[28] L. Rui, V. Aguirre, J. K. Kim, G. I. Shulman, A. Lee, A. Corbould, A. Dunaif, M. F. White, *J. Clin. Invest.* **2001**, *107*, 181.
[29] V. Aguirre, T. Uchida, L. Yenush, R. Davis, M. F. White, *J. Biol. Chem.* **2000**, *275*, 9047.
[30] J. H. Song, S. K. R. Padi, L. A. Luevano, M. D. Minden, D. J. Deangelo, G. Hardiman, L. E. Ball, N. A. Warfel, A. S. Kraft, *Oncotarget* **2016**, *7*, 20152.
[31] R. Ghemrawi, S. F. Battaglia-Hsu, C. Arnold, *Cells* **2018**, *7*, 63.
[32] X. Zhang, S. Yang, J. Chen, Z. Su, *Front. Endocrinol.* **2018**, *9*, 802.
[33] L. Salvadó, X. Palomer, E. Barroso, M. Vázquez-Carrera, *Trends Endocrinol. Metab.* **2015**, *26*, 438.
[34] L. P. Ren, X. Yu, G.-Y. Song, P. Zhang, L.-N. Sun, S.-C. Chen, Z.-J. Hu, X.-M. Zhang, *Mol. Med. Rep.* **2016**, *14*, 1649.
[35] T. A. Riaz, R. P. Junjappa, M. Handigund, J. Ferdous, H.-R. Kim, H.-J. Chae, *Cells* **2020**, *9*, 1160.
[36] H. Hu, M. Tian, C. Ding, S. Yu, *Front. Immunol.* **2018**, *9*, 3083.
[37] Y. Zhou, B. Dong, K. H. Kim, S. Choi, Z. Sun, N. Wu, Y. Wu, J. Scott, D. D. Moore, *Hepatology* **2020**, *71*, 1453.
[38] B. A. Ersoy, K. M. Maner-Smith, Y. Li, I. Alpertunga, D. E. Cohen, *J. Clin. Invest.* **2018**, *128*, 141.
[39] A. Tirosh, G. Tuncman, E. S. Calay, M. Rathaus, I. Ron, A. Tirosh, A. Yalcin, Y. G. Lee, R. Livne, S. Ron, N. Minsky, A. P. Arruda, G. S. Hotamisligil, *Cell Metab.* **2020**, *33*, 319.
[40] N. Kubota, T. Kubota, E. Kajiwara, T. Iwamura, H. Kumagai, T. Watanabe, M. Inoue, I. Takamoto, T. Sasako, K. Kumagai, M. Kohjima, M. Nakamuta, M. Moroi, K. Sugi, T. Noda, Y. Terauchi, K. Ueki, T. Kadowaki, *Nat. Commun.* **2016**, *7*, 12977.
[41] C. Krause, C. Geißler, H. Tackenberg, A. T. El Gammal, S. Wolter, J. Spranger, O. Mann, H. Lehnert, H. Kirchner, *Diabetologia* **2020**, *63*, 2182.
[42] P. L. Evans, S. L. McMillin, L. A. Weyrauch, C. A. Witczak, *Nutrients* **2019**, *11*, 2432.
[43] M. C. Petersen, G. I. Shulman, *Physiol. Rev.* **2018**, *98*, 2133.
[44] A. Klip, T. E. Mcgraw, D. E. James, *J. Biol. Chem.* **2019**, *294*, 11369.
[45] C. Affourtit, *Biochim. Biophys. Acta* **2016**, *1857*, 1678.
[46] R. Tunduguru, D. C. Thurmond, *Front. Endocrinol.* **2017**, *8*, 329.
[47] A. R. Martins, R. T. Nachbar, R. Gorjao, M. A. Vinolo, W. T. Festuccia, R. H. Lambertucci, M. F. Cury-Boaventura, L. R. Silveira, R. Curi, S. M. Hirabara, *Lipids Health Dis.* **2012**, *11*, 30.
[48] J. A. Seo, M.-C. Kang, W.-M. Yang, W. M. Hwang, S. S. Kim, S. H. Hong, J.-I. Heo, A. Vijyakumar, L. Pereira De Moura, A. Uner, H. Huang, S. H. Lee, I. S. Lima, K. S. Park, M. S. Kim, Y. Dagon, T. E. Willnow, V. Aroda, T. P. Ciaraldi, R. R. Henry, Y.-B. Kim, *Nat. Commun.* **2020**, *11*, 2024.
[49] P.-A. Just, S. Charawi, R. G. P. Denis, M. Savall, M. Traore, M. Foretz, S. Bastu, S. Magassa, N. Senni, P. Sohier, M. Wursmer, M. Vasseur-Cognet, A. Schmitt, M. Le Gall, M. Leduc, F. Guillonneau, J.-P. De Bandt, P. Mayeux, B. Romagnolo, S. Luquet, P. Bossard, C. Perret, *Nat. Commun.* **2020**, *11*, 6127.
[50] M. Rohm, A. Zeigerer, J. Machado, S. Herzig, *EMBO Rep.* **2019**, *20*, e47258.
[51] J. Mesinovic, A. Zengin, B. De Courten, P. R. Ebeling, D. Scott, *Diabetes, Metab. Syndr. Obes.* **2019**, *12*, 1057.

[52] M. Koziczak-Holbro, D. F. Rigel, B. Dumotier, D. A. Sykes, J. Tsao, N.-H. Nguyen, J. Bösch, M. Jourdain, L. Flotte, Y. Adachi, M. Kiffe, M. Azria, R. A. Fairhurst, S. J. Charlton, B. P. Richardson, E. Lach-Trifilieff, D. J. Glass, T. Ullrich, S. Hatakeyama, *J. Pharmacol. Exp. Ther.* **2019**, *369*, 188.
[53] Y. Kim, C.-S. Kim, Y. Joe, H. T. Chung, T. Y. Ha, R. Yu, *J. Med. Food* **2018**, *21*, 551.
[54] J.-P. G. Camporez, M. C. Petersen, A. Abudukadier, G. V. Moreira, M. J. Jurczak, G. Friedman, C. M. Haqq, K. F. Petersen, G. I. Shulman, *Proc. Natl. Acad. Sci. U. S. A.* **2016**, *113*, 2212.
[55] J. Dong, Y. Dong, Y. Dong, F. Chen, W. E. Mitch, L. Zhang, *Int. J. Obes.* **2016**, *40*, 434.
[56] L. A. Consitt, B. C. Clark, *J. Frailty Aging* **2018**, *7*, 21.
[57] T. Caputo, F. Gilardi, B. Desvergne, *FEBS Lett.* **2017**, *591*, 3061.
[58] F. Prattichizzo, V. De Nigris, L. La Sala, A. D. Procopio, F. Olivieri, A. Ceriello, *Oxid. Med. Cell. Longevity* **2016**, *2016*, 1810327.
[59] F. Prattichizzo, V. De Nigris, R. Spiga, E. Mancuso, L. La Sala, R. Antonicelli, R. Testa, A. D. Procopio, F. Olivieri, A. Ceriello, *Ageing Res. Rev.* **2018**, *41*, 1.
[60] A. Kuryłowicz, K. Koźniewski, *Molecules* **2020**, *25*, 2224.
[61] G. S. Hotamisligil, *Nature* **2017**, *542*, 177.
[62] G. S. Hotamisligil, *Immunity* **2017**, *47*, 406.
[63] P. E. Scherer, *Diabetologia* **2019**, *62*, 223.
[64] J. B. Seo, M. Riopel, P. Cabrales, J. Y. Huh, G. K. Bandyopadhyay, A. Y. Andreyev, A. N. Murphy, S. C. Beeman, G. I. Smith, S. Klein, Y. S. Lee, J. M. Olefsky, *Nat. Metab.* **2019**, *1*, 86.
[65] Y. S. Lee, J.-W. Kim, O. Osborne, D. Y. Oh, R. Sasik, S. Schenk, A. Chen, H. Chung, A. Murphy, S. M. Watkins, O. Quehenberger, R. S. Johnson, J. M. Olefsky, *Cell* **2014**, *157*, 1339.
[66] W. Ying, J. Wollam, J. M. Ofrecio, G. Bandyopadhyay, D. El Ouarrat, Y. S. Lee, D. Y. Oh, P. Li, O. Osborn, J. M. Olefsky, *J. Clin. Invest.* **2017**, *127*, 1019.
[67] W. Ying, M. Riopel, G. Bandyopadhyay, Y. Dong, A. Birmingham, J. B. Seo, J. M. Ofrecio, J. Wollam, A. Hernandez-Carretero, W. Fu, P. Li, J. M. Olefsky, *Cell* **2017**, *171*, 372.
[68] J. Xie, Y. Shao, J. Liu, M. Cui, X. Xiao, J. Gong, B. Xue, Q. Zhang, X. Hu, H. Duan, *Sci. Rep.* **2020**, *10*, 20038.
[69] B. Chaurasia, T. S. Tippetts, R. Mayoral Monibas, J. Liu, Y. Li, L. Wang, J. L. Wilkerson, C. R. Sweeney, R. F. Pereira, D. H. Sumida, J. A. Maschek, J. E. Cox, V. Kaddai, G. I. Lancaster, M. M. Siddique, A. Poss, M. Pearson, S. Satapati, H. Zhou, D. G. Mclaren, S. F. Previs, Y. Chen, Y. Qian, A. Petrov, M. Wu, X. Shen, J. Yao, C. N. Nunes, A. D. Howard, L. Wang, M. D. Erion, J. Rutter, W. L. Holland, D. E. Kelley, S. A. Summers, *Science* **2019**, *365*, 386.
[70] A. Staub, L. Sinn, O. K. Behrens, *J. Biol. Chem.* **1955**, *214*, 619.
[71] L. Janah, S. Kjeldsen, K. D. Galsgaard, M. Winther-Sørensen, E. Stojanovska, J. Pedersen, F. K. Knop, J. J. Holst, N. J. W. Albrechtsen, *Int. J. Mol. Sci.* **2019**, *20*, 3314.
[72] H. Yang, L. Yang, *J. Mol. Endocrinol.* **2016**, *57*, R93.
[73] S. Herzig, F. Long, U. S. Jhala, S. Hedrick, R. Quinn, A. Bauer, D. Rudolph, G. Schutz, C. Yoon, P. Puigserver, B. Spiegelman, M. Montminy, *Nature* **2001**, *413*, 179.
[74] P. G. Quinn, D. K. Granner, *Mol. Cell. Biol.* **1990**, *10*, 3357.
[75] J. Y. Altarejos, M. Montminy, *Nat. Rev. Mol. Cell Biol.* **2011**, *12*, 141.
[76] B. Lin, D. W. Morris, J. Y. Chou, *DNA Cell Biol.* **1998**, *17*, 967.
[77] P. Puigserver, J. Rhee, J. Donovan, C. J. Walkey, J. C. Yoon, F. Oriente, Y. Kitamura, J. Altomonte, H. Dong, D. Accili, B. M. Spiegelman, *Nature* **2003**, *423*, 550.
[78] J. Rhee, Y. Inoue, J. C. Yoon, P. Puigserver, M. Fan, F. J. Gonzalez, B. M. Spiegelman, *Proc. Natl. Acad. Sci. U. S. A.* **2003**, *100*, 4012.
[79] Y. Zhang, *Genes Dev.* **2004**, *18*, 157.
[80] H. Oberkofler, E. Schraml, F. Krempler, W. Patsch, *Biochem. J.* **2003**, *371*, 89.
[81] A. Cui, H. Fan, Y. Zhang, Y. Zhang, D. Niu, S. Liu, Q. Liu, W. Ma, Z. Shen, L. Shen, Y. Liu, H. Zhang, Y. Xue, Y. Cui, Q. Wang, X. Xiao, F. Fang, J. Yang, Q. Cui, Y. Chang, *J. Clin. Invest.* **2019**, *129*, 2266.
[82] H. Yan, W. Gu, J. Yang, V. Bi, Y. Shen, E. Lee, K. A. Winters, R. Komorowski, C. Zhang, J. J. Patel, D. Caughey, G. S. Elliott, Y. Y. Lau, J. Wang, Y.-S. Li, T. Boone, R. A. Lindberg, S. Hu, M. M. Véniant, *J. Pharmacol. Exp. Ther.* **2009**, *329*, 102.
[83] S. L. Conarello, G. Jiang, J. Mu, Z. Li, J. Woods, E. Zycband, J. Ronan, F. Liu, R. S. Roy, L. Zhu, M. J. Charron, B. B. Zhang, *Diabetologia* **2007**, *50*, 142.
[84] J. C. Parker, K. M. Andrews, M. R. Allen, J. L. Stock, J. D. Mcneish, *Biochem. Biophys. Res. Commun.* **2002**, *290*, 839.
[85] R. W. Gelling, X. Q. Du, D. S. Dichmann, J. Romer, H. Huang, L. Cui, S. Obici, B. Tang, J. J. Holst, C. Fledelius, P. B. Johansen, L. Rossetti, L. A. Jelicks, P. Serup, E. Nishimura, M. J. Charron, *Proc. Natl. Acad. Sci. U. S. A.* **2003**, *100*, 1438.
[86] L. Zhu, M. Rossi, Y. Cui, R. J. Lee, W. Sakamoto, N. A. Perry, N. M. Urs, M. G. Caron, V. V. Gurevich, G. Godlewski, G. Kunos, M. Chen, W. Chen, J. Wess, *J. Clin. Invest.* **2017**, *127*, 2941.
[87] L. Krilov, A. Nguyen, T. Miyazaki, C. G. Unson, R. Williams, N. H. Lee, S. Ceryak, B. Bouscarel, *Exp. Cell Res.* **2011**, *317*, 2981.
[88] N. R. Latorraca, M. Masureel, S. A. Hollingsworth, F. M. Heydenreich, C.-M. Suomivuori, C. Brinton, R. J. L. Townshend, M. Bouvier, B. K. Kobilka, R. O. Dror, *Cell* **2020**, *183*, 1813.
[89] L. A. Thielen, J. Chen, G. Jing, O. Moukha-Chafiq, G. Xu, S. Jo, T. B. Grayson, B. Lu, P. Li, C. E. Augelli-Szafran, M. J. Suto, M. Kanke, P. Sethupathy, J. K. Kim, A. Shalev, *Cell Metab.* **2020**, *32*, 353.
[90] C. B. Guzman, X. M. Zhang, R. Liu, A. Regev, S. Shankar, P. Garhyan, S. G. Pillai, C. Kazda, N. Chalasani, T. A. Hardy, *Diabetes, Obes. Metab.* **2017**, *19*, 1521.
[91] M. A. Sánchez-Garrido, S. J. Brandt, C. Clemmensen, T. D. Müller, R. D. Dimarchi, M. H. Tschöp, *Diabetologia* **2017**, *60*, 1851.
[92] D. M. Tanase, E. M. Gosav, E. Neculae, C. F. Costea, M. Ciocoiu, L. L. Hurjui, C. C. Tarniceriu, M. A. Maranduca, C. M. Lacatusu, M. Floria, I. L. Serban, *Nutrients* **2020**, *12*, 3719.
[93] M. Gurung, Z. Li, H. You, R. Rodrigues, D. B. Jump, A. Morgun, N. Shulzhenko, *EBioMedicine* **2020**, *51*, 102590.
[94] C. J. Lee, C. L. Sears, N. Maruthur, *Ann. N. Y. Acad. Sci.* **2020**, *1461*, 37.
[95] H. Herrema, J. H. Niess, *Diabetologia* **2020**, *63*, 2533.
[96] W.-Z. Li, K. Stirling, J.-J. Yang, L. Zhang, *World J. Diabetes* **2020**, *11*, 293.
[97] G. Falony, M. Joossens, S. Vieira-Silva, J. Wang, Y. Darzi, K. Faust, A. Kurilshikov, M. J. Bonder, M. Valles-Colomer, D. Vandeputte, R. Y. Tito, S. Chaffron, L. Rymenans, C. Verspecht, L. De Sutter, G. Lima-Mendez, K. D'hoe, K. Jonckheere, D. Homola, R. Garcia, E. F. Tigchelaar, L. Eeckhaudt, J. Fu, L. Henckaerts, A. Zhernakova, C. Wijmenga, J. Raes, *Science* **2016**, *352*, 560.
[98] D. Rothschild, O. Weissbrod, E. Barkan, A. Kurilshikov, T. Korem, D. Zeevi, P. I. Costea, A. Godneva, I. N. Kalka, N. Bar, S. Shilo, D. Lador, A. V. Vila, N. Zmora, M. Pevsner-Fischer, D. Israeli, N. Kosower, G. Malka, B. C. Wolf, T. Avnit-Sagi, M. Lotan-Pompan, A. Weinberger, Z. Halpern, S. Carmi, J. Fu, C. Wijmenga, A. Zhernakova, E. Elinav, E. Segal, *Nature* **2018**, *555*, 210.
[99] J. W. Ramadan, S. R. Steiner, C. M. O'neill, C. S. Nunemaker, *Cell Calcium* **2011**, *50*, 481.
[100] Z. Fu, E. R. Gilbert, D. Liu, *Curr. Diabetes Rev.* **2013**, *9*, 25.
[101] D. L. Eizirik, L. Pasquali, M. Cnop, *Nat. Rev. Endocrinol.* **2020**, *16*, 349.
[102] D. Raleigh, X. Zhang, B. Hastoy, A. Clark, *J. Mol. Endocrinol.* **2017**, *59*, R121.
[103] Ansarullah, C. Jain, F. F. Far, S. Homberg, K. Wißmiller, F. G. von Hahn, A. Raducanu, S. Schirge, M. Sterr, S. Bilekova, J. Siehler, J. Wiener, L. Oppenländer, A. Morshedi, A. Bastidas-Ponce,

G. Collden, M. Irmler, J. Beckers, A. Feuchtinger, M. Grzybek, C. Ahlbrecht, R. Feederle, O. Plettenburg, T. D. Müller, M. Meier, M. H. Tschöp, Ü. Coskun, H. Lickert, *Nature* **2021**, *590*, 326.
[104] H. Aljaibeji, D. Mukhopadhyay, A. K. Mohammed, S. Dhaiban, M. Y. Hachim, N. M. Elemam, N. Sulaiman, A. Salehi, J. Taneera, *Front. Endocrinol.* **2019**, *10*, 735.
[105] M. Bensellam, J.-C. Jonas, D. R. Laybutt, *J. Endocrinol.* **2018**, *236*, R109.
[106] Y. Tamura, N. Izumiyama-Shimomura, Y. Kimbara, K.-I. Nakamura, N. Ishikawa, J. Aida, Y. Chiba, S. Mori, T. Arai, T. Aizawa, A. Araki, K. Takubo, H. Ito, *J. Clin. Endocrinol. Metab.* **2014**, *99*, 2771.
[107] S. Lopes-Paciencia, E. Saint-Germain, M.-C. Rowell, A. F. Ruiz, P. Kalegari, G. Ferbeyre, *Cytokine* **2019**, *117*, 15.
[108] C. Aguayo-Mazzucato, J. Andle, T. B. Lee, A. Midha, L. Talemal, V. Chipashvili, J. Hollister-Lock, J. Van Deursen, G. Weir, S. Bonner-Weir, *Cell Metab.* **2019**, *30*, 129.
[109] J. Almaça, A. Caicedo, L. Landsman, *Diabetologia* **2020**, *63*, 2076.
[110] J. Houtz, P. Borden, A. Ceasrine, L. Minichiello, R. Kuruvilla, *Dev. Cell* **2016**, *39*, 329.
[111] L. Sakhneny, E. Rachi, A. Epshtein, H. C. Guez, S. Wald-Altman, M. Lisnyansky, L. Khalifa-Malka, A. Hazan, D. Baer, A. Priel, M. Weil, L. Landsman, *Diabetes* **2018**, *67*, 437.
[112] A. J. Scheen, *Expert Opin. Invest. Drugs* **2016**, *25*, 405.
[113] A. Perciaccante, A. Coralli, P. Charlier, R. Bianucci, O. Appenzeller, *Lancet Neurol.* **2017**, *16*, 268.
[114] I. M. Stratton, E. M. Kohner, S. J. Aldington, R. C. Turner, R. R. Holman, S. E. Manley, D. R. Matthews, *Diabetologia* **2001**, *44*, 156.
[115] H. Schatz, *Fortschr. Med.* **2009**, *151*, 42.
[116] I. M. Stratton, *BMJ* **2000**, *321*, 405.
[117] P. Gæde, P. Vedel, N. Larsen, G. V. H. Jensen, H.-H. Parving, O. Pedersen, *N. Engl. J. Med.* **2003**, *348*, 383.
[118] P. Gæde, H. Lund-Andersen, H.-H. Parving, O. Pedersen, *N. Engl. J. Med.* **2008**, *358*, 580.
[119] M. De Jong, H. B. Van Der Worp, Y. Van Der Graaf, F. L. J. Visseren, J. Westerink, *Cardiovasc. Diabetol.* **2017**, *16*, 134.
[120] M. Brownlee, *Nature* **2001**, *414*, 813.
[121] J. S. Nam, M. H. Cho, G. T. Lee, J. S. Park, C. W. Ahn, B. S. Cha, S. K. Lim, K. R. Kim, H. J. Ha, H. C. Lee, *Diabetes Res. Clin. Pract.* **2008**, *81*, 25.
[122] A. Moraru, J. Wiederstein, D. Pfaff, T. Fleming, A. K. Miller, P. Nawroth, A. A. Teleman, *Cell Metab.* **2018**, *27*, 926.
[123] E. Lodd, L. M. Wiggenhauser, J. Morgenstern, T. H. Fleming, G. Poschet, M. Büttner, C. T. Tabler, D. P. Wohlfart, P. P. Nawroth, J. Kroll, *JCI Insight* **2019**, *4*, e12615426.
[124] A. Schlotterer, M. Kolibabka, J. Lin, K. Acunman, N. Dietrichá, C. Sticht, T. Fleming, P. Nawroth, H.-P. Hammes, *FASEB J.* **2019**, *33*, 4141.
[125] D. Schumacher, J. Morgenstern, Y. Oguchi, N. Volk, S. Kopf, J. B. Groener, P. P. Nawroth, T. Fleming, M. Freichel, *Mol. Metab.* **2018**, *18*, 143.
[126] J. Morgenstern, T. Fleming, D. Schumacher, V. Eckstein, M. Freichel, S. Herzig, P. Nawroth, *J. Biol. Chem.* **2017**, *292*, 3224.
[127] S. G. Coca, F. Ismail-Beigi, N. Haq, H. M. Krumholz, C. R. Parikh, *Arch. Intern. Med.* **2012**, *172*, 761.
[128] A. Falkevall, A. Mehlem, I. Palombo, B. Heller Sahlgren, L. Ebarasi, L. He, A. J. Ytterberg, H. Olauson, J. Axelsson, B. Sundelin, J. Patrakka, P. Scotney, A. Nash, U. Eriksson, *Cell Metab.* **2017**, *25*, 713.
[129] S. Tonna, A. El-Osta, M. E. Cooper, C. Tikellis, *Nat. Rev. Nephrol.* **2010**, *6*, 332.
[130] S. Kumar, H. Pamulapati, K. Tikoo, *Mol. Cell. Endocrinol.* **2016**, *422*, 233.
[131] Writing Team for the Diabetes Control and Complications Trial/Epidemiology of Diabetes Interventions and Complications Research Group, *JAMA, J. Am. Med. Assoc.* **2002**, *287*, 2563.
[132] Diabetes Control and Complications Trial Research Group, D. M. Nathan, S. Genuth, J. Lachin, P. Cleary, O. Crofford, M. Davis, L. Rand, C. Siebert, *N. Engl. J. Med.* **1993**, *329*, 977.
[133] Writing Team for the Diabetes Control and Complications Trial/Epidemiology of Diabetes Interventions and Complications Research Group, *JAMA, J. Am. Med. Assoc.* **2003**, *290*, 2159.
[134] R. R. Holman, S. K. Paul, M. A. Bethel, D. R. Matthews, H. A. W. Neil, *N. Engl. J. Med.* **2008**, *359*, 1577.
[135] R. R. Holman, S. K. Paul, M. A. Bethel, H. A. W. Neil, D. R. Matthews, *N. Engl. J. Med.* **2008**, *359*, 1565.
[136] R. Natarajan, *Diabetes* **2021**, *70*, 328.
[137] T. Nishikawa, E. Araki, *J. Diabetes Invest.* **2016**, *7*, 297.
[138] C. Lee, D. An, J. Park, *Horm. Mol. Biol. Clin. Invest.* **2016**, *26*, 77.
[139] P. Bheda, *Mol. Metab.* **2020**, *38*, 100955.
[140] X.-M. Meng, P. M.-K. Tang, J. Li, H. Y. Lan, *Front. Physiol.* **2015**, *6*, 82.
[141] F. Yang, A. C. K. Chung, X. R. Huang, H. Y. Lan, *Hypertension* **2009**, *54*, 877.
[142] A. S. Chang, C. K. Hathaway, O. Smithies, M. Kakoki, *Am. J. Physiol. Renal. Physiol.* **2016**, *310*, F689.
[143] J. Wu, J. Han, B. Hou, C. Deng, H. Wu, L. Shen, *Oncol. Rep.* **2016**, *35*, 2977.
[144] K. R. Tuttle, F. C. Brosius, S. G. Adler, M. Kretzler, R. L. Mehta, J. A. Tumlin, Y. Tanaka, M. Haneda, J. Liu, M. E. Silk, T. E. Cardillo, K. L. Duffin, J. V. Haas, W. L. Macias, F. P. Nunes, J. M. Janes, *Nephrol., Dial., Transplant.* **2018**, *33*, 1950.
[145] F. C. Brosius, K. R. Tuttle, M. Kretzler, *Diabetologia* **2016**, *59*, 1624.
[146] A. S. Krolewski, J. Skupien, P. Rossing, J. H. Warram, *Kidney Int.* **2017**, *91*, 1300.
[147] L. Zhao, Y. Zou, F. Liu, *Front. Cell Dev. Biol.* **2020**, *8*, 187.
[148] Q. Lu, W.-W. Wang, M.-Z. Zhang, Z.-X. Ma, X.-R. Qiu, M. Shen, X.-X. Yin, *Exp. Ther. Med.* **2019**, *17*, 835.
[149] W. Lv, G. W. Booz, Y. Wang, F. Fan, R. J. Roman, *Eur. J. Pharmacol.* **2018**, *820*, 65.
[150] Y. Chang, W. L. Lau, H. Jo, K. Tsujino, L. Gewin, N. I. Reed, A. Atakilit, A. C. F. Nunes, W. F. Degrado, D. Sheppard, *J. Am. Soc. Nephrol.* **2017**, *28*, 1998.
[151] T.-H. Yoo, C. E. Pedigo, J. Guzman, M. Correa-Medina, C. Wei, R. Villarreal, A. Mitrofanova, F. Leclercq, C. Faul, J. Li, M. Kretzler, R. G. Nelson, M. Lehto, C. Forsblom, P.-H. Groop, J. Reiser, G. W. Burke, A. Fornoni, S. Merscher, *J. Am. Soc. Nephrol.* **2015**, *26*, 133.
[152] A. Mitrofanova, S. K. Mallela, G. M. Ducasa, T. H. Yoo, E. Rosenfeld-Gur, I. D. Zelnik, J. Molina, J. Varona Santos, M. Ge, A. Sloan, J. J. Kim, C. Pedigo, J. Bryn, I. Volosenco, C. Faul, Y. H. Zeidan, C. Garcia Hernandez, A. J. Mendez, I. Leibiger, G. W. Burke, A. H. Futerman, L. Barisoni, Y. Ishimoto, R. Inagi, S. Merscher, A. Fornoni, *Nat. Commun.* **2019**, *10*, 2692.
[153] L. Thongnak, A. Pongchaidecha, A. Lungkaphin, *Am. J. Med. Sci.* **2020**, *359*, 84.
[154] Y. Fu, Yu Sun, M. Wang, Y. Hou, W. Huang, D. Zhou, Z. Wang, S. Yang, W. Tang, J. Zhen, Y. Li, X. Wang, M. Liu, Y. Zhang, B. Wang, G. Liu, X. Yu, J. Sun, C. Zhang, F. Yi, *Cell Metab.* **2020**, *32*, 1052.
[155] B. Neal, V. Perkovic, K. W. Mahaffey, D. De Zeeuw, G. Fulcher, N. Erondu, W. Shaw, G. Law, M. Desai, D. R. Matthews, *N. Engl. J. Med.* **2017**, *377*, 644.
[156] C. Wanner, S. E. Inzucchi, J. M. Lachin, D. Fitchett, M. Von Eynatten, M. Mattheus, O. E. Johansen, H. J. Woerle, U. C. Broedl, B. Zinman, *N. Engl. J. Med.* **2016**, *375*, 323.
[157] D. Cherney, B. A. Perkins, Y. Lytvyn, H. Heerspink, M. E. Rodríguez-Ortiz, H. Mischak, *PLoS One* **2017**, *12*, e0186910.
[158] B. L. Neuen, T. Young, H. J. L. Heerspink, B. Neal, V. Perkovic, L. Billot, K. W. Mahaffey, D. M. Charytan, D. C. Wheeler, C. Arnott, S. Bompoint, A. Levin, M. J. Jardine, *Lancet Diabetes Endocrinol.* **2019**, *7*, 845.

[159] X. Luo, J. Wu, S. Jing, L.-J. Yan, *Aging Dis.* **2016**, *7*, 90.
[160] V. Perkovic, M. J. Jardine, B. Neal, S. Bompoint, H. J. L. Heerspink, D. M. Charytan, R. Edwards, R. Agarwal, G. Bakris, S. Bull, C. P. Cannon, G. Capuano, P.-L. Chu, D. De Zeeuw, T. Greene, A. Levin, C. Pollock, D. C. Wheeler, Y. Yavin, H. Zhang, B. Zinman, G. Meininger, B. M. Brenner, K. W. Mahaffey, *N. Engl. J. Med.* **2019**, *380*, 2295.
[161] I. Tomita, S. Kume, S. Sugahara, N. Osawa, K. Yamahara, M. Yasuda-Yamahara, N. Takeda, M. Chin-Kanasaki, T. Kaneko, E. Mayoux, M. Mark, M. Yanagita, H. Ogita, S.-I. Araki, H. Maegawa, *Cell Metab.* **2020**, *32*, 404.
[162] H. Mori, K. Inoki, K. Masutani, Y. Wakabayashi, K. Komai, R. Nakagawa, K.-L. Guan, A. Yoshimura, *Biochem. Biophys. Res. Commun.* **2009**, *384*, 471.
[163] K. Inoki, *Diabetes Res. Clin. Pract.* **2008**, *82*, S59.
[164] M. Gödel, B. Hartleben, N. Herbach, S. Liu, S. Zschiedrich, S. Lu, A. Debreczeni-Mór, M. T. Lindenmeyer, M.-P. Rastaldi, G. Hartleben, T. Wiech, A. Fornoni, R. G. Nelson, M. Kretzler, R. Wanke, H. Pavenstädt, D. Kerjaschki, C. D. Cohen, M. N. Hall, M. A. Rüegg, K. Inoki, G. Walz, T. B. Huber, *J. Clin. Invest.* **2011**, *121*, 2197.
[165] S. Hattori, *Diabetol. Metab. Syndr.* **2018**, *10*, 93.
[166] W. T. Garvey, L. Van Gaal, L. A. Leiter, U. Vijapurkar, J. List, R. Cuddihy, J. Ren, M. J. Davies, *Metabolism* **2018**, *85*, 32.
[167] W. Leng, X. Ouyang, X. Lei, M. Wu, L. Chen, Q. Wu, W. Deng, Z. Liang, *Mediators Inflammation* **2016**, *2016*, 6305735.
[168] S. Tanaka, Y. Sugiura, H. Saito, M. Sugahara, Y. Higashijima, J. Yamaguchi, R. Inagi, M. Suematsu, M. Nangaku, T. Tanaka, *Kidney Int.* **2018**, *94*, 912.
[169] M. A. Weber, T. A. Mansfield, F. Alessi, N. Iqbal, S. Parikh, A. Ptaszynska, *Blood Press.* **2016**, *25*, 93.
[170] L. Tang, Y. Wu, M. Tian, C. D. Sjöström, U. Johansson, X.-R. Peng, D. M. Smith, Y. Huang, *Am. J. Physiol. Endocrinol. Metab.* **2017**, *313*, E563.
[171] T. A. Zelniker, E. Braunwald, *J. Am. Coll. Cardiol.* **2020**, *75*, 422.
[172] T. R. Einarson, A. Acs, C. Ludwig, U. H. Panton, *Cardiovasc. Diabetol.* **2018**, *17*, 83.
[173] K. E. Bornfeldt, I. Tabas, *Cell Metab.* **2011**, *14*, 575.
[174] C. C. Low Wang, C. N. Hess, W. R. Hiatt, A. B. Goldfine, *Circulation* **2016**, *133*, 2459.
[175] M. A. Reddy, S. Das, C. Zhuo, W. Jin, M. Wang, L. Lanting, R. Natarajan, *Arterioscler., Thromb., Vasc. Biol.* **2016**, *36*, 864.
[176] C. Yang, M. Eleftheriadou, S. Kelaini, T. Morrison, M. V. González, R. Caines, N. Edwards, A. Yacoub, K. Edgar, A. Moez, A. Ivetic, A. Zampetaki, L. Zeng, F. L. Wilkinson, N. Lois, A. W. Stitt, D. J. Grieve, A. Margariti, *Nat. Commun.* **2020**, *11*, 3812.
[177] K. Park, Mima A., Q. Li, C. Rask-Madsen, P. N. He, K. Mizutani, S. Katagiri, Y. Maeda, I. H. Wu, M. Khamaisi, S. R. Preil, E. Maddaloni, D. Sorensen, L. M. Rasmussen, P. L. Huang, G. L. King, Insulin decreases atherosclerosis by inducing endothelin receptor B expression *JCI Insight* **2016**, *1*, e86574.
[178] Z. Liu, Y. Zhang, C. Qiu, H. Zhu, S. Pan, H. Jia, H. Kang, G. Guan, R. Hui, L. Zhu, J. Wang, *ESC Heart Failure* **2020**, *7*, 1935.
[179] M. Kronlage, M. Dewenter, J. Grosso, T. Fleming, U. Oehl, L. H. Lehmann, I. Falcão-Pires, A. F. Leite-Moreira, N. Volk, H.-J. Gröne, O. J. Müller, A. Sickmann, H. A. Katus, J. Backs, *Circulation* **2019**, *140*, 580.
[180] J. A. Nicolás-Ávila, A. V. Lechuga-Vieco, L. Esteban-Martínez, M. Sánchez-Díaz, E. Díaz-García, D. J. Santiago, A. Rubio-Ponce, J. L. Li, A. Balachander, J. A. Quintana, R. Martínez-De-Mena, B. Castejón-Vega, A. Pun-García, P. G. Través, E. Bonzón-Kulichenko, F. García-Marqués, L. Cussó, N. A-González, A. González-Guerra, M. Roche-Molina, S. Martin-Salamanca, G. Crainiciuc, G. Guzmán, J. Larrazabal, E. Herrero-Galán, J. Alegre-Cebollada, G. Lemke, C. V. Rothlin, L. J. Jimenez-Borreguero, G. Reyes, et al., *Cell* **2020**, *183*, 94.
[181] K. Miloudi, M. Oubaha, C. Ménard, A. Dejda, V. Guber, G. Cagnone, A. M. Wilson, N. Tétreault, G. Mawambo, F. Binet, R. Chidiac, C. Delisle, M. Buscarlet, A. Cerani, S. Crespo-Garcia, K. Bentley, F. Rezende, J.-S. Joyal, F. A. Mallette, J.-P. Gratton, B. Larrivée, P. Sapieha, *Proc. Natl. Acad. Sci. U. S. A.* **2019**, *116*, 4538.
[182] H. Liu, W. Zhang, B. Lilly, *J. Vasc. Res.* **2018**, *55*, 308.
[183] J. H. Wu, Y.-N. Li, A.-Q. Chen, C.-D. Hong, C.-L. Zhang, H.-L. Wang, Y.-F. Zhou, P.-C. Li, Y. Wang, L. Mao, Y.-P. Xia, Q.-W. He, H.-J. Jin, Z.-Y. Yue, B. Hu, *EMBO Mol. Med.* **2020**, *12*, e10154.
[184] M. Whitehead, A. Osborne, P. S. Widdowson, P. Yu-Wai-Man, K. R. Martin, *J. Diabetes Res.* **2019**, *2019*, 5140521.
[185] D. Ferland-Mccollough, S. Slater, J. Richard, C. Reni, G. Mangialardi, *Pharmacol. Ther.* **2017**, *171*, 30.
[186] C. Liu, H.-M. Ge, B.-H. Liu, R. Dong, K. Shan, X. Chen, M.-D. Yao, X.-M. Li, J. Yao, R.-M. Zhou, S.-J. Zhang, Q. Jiang, C. Zhao, B. Yan, *Proc. Natl. Acad. Sci. U. S. A.* **2019**, *116*, 7455.
[187] Q. Jiang, C. Liu, C.-P. Li, S.-S. Xu, M.-D. Yao, H.-M. Ge, Y.-N. Sun, X.-M. Li, S.-J. Zhang, K. Shan, B.-H. Liu, J. Yao, C. Zhao, B. Yan, *J. Clin. Invest.* **2020**, *130*, 3833.
[188] S. I. Lindstrom, S. Sigurdardottir, T. E. Zapadka, J. Tang, H. Liu, B. E. Taylor, D. G. Smith, C. A. Lee, J. Deangelis, T. S. Kern, P. R. Taylor, *J. Diabetes Complications* **2019**, *33*, 668.
[189] M. Mesquida, F. Drawnel, S. Fauser, *Semin. Immunopathol.* **2019**, *41*, 427.
[190] M. Wang, Y. Wang, T. Xie, P. Zhan, J. Zou, X. Nie, J. Shao, M. Zhuang, C. Tan, J. Tan, Y. Dai, J. Sun, J. Li, Y. Li, Q. Shi, J. Leng, X. Wang, Y. Yao, *Diabetologia* **2019**, *62*, 335.
[191] W. Dai, W. P. Miller, A. L. Toro, A. J. Black, S. K. Dierschke, R. P. Feehan, S. R. Kimball, M. D. Dennis, *FASEB J.* **2018**, *32*, 6883.
[192] K. Elmasry, A. S. Ibrahim, S. Abdulmoneim, M. Al-Shabrawey, *Br. J. Pharmacol.* **2019**, *176*, 93.
[193] M. Kolibabka, N. Dietrich, T. Klein, H.-P. Hammes, *Diabetologia* **2018**, *61*, 2412.
[194] M. Pham, D. Oikonomou, P. Baumer, A. Bierhaus, S. Heiland, P. M. Humpert, P. P. Nawroth, M. Bendszus, *Diabetes Care* **2011**, *34*, 721.
[195] M. Pham, D. Oikonomou, B. Hornung, M. Weiler, S. Heiland, P. Bäumer, J. Kollmer, P. P. Nawroth, M. Bendszus, *Ann. Neurol.* **2015**, *78*, 939.
[196] D. Schwarz, A. S. Hidmark, V. Sturm, M. Fischer, D. Milford, I. Hausser, F. Sahm, M. O. Breckwoldt, N. Agarwal, R. Kuner, M. Bendszus, P. P. Nawroth, S. Heiland, T. Fleming, *Sci. Rep.* **2020**, *10*, 7593.
[197] A. Bierhaus, T. Fleming, S. Stoyanov, A. Leffler, A. Babes, C. Neacsu, S. K. Sauer, M. Eberhardt, M. Schnölzer, F. Lasitschka, W. L. Neuhuber, T. I. Kichko, I. Konrade, R. Elvert, W. Mier, V. Pirags, I. K. Lukic, M. Morcos, T. Dehmer, N. Rabbani, P. J. Thornalley, D. Edelstein, C. Nau, J. Forbes, P. M. Humpert, M. Schwaninger, D. Ziegler, D. M. Stern, M. E. Cooper, U. Haberkorn, M. Brownlee, P. W. Reeh, P. P. Nawroth, *Nat. Med.* **2012**, *18*, 926.
[198] C. Tsantoulas, S. Laínez, S. Wong, I. Mehta, B. Vilar, P. A. Mcnaughton, *Sci. Transl. Med.* **2017**, *9*, eaam6072.
[199] N. D. Jayaraj, B. J. Bhattacharyya, A. A. Belmadani, D. Ren, C. A. Rathwell, S. Hackelberg, B. E. Hopkins, H. R. Gupta, R. J. Miller, D. M. Menichella, *J. Clin. Invest.* **2018**, *128*, 2205.
[200] D. A. Andersson, C. Gentry, E. Light, N. Vastani, J. Vallortigara, A. Bierhaus, T. Fleming, S. Bevan, *PLoS One* **2013**, *8*, e77986.
[201] J. Hur, K. A. Sullivan, M. Pande, Y. Hong, A. A. F. Sima, H. V. Jagadish, M. Kretzler, E. L. Feldman, *Brain* **2011**, *134*, 3222.
[202] I. I. Witzel, H. F. Jelinek, K. Khalaf, S. Lee, A. H. Khandoker, H. Alsafar, *Front. Endocrinol.* **2015**, *6*, 88.
[203] E. L. Feldman, K.-A. Nave, T. S. Jensen, D. L. H. Bennett, *Neuron* **2017**, *93*, 1296.
[204] T. Chen, H. Li, Y. Yin, Y. Zhang, Z. Liu, H. Liu, *Sci. Rep.* **2017**, *7*, 14923.
[205] C. W. Grote, D. E. Wright, *Front. Neurosci.* **2016**, *10*, 581.

[206] N. P. Gonçalves, C. B. Vægter, H. Andersen, L. Østergaard, N. A. Calcutt, T. S. Jensen, *Nat. Rev. Neurol.* **2017**, *13*, 135.
[207] Q. Zhao, J. Liu, H. Deng, R. Ma, J.-Y. Liao, H. Liang, J. Hu, J. Li, Z. Guo, J. Cai, X. Xu, Z. Gao, S. Su, *Cell* **2020**, *183*, 76.
[208] P. Zhao, X. Sun, C. Chaggan, Z. Liao, K. In Wong, F. He, S. Singh, R. Loomba, M. Karin, J. L. Witztum, A. R. Saltiel, *Science* **2020**, *367*, 652.
[209] X. Wang, A. Cui, F. Chen, L. Xu, Z. Hu, K. Jiang, L. Shang, J. Chu, *Small* **2019**, *15*, 1903106.
[210] X. Wang, Z. Zheng, J. M. Caviglia, K. E. Corey, T. M. Herfel, B. Cai, R. Masia, R. T. Chung, J. H. Lefkowitch, R. F. Schwabe, I. Tabas, *Cell Metab.* **2016**, *24*, 848.
[211] S. Kopf, J. B. Groener, Z. Kender, T. Fleming, M. Brune, C. Riedinger, N. Volk, E. Herpel, D. Pesta, J. Szendrödi, M. O. Wielpütz, H.-U. Kauczor, H. A. Katus, M. Kreuter, P. P. Nawroth, *Respiration* **2018**, *96*, 29.
[212] S. Kopf, P. P. Nawroth, *Exp. Clin. Endocrinol. Diabetes* **2018**, *126*, 590.
[213] V. Kumar, R. Agrawal, A. Pandey, S. Kopf, M. Hoeffgen, S. Kaymak, O. R. Bandapalli, V. Gorbunova, A. Seluanov, M. A. Mall, S. Herzig, P. P. Nawroth, *EMBO J.* **2020**, *39*, e103477.
[214] V. Kumar, T. Fleming, S. Terjung, C. Gorzelanny, C. Gebhardt, R. Agrawal, M. A. Mall, J. Ranzinger, M. Zeier, T. Madhusudhan, S. Ranjan, B. Isermann, A. Liesz, D. Deshpande, H.-U. Häring, S. K. Biswas, P. R. Reynolds, H.-P. Hammes, R. Peperkok, P. Angel, S. Herzig, P. P. Nawroth, *Nucleic Acids Res.* **2017**, *45*, 10595.
[215] H. J. Lee, H. I. Seo, H. Y. Cha, Y. J. Yang, S. H. Kwon, S. J. Yang, *Clin. Nutr. Res.* **2018**, *7*, 229.
[216] D. K. Mcguire, W. J. Shih, F. Cosentino, B. Charbonnel, D. Z. I. Cherney, S. Dagogo-Jack, R. Pratley, M. Greenberg, S. Wang, S. Huyck, I. Gantz, S. G. Terra, U. Masiukiewicz, C. P. Cannon, *JAMA Cardiol.* **2021**, *6*, 148.
[217] S. L. Kristensen, R. Rørth, P. S. Jhund, K. F. Docherty, N. Sattar, D. Preiss, L. Køber, M. C. Petrie, J. J. V. Mcmurray, *Lancet Diabetes Endocrinol.* **2019**, *7*, 776.

Sevgican Demir graduated from the Department of Molecular Biology and Genetics at Bilkent University in Ankara, Turkey. After graduation, she moved to Germany and received her M.Sc. degree in Regenerative Biology and Medicine Program at Technische Universität Dresden. Currently, she is pursuing her Ph.D. degree at the Ruprechts Karl University of Heidelberg in the research laboratory of Dr. Bilgen Ekim Üstünel.

Bilgen Ekim Üstünel received her B.Sc. degree in Molecular Biology and Genetics at Middle East Technical University in Ankara, Turkey. In 2012, she earned her Ph.D. degree in Cell and Developmental Biology at the University of Michigan—Ann Arbor, USA and moved to Germany for her postdoctoral studies at German Cancer Research Center (DKFZ, Heidelberg). Since 2017, she is a junior group leader at the Joint Heidelberg—Institute for Diabetes and Cancer (IDC) Translational Diabetes Program at Heidelberg University Hospital. Her research interests focus on identification of novel targets in type 2 diabetes and investigating their mechanism of action.

